AIMS Mathematics

http://www.aimspress.com/journal/Math

AIMS Mathematics, 11(7): 20815–20874.
DOI: 10.3934/math.2026846
Received: 11 February 2026
Revised: 06 June 2026
Accepted: 22 June 2026
Published: 15 July 2026

Research article

A golden-section-based group decision framework for software quality assessment under complex spherical fuzzy environments

Chuan Yue*

College of Mathematics and Computer Science, Guangdong Ocean University, Haida Road 1st, Zhanjiang, 524088, Guangdong, China

* **Correspondence:** Email: yuechuan-1988@163.com.

Abstract: This study introduces a novel group decision-making (GDM) framework under a complex spherical fuzzy environment, extending the golden section (GS) principle from a one-dimensional interval to a high-dimensional data center to address the core challenges of determining decision-maker (DM) weights and ranking alternatives. A rigorous theoretical justification is established, comprising four formal properties (self-similarity, optimal balance, convergence, and geometric center) that mathematically justify the GS ratio as aggregation weights for combining minimum and maximum matrices. An entropy-based method quantifies data quality for DM weight allocation, while a normalized Euclidean distance ranks the options. Eight experimental findings demonstrate the superiority of the GS-based approach: it enhances DM weight stability by a factor of 4.76 (376%) and improves ranking robustness by 8.33% compared to an arithmetic-mean-based center; against a direct extreme-value method, it achieves a 9.74-fold (874%) improvement in weight discrimination and a 0.42% sharper distinction among top alternatives. Dynamic experiments validate that the GS point 0.618 serves as a pivotal partition within [0, 1], with stable ordinal relations over 61.2% of the parameter space. Sensitivity analysis under ±50% weight variations (18 scenarios) confirms that the optimal alternative remains first in 100% of scenarios with minimal RC variability (std = 0.0013/0.0033). Comparisons with CSFN-TOPSIS and entropy-weighted methods show that the proposed method achieves the highest ranking discrimination (RDI = 0.8777). The proposed framework provides a robust, theoretically grounded methodology for reliable decision support in applications such as software quality assessment.

Keywords: group decision making; golden section; complex spherical fuzzy number; entropy; periodicity; software quality evaluation
Mathematics Subject Classification: 03E72, 90B50

1. Introduction

1.1. Background

The rapid proliferation of software across all sectors of society has precipitated a corresponding surge in demand for higher software quality. As defined by the International Standards Organization (ISO), software quality denotes the degree to which a system conforms to specified requirements, standards, and user expectations [1]. This encompasses a multifaceted spectrum of attributes, including functionality, reliability, performance, maintainability, usability, and security. The overarching objective is to deliver a product that is not only reliable and efficient but also user-friendly [2] and aligned with the needs of its intended users [3].

The evaluation of software quality can be approached from diverse perspectives [4]. This work centers on two pivotal, yet often underexplored, dimensions: (1) the inherent *periodicity* of software quality metrics and (2) the *diversity and multiplicity* of participants—ranging from end-users to domain experts—involved in the assessment process. The periodic nature of software quality is intrinsically linked to the stages of the software development lifecycle and the dynamic patterns of software usage in operation. By systematically analyzing these periodic patterns, one can more effectively identify, diagnose, and remediate recurrent quality issues.

1.2. Significance of periodicity in software quality

Post-deployment, numerous software quality indicators exhibit discernible periodic fluctuations, often correlating with usage patterns, business cycles, or maintenance schedules. Key metrics demonstrating such periodicity include:

- **Availability:** The system's ability to deliver service during specific intervals may fluctuate periodically, often degrading during predictable peak usage hours due to increased load [5].
- **Performance:** Metrics like response time and throughput can show cyclical variations, influenced by periodic high-demand scenarios in business applications [6].
- **Security:** Vulnerability exposure and attack vectors frequently follow temporal patterns, with malicious actors exploiting weaknesses during specific, predictable periods [7].
- **User satisfaction:** Feedback and satisfaction levels often vary cyclically, correlating with feature release schedules, update cycles, or seasonal usage changes [8].

Recognizing and modeling these periodic variations is crucial for proactive quality management, enabling development teams to anticipate issues, allocate resources efficiently, and enhance both software stability and user satisfaction.

1.3. Challenges in quantitative modeling

Accurately modeling software quality for assessment purposes presents several intertwined challenges:

- **Multidimensional uncertainty:** Software quality evaluation inherently involves fuzziness (partial truth) [9], hesitation (experts' uncertainty) [10], and the aforementioned periodicity. Traditional fuzzy sets fail to encapsulate this triad simultaneously.
- **Dynamic and periodic information:** Conventional methods often treat quality as a static snapshot, unable to distinguish between, for example, latency during peak versus off-peak periods, as both might be assigned a similar "high" fuzzy value despite their contextual difference.
- **Group decision-making (GDM) [11] complexity:** With the expansion of software user bases, quality assessment increasingly involves multiple stakeholders or decision-makers (DMs) [12, 13]. Effectively aggregating diverse, potentially conflicting evaluations and assigning appropriate weights to each DM based on their data's reliability [14] is a non-trivial problem. The core challenge lies in quantifying the *quality of decision data* itself to inform DM weighting.

These challenges crystallize into the first research question (RQ):

RQ 1. *How can the quality of decision data provided by multiple DMs be objectively quantified? Furthermore, is it possible to establish a neutral, objective reference data center within a GDM [15–17] environment against which individual DM data can be compared?*

1.4. Proposed conceptual framework

To address these challenges, this study proposes an integrated framework anchored on two core concepts:

(1). Complex spherical fuzzy sets (CSFSs) for periodic modeling: This study employs CSFSs [18] as a foundational quantitative tool. A CSFS represents membership, non-membership, and hesitation degrees using three-dimensional complex numbers. This structure offers unique advantages:

- **Periodicity encoding:** The phase component of the complex number naturally models temporal shifts (e.g., release cycles, usage waves), while the modulus represents the intensity of a quality attribute.
- **Unified uncertainty handling:** It concurrently captures fuzziness, hesitation, and periodicity, overcoming the limitations of traditional fuzzy sets in dynamic contexts.
- **Computational and geometric advantage:** Compared to pure temporal fuzzy logic, it reduces computational complexity while offering the geometric intuitiveness of the complex plane for operations like comparing fluctuation patterns across cycles.

(2). Golden section (GS) principle for establishing a data center: To answer RQ1 and establish a reference point, this work draws inspiration from the GS [19, 20], a proportional ratio ($\alpha \approx 0.618$) prevalent in natural patterns. The GS principle finds an ideal point C within an interval $[A, B]$ such that $(C - A)/(B - A) = (B - C)/(C - A) = \alpha$. The research ambition is to extend this one-dimensional ideal to a high-dimensional decision space, leading to the second RQ:

RQ 2. *How can the one-dimensional GS interval* $[A, B]$ *be extended to a high-dimensional dataset? Specifically, how can the boundary points A, B and the ideal point C be conceptualized and computed as complete decision/evaluation matrices?*

Once a reference data center (C) is established via the GS principle, the next step is to quantify each DM's deviation from this center, which relates to their data quality. This introduces the third RQ:

RQ 3. *How can the quality of an individual DM's evaluation data be quantified, particularly in terms of its information content and reliability relative to the established golden reference?*

To address RQ3, this study proposes the use of *entropy measures* [21,22]. Entropy, as a measure of disorder or uncertainty in a dataset, provides a scientific basis for quantifying the information quality and consistency of a DM's evaluations. Lower entropy (higher order) relative to the golden center may indicate more reliable and focused data, thus justifying a higher weight for that DM.

1.5. Research motivations and contributions

Driven by the three RQs, the core motivations of this research are:

1. To propose a novel method for determining a reference data center in GDM using the GS principle (addressing RQ1 and RQ2).
2. To extend the GS concept from a one-dimensional interval to a high-dimensional fuzzy decision matrix (addressing RQ2).
3. To utilize entropy measures for quantifying DM data quality and deriving objective DM weights based on this quantification (addressing RQ3).
4. To integrate the above into a new GDM method within a complex spherical fuzzy environment and apply it to the practical problem of periodic software quality assessment.

Accordingly, this paper makes the following key contributions:

1. Establishes a novel, geometrically-inspired **golden data center** for GDM based on the GS principle.
2. Proposes a methodology for **extending the GS** to operate on high-dimensional complex spherical fuzzy datasets.
3. Develops a **data quality measurement scheme** using entropy measures, linking data reliability to DM weighting.
4. Designs a **new GDM method** that integrates the golden data center and entropy-based weighting within a CSFSs framework.
5. Demonstrates the **practical applicability and value** of the proposed method through a case study on software quality assessment with periodic phenomena, supported by experimental analysis.

Scope and organization of this paper. The primary contribution of this study lies in the proposed CSFN-based decision methodology, rather than empirical findings. The illustrative example in Section 5.1 is intended solely to demonstrate the application procedure of the proposed method.

Proved results: Section 3.3 establishes four formal properties of the GS ratio (self-similarity, optimal balance, fixed-point convergence, and geometric center) that mathematically justify the use of the GS ratio as aggregation weights. These properties are proved analytically, independent of any specific dataset.

Observed results: Section 5 reports eight experimental findings based on the illustrative example, including robustness to weight perturbations, enhanced stability of DM weights, and superiority over alternative GDM methods. These findings are derived from a single illustrative dataset (four DMs, four alternatives). The reported improvement factors (e.g., 4.76-fold stability increase, 9.74-fold discrimination enhancement) represent relative performance comparisons under the specified experimental conditions and should be interpreted as indicative rather than absolute claims.

Future work: Section 6 discusses the limitations of this study and outlines 10 future research directions, including multi-dataset validation, statistical testing (e.g., t-tests, ANOVA, Monte Carlo simulations), real-time decision support, and applications to other domains. This paper acknowledges that multi-dataset validation is required to establish the generalizability of the observed findings.

1.6. Paper structure

The remainder of this paper is structured as follows: Section 2 reviews related work in GDM, entropy-based weighting methods, and the application of the GS principle. Section 3 presents the mathematical preliminaries, including CSFS, essential operations and measures for complex spherical fuzzy numbers (CSFNs), and the GS principle. Section 4 presents the proposed GDM methodology and outlines the step-by-step implementation procedure. Section 5 conducts an experimental analysis to validate the proposed method. This section includes an illustrative example (Subsection 5.1), sensitivity analyses, comparative studies, and dynamic experiments. Finally, Section 6 concludes the paper by summarizing the principal contributions and findings, discussing implications, and offering future research directions.

2. Related work

A structured review of the literature reveals two principal research streams directly relevant to this work: (1) the evolution of fuzzy set theories for modeling complex uncertainty, culminating in CSFSs, and (2) methodologies for determining DM weights in GDM [23]. This section synthesizes these streams, identifies persisting research gaps, and positions the present study's contributions as a targeted response to these gaps.

2.1. Evolution of fuzzy sets for complex uncertainty

The need to model imprecision and subjectivity in decision-making led to the seminal development of the ordinary fuzzy set (FS) by Zadeh [24], where membership is represented by a value μ in $[0, 1]$. While foundational, FSs exhibit key limitations: they cannot model periodicity, and the non-membership degree is rigidly defined as the complement of membership.

Subsequent extensions sought greater expressiveness:

- **Intuitionistic fuzzy sets (IFS)** by Atanassov [25] introduced an independent non-membership degree, satisfying $\mu + \nu \leq 1$. This captured hesitancy but remained static and one-dimensional. For brevity, the pair (μ, ν) is called an **intuitionistic fuzzy number (IFN)**.
- **Pythagorean fuzzy sets (PyFS)** by Yager [26] relaxed the constraint to $\mu^2 + \nu^2 \leq 1$, expanding the feasible domain for modeling stronger uncertainty. The pair (μ, ν) is correspondingly referred to as

a **Pythagorean fuzzy number (PyFN)**.

- **Picture fuzzy sets (PFS)** by Cuong [27] added a neutral/abstention degree η, governed by $\mu+\eta+\nu \leq 1$, to model voting-style hesitancy more granularly. The triplet (μ, η, ν) is known as a **Picture fuzzy number (PFN)**.

- **Spherical fuzzy sets (SFS)** by Mahmood et al. [28] further generalized PFS with the squared sum constraint $\mu^2 + \eta^2 + \nu^2 \leq 1$, accommodating a significantly broader range of expert judgments. The triplet (μ, η, ν) is accordingly called a **spherical fuzzy number (SFN)**.

The incorporation of periodicity: A parallel line of research addressed temporal or phase-based information. Ramot et al. [29] pioneered the concept of **complex fuzzy sets (CFS)**, represented as $\mu(x)e^{i2\pi f(x)}$, thereby extending the membership domain to the unit circle in the complex plane. In this representation, the modulus reflects the intensity of membership, while the phase encodes periodic shifts. The expression $\mu e^{i2\pi f}$ is termed a **complex fuzzy number (CFN)**.

This idea was later integrated into more advanced fuzzy frameworks, giving rise to several higher-order extensions:

- **Complex intuitionistic fuzzy sets (CIFS)** [30], characterized by the pair $(\mu(x)e^{i2\pi f(x)},\ \nu(x)e^{i2\pi g(x)})$.

- **Complex pythagorean fuzzy sets (CPyFS)** [31], also described by the pair $(\mu(x)e^{i2\pi f(x)},\ \nu(x)e^{i2\pi g(x)})$.

- **Complex picture fuzzy sets (CPFS)** [32], defined by the triplet $(\mu(x)e^{i2\pi f(x)},\ \eta(x)e^{i2\pi g(x)},\ \nu(x)e^{i2\pi h(x)})$.

For conciseness, the notation $(\mu e^{i2\pi f}, \nu e^{i2\pi g})$ is referred to as a **complex intuitionistic fuzzy number (CIFN)** and also as a **complex pythagorean fuzzy number (CPyFN)**—the distinction lying in the respective set constraints. The triplet $(\mu e^{i2\pi f}, \eta e^{i2\pi g}, \nu e^{i2\pi h})$ is called a **complex picture fuzzy number (CPFN)**.

The most recent and comprehensive synthesis is the **CSFS** [33]. A CSFS represents membership $(\mu e^{i2\pi f})$, neutrality $(\eta e^{i2\pi g})$, and non-membership $(\nu e^{i2\pi h})$ as three-dimensional complex numbers on a unit sphere in the complex space, governed by $\mu^2 + \eta^2 + \nu^2 \leq 1$ and $f^2 + g^2 + h^2 \leq 1$. This structure *simultaneously* captures (a) magnitude-based fuzziness, (b) tri-partite hesitation (support, neutral, against), and (c) periodic/phase information.

The relevant relationships of the complex fuzzy numbers introduced above can be represented in a single diagram, as shown in Figure 1.

Research gap and contribution linkage: While CSFSs provide a powerful, unified representation for time-varying, uncertain judgments, their application in practical GDM—particularly for problems exhibiting inherent periodicity like software quality assessment—remains underexplored. This study directly addresses this gap by adopting CSFSs as the fundamental representation scheme, thereby enabling the modeling of periodic software quality metrics within a GDM framework (linking to Contribution 5).

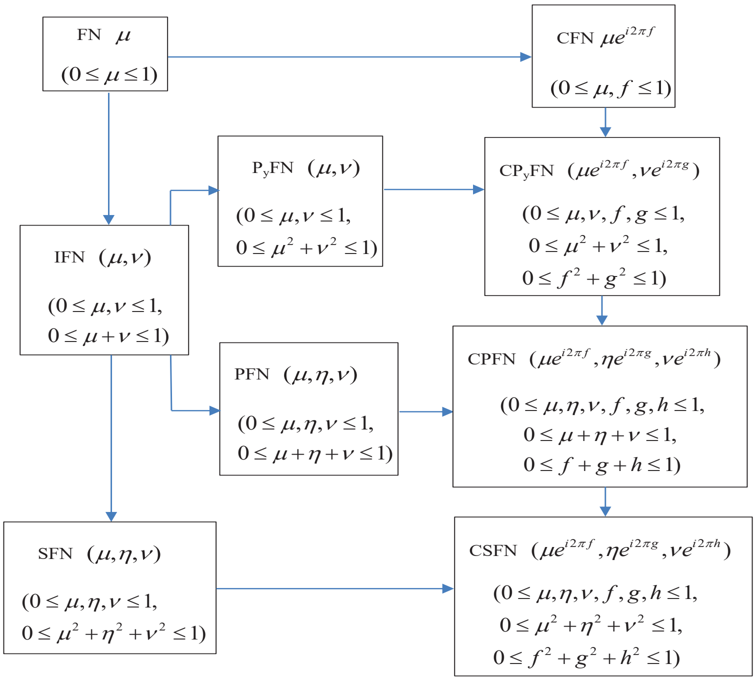

Figure 1. Graphical framework of some fuzzy numbers.

2.2. *Methodologies for determining DM weights*

The determination of DM weights is critical, as it directly impacts the GDM outcome. As noted by [34], research on DM weighting is less extensive than on attribute weighting. Existing objective methods can be categorized as follows:

- **Type I: Group position methods:** Weights are derived from a DM's position relative to a group reference concept (e.g., trust [35], consensus [36]). DMs closer to a positive ideal (or farther from a negative one) receive higher weights.
- **Type II: Group centroid methods:** A group centroid (e.g., mean [37], an ideal decision matrix [38]) is calculated. Weights are assigned based on the closeness (distance, similarity, projection [39, 40]) of an individual's assessment to this centroid.
- **Type III: Optimization methods:** Weights are obtained by solving an optimization model targeting objectives like maximizing consensus [41] or minimizing discordance/risk [42].
- **Type IV: Quality assessment methods:** The intrinsic *quality* of a DM's provided data is evaluated using measures such as entropy [43], consistency [44], certainty [45], or reliability [46]. Higher data quality translates to a higher DM weight. This approach is gaining traction [47, 48].
- **Type V: Integrated methods:** Hybrid approaches combine multiple techniques (e.g., optimization with similarity [49], entropy with VIKOR [50]).

Critical analysis and research gaps: While Types I–IV provide robust frameworks, they often rely on references that are *derived from the group data itself* (e.g., mean, consensus state). This creates a circular dependency where the reference and the weights are mutually defined. More fundamentally, there is a lack of an *independent, geometrically principled reference point* against which to impartially gauge individual DM data quality.

This directly relates to **RQ1** and reveals a significant gap: *the absence of a method to establish an objective, data-driven "golden" reference center that is not a simple statistical aggregate (like mean or mode) but is rooted in a formal geometric principle.* Furthermore, while entropy is recognized as a viable tool for quality assessment (Type IV), its application is typically divorced from such a principled reference center.

Positioning of this work's contributions: This paper directly targets these intertwined gaps. It introduces the **GS** principle [19, 51]—a classical concept of ideal proportion—into the GDM domain. The core innovation is the extension of the one-dimensional GS to define a *high-dimensional golden data center* within the CSFS space (Contributions 1 and 2). This center serves as an independent, geometrically–motivated ideal against which all DM evaluations are compared.

Subsequently, it develops an *entropy-based measurement scheme* to quantify the deviation of a DM's data from this golden center, explicitly linking data reliability to weight assignment (Contribution 3). Finally, it integrates these components into a novel, end-to-end GDM methodology within the CSFS framework (Contribution 4). Therefore, this work bridges the identified gaps by fusing a *principled reference construction method* (GS-based center) with a *sophisticated data quality assessment technique* (entropy on CSFS) within a *comprehensive uncertainty modeling environment* (CSFS), culminating in a new and applicable GDM method validated in a practical domain (Contribution 5).

3. Preliminaries

This section briefly reviews the fundamental concepts underpinning this research, including the evolution of fuzzy sets toward the CSFS, key operations and measures for CSFNs, and the GS principle. These concepts form the essential mathematical foundation for the proposed methodology. Only the prerequisites that are essential for understanding the subsequent methodology are presented, and each concept is accompanied by an intuitive explanation of its role in the proposed framework.

3.1. Complex spherical fuzzy sets

The most expressive synthesis, and the one adopted in this work, is the **CSFS** introduced by [33]. A CSFS element is represented by a triplet of complex numbers:

$$(\mu e^{i2\pi f},\ \eta e^{i2\pi g},\ \nu e^{i2\pi h})$$

where $\mu, \eta, \nu \in [0, 1]$ are the amplitude terms for membership, neutrality, and non-membership, respectively, satisfying $\mu^2 + \eta^2 + \nu^2 \leq 1$. The corresponding phase terms $f, g, h \in [0, 1]$ satisfy $f^2 + g^2 + h^2 \leq 1$. This structure *simultaneously* captures three-dimensional fuzziness (support, neutral, against), the associated hesitation, and periodic/phase information within a unified framework. For conciseness, such a triplet is termed a complex spherical fuzzy number (CSFN).

Role in the proposed methodology: The CSFN serves as the fundamental information representation unit throughout this study. It enables the modeling of e-commerce software evaluations that vary between peak and off-peak periods, capturing both the intensity (via amplitude terms) and the periodicity (via phase terms) of user assessments. Every evaluation matrix entry in the methodology (Section 4) is expressed as a CSFN.

Theoretical basis for processing periodic phenomena using complex spherical fuzzy information. The primary advantage of CSFNs over conventional fuzzy sets is their inherent ability to represent periodic information through the phase term $e^{i2\pi\cdot(\cdot)}$. This subsection provides the theoretical justification for using CSFN to process periodic phenomena.

Phase-term encoding of temporal dynamics. In conventional fuzzy sets, an evaluation is represented as a static scalar value $\mu \in [0, 1]$, which cannot distinguish between different temporal phases of the same phenomenon. For example, a software system may be rated "good" with $\mu = 0.8$ during both peak and off-peak periods, but the underlying user perception and system behavior may differ significantly. The CSFN addresses this limitation by encoding the temporal context into the phase term. Specifically, the phase term $e^{i2\pi f}$ for membership, $e^{i2\pi g}$ for neutrality, and $e^{i2\pi h}$ for non-membership capture the periodic characteristics (e.g., peak vs. off-peak) of the evaluation.

Circular representation via Euler's formula. By Euler's formula $e^{i\theta} = \cos\theta + i\sin\theta$ [52], the complex-valued membership can be decomposed into real and imaginary components:

$$\mu e^{i2\pi f} = \mu(\cos 2\pi f + i\sin 2\pi f).$$

This decomposition provides a geometric interpretation on the unit circle, where the phase $2\pi f$ represents the angular position corresponding to a specific periodic state. As f varies from 0 to 1, the complex number traces a full circle, allowing the representation of any cyclical phase. This circular representation is particularly suitable for modeling phenomena that repeat periodically, such as seasonal fluctuations, daily traffic patterns, or shopping festival cycles.

Distinguishing different temporal phases. A key theoretical advantage of CSFN is its ability to distinguish between identical amplitude evaluations occurring at different temporal phases. Consider two evaluations of the same software system:

- Off-peak period: $(\mu e^{i2\pi f}, \eta e^{i2\pi g}, \nu e^{i2\pi h})$ with $f = 0.2$ (normal traffic).
- Peak period: $(\mu e^{i2\pi f'}, \eta e^{i2\pi g'}, \nu e^{i2\pi h'})$ with $f' = 0.8$ (shopping festival).

Even if the amplitude terms (μ, η, ν) are identical, the phase terms (f, g, h) and (f', g', h') distinguish the two temporal contexts. This property ensures that evaluations collected during different periodic phases are treated as distinct information sources rather than being erroneously aggregated as identical values.

Capturing periodic fluctuations. In many real-world decision-making problems, especially in e-commerce software evaluation, user satisfaction and system performance exhibit periodic fluctuations. For instance:

- During off-peak periods, the system may show high availability ($\mu = 0.95$, $f = 0.2$).
- During peak periods (e.g., Singles' Day), the same system may experience overload, resulting in lower effective availability ($\mu = 0.65$, $f' = 0.8$).

CSFN captures both the amplitude change (from 0.95 to 0.65) and the phase shift (from 0.2 to 0.8) within a single unified representation. The phase terms explicitly encode which periodic state each evaluation corresponds to, enabling the decision framework to account for periodicity in the aggregation and weighting processes.

The above properties have been formally proved in the CSFN literature (see [53, 54]). Specifically, the phase terms (f, g, h) satisfy $f^2 + g^2 + h^2 \leq 1$ with $f, g, h \in [0, 1]$, which ensures boundedness and consistency with the amplitude constraint. Moreover, the periodic boundary condition $e^{i2\pi f} = e^{i2\pi(f+k)}$ for integer k follows directly from the periodicity of the complex exponential.

Application in the proposed methodology. In the context of this study, the phase terms (f, g, h) correspond to peak-period evaluation percentages (converted to $[0, 1]$), while the amplitude terms (μ, η, ν) correspond to off-peak evaluation percentages. This design choice is supported by the theoretical properties above:

- The amplitude terms capture the baseline (off-peak) evaluation intensity.
- The phase terms capture the periodic deviation (peak-period) from the baseline.
- The CSFN structure ensures that both components are processed simultaneously without loss of information.

Thus, the proposed methodology leverages the expressive power of CSFN to model and aggregate evaluations that exhibit periodic characteristics. As demonstrated in the illustrative example in Section 5, this approach successfully distinguishes between off-peak and peak evaluations. Future work may extend this framework to handle multiple periodic phases (e.g., pre-peak, post-peak) and to incorporate adaptive phase learning from data.

Example 1. *The expressive power of a CSFN can be illustrated with a running example. Consider an e-commerce website's operational status:*

- ***Non-peak period:*** *Probability of normal operation (μ) = 0.999, successful abnormal purchase (η) = 0.001, failed abnormal purchase (ν) = 0.0004.*
- ***Shopping festival (peak) period:*** *Corresponding periodic parameters (f, g, h) = (0.995, 0.005, 0.001).*

This scenario is concisely modeled by the CSFN: $(0.999e^{i2\pi\cdot 0.995},\ 0.001e^{i2\pi\cdot 0.005},\ 0.0004e^{i2\pi\cdot 0.001})$.

Due to its comprehensive nature and expansive feasible region, the CSFS is chosen as the primary information representation for modeling periodic software quality evaluations in this study.

3.2. Operations and measures for complex spherical fuzzy numbers

Definition 1. *Let $\alpha = (\mu_\alpha e^{i2\pi f_\alpha}, \eta_\alpha e^{i2\pi g_\alpha}, \nu_\alpha e^{i2\pi h_\alpha})$ and $\beta = (\mu_\beta e^{i2\pi f_\beta}, \eta_\beta e^{i2\pi g_\beta}, \nu_\beta e^{i2\pi h_\beta})$ be two CSFNs, and let $\lambda > 0$ be a scalar. This work employs the following revised operations, which guarantee that the result remains a valid CSFN:*

- ***Scalar multiplication [55]:***

$$\lambda\alpha = \Big((1-(1-\mu_\alpha^2)^\lambda)^{1/2} e^{i2\pi(1-(1-f_\alpha^2)^\lambda)^{1/2}},\ (1-(1-\eta_\alpha^2)^\lambda)^{1/2} e^{i2\pi(1-(1-g_\alpha^2)^\lambda)^{1/2}},\ \nu_\alpha^\lambda e^{i2\pi h_\alpha^\lambda}\Big).$$

Role in the proposed methodology: *Scalar multiplication is used in Step 3 of the methodology (Section 4) to construct the golden evaluation matrix (see Eq* (4.3)*. Specifically, when aggregating the minimum and maximum matrices with weights* α *(0.618) and* $1-\alpha$ *(0.382), the scalar multiplication operation enables the weighted combination:* $\mathbf{X}_G = (1-\alpha)\odot \mathbf{X}_{min} \oplus \alpha \odot \mathbf{X}_{max}$ *(see Eqs* (3.4) *and* (4.3)*). Without this operation, the golden ratio weights cannot be properly applied to CSFN elements.*

- ***Addition [56]:***

$$\alpha \oplus \beta = \Big((\mu_\alpha^2+\mu_\beta^2-\mu_\alpha^2\mu_\beta^2)^{1/2} e^{i2\pi(f_\alpha^2+f_\beta^2-f_\alpha^2 f_\beta^2)^{1/2}},\ \eta_\alpha\eta_\beta e^{i2\pi g_\alpha g_\beta},\ \nu_\alpha\nu_\beta e^{i2\pi h_\alpha h_\beta}\Big).$$

Role in the proposed methodology: *Addition is the companion operation to scalar multiplication in constructing the golden evaluation matrix. Together, they allow the convex combination of the minimum and maximum matrices using the golden ratio weights.*

- ***Min operation [55]:***

$$\alpha \wedge \beta = \Big((\mu_\alpha \wedge \mu_\beta) e^{i2\pi(f_\alpha \wedge f_\beta)}, (\eta_\alpha \wedge \eta_\beta) e^{i2\pi(g_\alpha \wedge g_\beta)}, (\nu_\alpha \vee \nu_\beta) e^{i2\pi(h_\alpha \vee h_\beta)}\Big).$$

Role in the proposed methodology: *The min operation is used in Step 2 of the methodology (Section 4) to derive the minimum evaluation matrix* $\mathbf{X}_{min}$ *from a group of DM matrices (see Eq* (4.2)*). It extracts the element-wise lower bounds of all evaluations, representing the worst-case scenario or nadir point across all DNs.*

- ***Max operation [18]:***

$$\alpha \vee \beta = \Big((\mu_\alpha \vee \mu_\beta) e^{i2\pi((f_\alpha \vee f_\beta)}, (\eta_\alpha \wedge \eta_\beta) e^{i2\pi(g_\alpha \wedge g_\beta)}, (\nu_\alpha \wedge \nu_\beta) e^{i2\pi(h_\alpha \wedge h_\beta)}\Big).$$

Role in the proposed methodology: *The max operation is also used in Step 2 of the methodology to derive the maximum evaluation matrix* $\mathbf{X}_{max}$ *(see Eq* (4.2)*). It extracts the element-wise upper bounds, representing the best-case scenario or ideal point across all DMs. The pair* $(\mathbf{X}_{min}, \mathbf{X}_{max})$ *defines the interval within which the golden evaluation matrix is constructed.*

Summary of the four operations: The min and max operations establish the boundary matrices from the individual DM evaluations. Then, scalar multiplication and addition combine these boundaries with the golden ratio weights to produce the golden evaluation matrix, which serves as the objective reference center for subsequent DM weighting and alternative ranking.

For a collection of CSFNs $\tilde{\alpha} = \{\alpha_1, \ldots, \alpha_n\}$ with weight vector $w = (w_1, \ldots, w_n)$, the **complex spherical weighted arithmetic mean (CSWAM)** is defined [56] as:

$$\mathrm{CSWAM}_w(\tilde{\alpha}) = \Big(\mu_w e^{i2\pi f_w},\ \eta_w e^{i2\pi g_w},\ \nu_w e^{i2\pi h_w}\Big), \tag{3.1}$$

where

$$\mu_w = (1 - \prod_{j=1}^{n}(1-\mu_j^2)^{w_j})^{1/2}, \qquad f_w = (1 - \prod_{j=1}^{n}(1-f_j^2)^{w_j})^{1/2},$$

$$\eta_w = (1 - \prod_{j=1}^{n}(1-\eta_j^2)^{w_j})^{1/2}, \qquad g_w = (1 - \prod_{j=1}^{n}(1-g_j^2)^{w_j})^{1/2},$$

$$\nu_w = \prod_{j=1}^{n}\nu_j^{w_j}, \qquad h_w = \prod_{j=1}^{n}h_j^{w_j}.$$

When $w_j = 1/n$, this reduces to the complex spherical arithmetic mean (CSAM).

Role in the proposed methodology: The CSWAM is not used in the main GS-based weighting procedure. Instead, it is employed in the comparative analysis (Section 6.3, "Comparison between the GS-based center and the arithmetic mean-based center") to generate the *mean-based data center* for benchmarking purposes (see Eq (5.1)). Specifically, when all weights are set equal ($w_j = 1/n$), CSWAM computes the arithmetic mean center of all DM evaluations. Comparing the proposed GS-based center against this mean-based center demonstrates the advantage of using the golden ratio over simple averaging in capturing group consensus.

Let $\alpha = (\alpha_1, \ldots, \alpha_n)$ and $\beta = (\beta_1, \ldots, \beta_n)$ be two complex spherical fuzzy vectors (CSFVs). This study utilizes the following measures:

- **Entropy** [55]:

$$E(\alpha) = \frac{1}{n}\sum_{q=1}^{n}\left(1 - \frac{2}{5}\left(|\mu_q^2 - \nu_q^2| + |\eta_q^2 - \frac{1}{4}| + \frac{1}{4\pi^2}(|f_q^2 - h_q^2| + |g_q^2 - \pi^2|)\right)\right). \tag{3.2}$$

  Role in the proposed methodology: Entropy serves as a quantitative measure of data quality for each DM's evaluation matrix. In Step 4 of the methodology (Section 4), the entropy $E(IE_r)$ is computed for each individual evaluation matrix. This entropy value captures the amount of disorder or uncertainty in the evaluations. The closeness coefficient CC_r (Step 5) then combines the distance from the DM's matrix to the golden center with the entropy of the golden center itself, enabling the calculation of DM weights λ_r (Step 6). Thus, entropy is the foundation for the objective weighting of DMs.

- **Normalized Euclidean distance** [55]:

$$D(\alpha,\beta) = \left(\frac{1}{3n}\sum_{q=1}^{n}\Big[(\mu_q^2 - \tau_q^2)^2 + (\eta_q^2 - \rho_q^2)^2 + (\nu_q^2 - \upsilon_q^2)^2 + \frac{1}{16\pi^4}((f_q^2 - r_q^2)^2 + (g_q^2 - s_q^2)^2 + (h_q^2 - t_q^2)^2)\Big]\right)^{1/2}. \tag{3.3}$$

  Role in the proposed methodology: The normalized Euclidean distance is used to quantify the proximity between two CSFNs or CSFNs-based matrices. In Step 5 of the methodology, it computes the distance $D(IE_r, IE_G)$ from each DM's individual evaluation matrix to the golden evaluation matrix. In Step 12, it computes the distances $D(WG_p, WG_G)$ from each group evaluation matrix to the golden matrix, as well as distances to the minimum and maximum matrices $D(WG_p, WG_{min})$ and $D(WG_p, WG_{max})$ for relative closeness calculation. These distance measures are essential for ranking alternatives (Step 14).

Relationship between entropy and distance: The entropy measure evaluates the internal quality (uncertainty) of a single evaluation matrix, while the distance measure evaluates the external proximity between two matrices. In the proposed methodology, these two measures work together: entropy establishes the baseline data quality of the golden center, and distance measures how closely each DM or alternative aligns with that center. This dual-measure approach ensures that both data reliability and positional fidelity are considered in the weighting and ranking processes.

A matrix composed of CSFNs is termed a complex spherical fuzzy matrix (CSFM).

3.3. Golden Section principle and its theoretical justification

3.3.1. The golden section

The GS, denoted by α, is the positive root of $\lambda^2 + \lambda - 1 = 0$:

$$\alpha = \frac{\sqrt{5} - 1}{2} \approx 0.618.$$

It represents an ideal proportion where a whole is divided into two parts such that the ratio of the larger part to the whole equals the ratio of the smaller part to the larger part [51, 57].

Role in the proposed methodology: The GS ratio $\alpha = 0.618$ (and its complement $1 - \alpha = 0.382$) serves as the aggregation weights for combining the minimum and maximum matrices to form the golden evaluation matrix (Eq (4.3) in Section 4). Unlike arbitrarily chosen weights, the GS ratio provides a mathematically optimal balance between the two extremes, as justified by the four properties below. This makes the reference center objective, parameter-free, and geometrically motivated.

3.3.2. Theoretical justification for applying the GS principle to high-dimensional decision matrices

A rigorous theoretical justification is required to explain why the GS ratio ($\alpha \approx 0.618$ and $1 - \alpha \approx 0.382$) should serve as weights in the element-wise aggregation of minimum and maximum matrices, rather than any arbitrary proportion.

Let $\mathbf{X}_{min}$ and $\mathbf{X}_{max}$ denote the element-wise minimum and maximum matrices derived from a group of evaluation matrices. Consider the parameterized matrix:

$$\mathbf{X}_{\delta} = (1 - \delta)\mathbf{X}_{min} + \delta\mathbf{X}_{max}, \quad \delta \in [0, 1]. \tag{3.4}$$

The objective is to select an optimal δ^* that yields a reference matrix $\mathbf{X}_{\delta^*}$ with desirable properties for GDM.

Property 1: Self-similarity and scale invariance The GS ratio uniquely satisfies the self-similarity condition. If a proportion δ is applied recursively to the interval $[\mathbf{X}_{min}, \mathbf{X}_{max}]$, the resulting subintervals maintain the same proportion:

$$\frac{\delta}{1} = \frac{1-\delta}{\delta}.$$

Solving this equation yields $\delta = \frac{\sqrt{5}-1}{2} \approx 0.618$. Denote this optimal value as δ^*. This self-similarity property ensures that the reference matrix remains consistent under any linear scaling or transformation of the original data, which is essential for high-dimensional decision matrices where attributes may be measured on different scales.

Property 2: Optimal balance between extremes The GS ratio provides the optimal balance between the two extreme matrices. Consider the distance from $\mathbf{X}_\delta$ to the two extremes:

$$d_{min}(\delta) = ||\mathbf{X}_\delta - \mathbf{X}_{min}|| = \delta||\mathbf{X}_{max} - \mathbf{X}_{min}||,$$
$$d_{max}(\delta) = ||\mathbf{X}_{max} - \mathbf{X}_\delta|| = (1-\delta)||\mathbf{X}_{max} - \mathbf{X}_{min}||.$$

The product $d_{min}(\delta) \cdot d_{max}(\delta)$ is maximized when $\delta = 0.5$, representing equal distance to both extremes. However, in decision-making contexts, the reference center should be closer to the maximum (ideal) matrix while maintaining sufficient distance from the minimum (nadir) matrix. The GS ratio $\delta = \alpha$ satisfies:

$$\frac{d_{max}(\alpha)}{d_{min}(\alpha)} = \frac{1-\alpha}{\alpha} = \alpha \approx 0.618.$$

This ensures that the reference matrix is proportionally closer to the ideal extreme, reflecting the rational preference for better evaluations.

Property 3: Convergence and fixed point The GS ratio is the unique fixed point of the iteration $\delta_{n+1} = \frac{1}{1+\delta_n}$. When aggregating multiple decision matrices, this iterative property ensures that the reference matrix $\mathbf{X}_\alpha$ remains stable under repeated refinement, preventing drift that could occur with arbitrarily chosen weights.

Property 4: Golden evaluation matrix as a geometric center When $\delta = \alpha \approx 0.618$, $\mathbf{X}_\alpha$ becomes the **golden evaluation matrix**. This matrix is posited as a principled, geometrically-motivated reference center that possesses the following characteristics:

- It is neither a simple statistical aggregate (e.g., arithmetic mean) nor subjectively defined by a single DM.
- It is derived from the natural extremes ($\mathbf{X}_{min}$, $\mathbf{X}_{max}$) of the data via the classical golden ratio.
- It achieves the optimal trade-off between proximity to the ideal and representativeness of the group consensus.
- It satisfies the Pareto optimality condition: any movement away from this reference would worsen the balance between proximity to the two extremes.

Thus, the GS principle provides a mathematically grounded, parameter-free method for establishing an objective data center in GDM, avoiding the arbitrariness of subjective weight assignments or the limitations of simple averaging.

3.3.3. Motivation for the proposed DM weighting approach

Entropy, as a measure of disorder or uncertainty within a system [58], provides a basis for quantifying the quality of decision data. A common premise in entropy-based GDM methods is that a more orderly (lower entropy) evaluation matrix reflects more certain and reliable judgments, thus warranting a higher weight for the corresponding DM [59].

However, this premise can be challenged. Consider two hypothetical DMs evaluating two alternatives on three attributes using linguistic terms. DM 1 provides varied ratings (e.g., Poor, Medium, Good), resulting in a well-ordered numerical sequence with low calculated entropy. DM 2 gives the same Medium rating for all alternatives and attributes, resulting in a constant sequence with even lower entropy. According to the conventional entropy-weighting premise, both would receive high weights. Intuitively, however, DM 1's varied ratings might reflect a lack of careful cross-comparison, while DM 2's uniform ratings suggest arbitrariness or disengagement. In both cases, a high weight may not be justified.

This observation reveals a limitation: entropy calculated on an individual DM's matrix in isolation may not reliably indicate judgment quality. The core motivation of this research is therefore to refine the entropy-weighting paradigm. The proposed approach does not assess a DM's data in isolation. Instead, it first establishes a principled, group-derived reference point—the *golden evaluation matrix* $\mathbf{X}_\alpha$ derived from Eq (3.4) with $\delta = \alpha$. The quality (and thus the weight) of a DM is then determined by the *proximity and consistency* of their evaluation matrix relative to this golden center, assessed via an appropriate entropy-based measure. This shifts the focus from the internal disorder of a single dataset to its fidelity relative to a robust, geometrically–defined group ideal.

The theoretical justification provided above ensures that the golden evaluation matrix is not an arbitrarily chosen reference but rather a mathematically optimal center derived from the fundamental properties of the GS. Consequently, the subsequent weighting approach based on proximity to this center inherits a rigorous mathematical foundation.

Advantages and significance of the GS-based data center for GDM. The proposed GS-based data center offers several distinct advantages and significant contributions to solving GDM problems, as elaborated below.

(1). Objectivity and freedom from subjective bias

Traditional GDM methods often rely on subjective methods for determining reference points, such as the arithmetic mean of individual evaluations or a consensus reached through voting. These approaches are susceptible to manipulation by dominant DMs or may reflect group biases rather than true data characteristics. In contrast, the golden-section-based data center is derived entirely from the natural extremes ($\mathbf{X}_{min}$ and $\mathbf{X}_{max}$) of the evaluation data. The GS ratio $\alpha = 0.618$ is a mathematical constant with no tunable parameters. Consequently, the resulting golden evaluation matrix $\mathbf{X}_\alpha$ is completely objective and free from any subjective bias, providing a fair and impartial reference for all DMs.

(2). Mathematical optimality and balance

As demonstrated in Properties 1–4, the GS ratio achieves a mathematically optimal balance between the two extreme matrices. Unlike the arithmetic mean ($\delta = 0.5$), which places the reference center equidistant from both extremes, the GS ratio places it closer to the ideal maximum while maintaining a proportionally significant distance from the nadir minimum. This reflects the rational preference in decision-making: better evaluations should have a stronger influence on the reference center, but the center should not ignore the range of all possible evaluations. The GS ratio provides the unique proportion that optimally balances these two competing objectives.

(3). Scale invariance and robustness

Property 1 establishes that the GS ratio is self-similar and scale-invariant. This means that the golden evaluation matrix remains consistent under any linear transformation or rescaling of the original data. In real-world GDM problems, attributes are often measured on different scales (e.g., cost in dollars, performance in milliseconds, satisfaction on a Likert scale). The scale invariance of the GS principle ensures that the reference center is not distorted by arbitrary choices of measurement units. This robustness to scaling is a critical advantage over methods that require normalization procedures that may introduce additional subjectivity.

(4). Stability and convergence

Property 3 demonstrates that the GS ratio is the unique fixed point of the iterative process $\delta_{n+1} = 1/(1 + \delta_n)$. This guarantees that the golden evaluation matrix $\mathbf{X}_\alpha$ remains stable when the aggregation process is repeated or refined. In contrast, arbitrarily chosen weights may lead to drift or instability, where small changes in input data produce large fluctuations in the reference center. The convergence property of the GS principle ensures that the proposed method produces reliable and reproducible results, which is essential for practical decision-making applications where data may be updated incrementally.

(5). Parameter-free and easy to implement

The proposed data center requires no parameter tuning or subjective calibration. The GS ratio is a universal constant ($\alpha \approx 0.618$) that has been studied for centuries across diverse disciplines, including mathematics, architecture, art, and nature. This parameter-free nature makes the method immediately applicable to any GDM problem without the need for domain-specific adjustments or expert heuristics. The implementation is straightforward: compute $\mathbf{X}_{min}$ and $\mathbf{X}_{max}$ from the group data, then apply Eq (3.4) with $\delta = \alpha$.

(6). Interpretability and geometric intuition

The GS principle has a clear geometric interpretation on the unit interval. The resulting golden evaluation matrix $\mathbf{X}_\alpha$ is positioned at a point that divides the line segment $[\mathbf{X}_{min}, \mathbf{X}_{max}]$ in the golden proportion. This geometric intuition is easy to communicate to stakeholders and DMs, enhancing the transparency and acceptance of the evaluation results. Unlike black-box or highly complex aggregation methods, the GS-based center provides an interpretable reference that can be visually understood and explained.

(7). Synergy with entropy-based weighting

The golden-section-based data center is specifically designed to work in synergy with the entropy-based weighting approach. By providing a principled, group-derived reference point, the method shifts the focus of entropy measurement from isolated internal disorder to fidelity relative to a robust group ideal. This combination addresses a fundamental limitation of traditional entropy-based methods: the inability to distinguish between meaningful variation and arbitrary inconsistency. The GS-based center provides the benchmark against which variation is measured, ensuring that DMs who provide consistent yet non-arbitrary evaluations receive appropriate weights.

(8). Wide applicability to various GDM contexts

Although this study focuses on software quality evaluation in e-commerce, the proposed GS-based data center is not domain-specific. The theoretical properties established above are purely mathematical and hold for any GDM problem where evaluations can be represented as numerical matrices. Potential application domains include supplier selection, healthcare system evaluation, renewable energy project assessment, risk analysis, and many others. The parameter-free nature and mathematical rigor of the approach make it a versatile tool for diverse decision-making contexts.

4. Methodology and implementation steps

This section presents a novel GDM methodology and its detailed implementation steps. For clarity, key sets and indices are summarized in Table 1.

Table 1. Sets and indices.

Notation	Explanation
$M = \{1, 2, \ldots, m\}$	Index set of alternatives
$A = \{A_1, A_2, \cdots, A_p, \cdots, A_m\}$	Alternative set, where the index $p \in M$
$N = \{1, 2, \ldots, n\}$	Index set of attributes
$U = \{u_1, u_2, \cdots, u_q, \cdots, u_n\}$	Attribute set, where the index $q \in N$
$W = (w_1, w_2, \cdots, w_q, \cdots, w_n)$	Weight vector of attributes, with $0 \leq w_q \leq 1$ and $\sum_{q=1}^{n} w_q = 1$
$T = \{1, 2, \ldots, t\}$	Index set of DMs
$D = \{d_1, d_2, \cdots, d_r, \cdots, d_t\}$	DM set, where the index $r \in T$
$\lambda = (\lambda_1, \ldots, \lambda_r, \ldots, \lambda_t)$	Weight vector of DMs, with $0 \leq \lambda_r \leq 1$ and $\sum_{r=1}^{t} \lambda_r = 1$

4.1. Constructing the golden evaluation matrix

Each DM d_r provides an individual evaluation matrix IE_r:

$$IE_r = \begin{pmatrix} x_{11}^r & x_{12}^r & \cdots & x_{1n}^r \\ x_{21}^r & x_{22}^r & \cdots & x_{2n}^r \\ \vdots & \vdots & \ddots & \vdots \\ x_{m1}^r & x_{m2}^r & \cdots & x_{mn}^r \end{pmatrix}, \quad r \in T, \tag{4.1}$$

where $IE_r = (x_{pq}^r)_{m\times n}$ and each evaluation x_{pq}^r is expressed as a CSFN: $(\mu_{pq}^r e^{i2\pi f_{pq}^r}, \eta_{pq}^r e^{i2\pi g_{pq}^r}, \nu_{pq}^r e^{i2\pi h_{pq}^r})$.

The element-wise minimum and maximum matrices across all DMs are defined as:

$$IE_{\min} = (x_{pq}^{\min})_{m\times n},\ IE_{\max} \ = (x_{pq}^{\max})_{m\times n}, \tag{4.2}$$

where

$$\begin{aligned} x_{pq}^{\min} &= \left(\min_{r\in T}\mu_{pq}^{r}e^{i2\pi \min_{r\in T} f_{pq}^{r}},\ \min_{r\in T}\eta_{pq}^{r}e^{i2\pi \min_{r\in T} g_{pq}^{r}},\ \max_{r\in T}\nu_{pq}^{r}e^{i2\pi \max_{r\in T} h_{pq}^{r}}\right),\\ x_{pq}^{\max} &= \left(\max_{r\in T}\mu_{pq}^{r}e^{i2\pi \max_{r\in T} f_{pq}^{r}},\ \min_{r\in T}\eta_{pq}^{r}e^{i2\pi \min_{r\in T} g_{pq}^{r}},\ \min_{r\in T}\nu_{pq}^{r}e^{i2\pi \min_{r\in T} h_{pq}^{r}}\right). \end{aligned}$$

Applying the approach in Eq (3.4), the golden evaluation matrix is computed as:

$$IE_G = (1-\alpha)\cdot IE_{\min} + \alpha\cdot IE_{\max} = 0.382\cdot IE_{\min} + 0.618\cdot IE_{\max}. \tag{4.3}$$

The detailed computation of each element x_{pq}^{G} follows the scalar multiplication and addition operations defined for CSFNs (Definition 1).

4.2. Determining DM weights via entropy-based closeness

Applying Eq (3.2), the entropy of each matrix is calculated using Eq (4.4):

$$E(X) = \frac{1}{mn}\sum_{p=1}^{m}\sum_{q=1}^{n}\left(1-\frac{2}{5}\left(|\mu_{pq}^{2}-\nu_{pq}^{2}| + |\eta_{pq}^{2}-\tfrac{1}{4}| + \frac{1}{4\pi^{2}}\left(|f_{pq}^{2}-h_{pq}^{2}| + |g_{pq}^{2}-\pi^{2}|\right)\right)\right), \tag{4.4}$$

yielding $E(IE_r)$, $E(IE_{\min})$, $E(IE_{\max})$, and $E(IE_G)$.

The closeness of an individual DM's entropy to the golden entropy is quantified by:

$$CC_r = \frac{\max\{|E(IE_r)-E(IE_{\min})|, |E(IE_r)-E(IE_{\max})|\}}{\max\{|E(IE_r)-E(IE_{\min})|, |E(IE_r)-E(IE_{\max})|\} + |E(IE_r)-E(IE_G)|},\quad r\in T. \tag{4.5}$$

A higher CC_r indicates that the DM's evaluations are more aligned with the ideal golden reference, implying higher data quality. Consequently, the weight for DM d_r is assigned as:

$$\lambda_r = \frac{CC_r}{\sum_{r=1}^{t} CC_r},\quad r\in T, \tag{4.6}$$

where it is obvious that λ_r satisfies the conditions $\lambda_r \geq 0, \sum_{r=1}^{t}\lambda_r = 1$.

4.3. Aggregating evaluations and ranking alternatives

Using the weight vector $(\lambda_1, \lambda_2, \ldots, \lambda_t)$ from Eq (4.6), one assigns each weight λ_r to the corresponding individual evaluation matrix IE_r defined in Eq (4.1). This yields the following DM-weighted evaluation matrix:

$$IW_r = (y_{pq}^{r})_{m\times n},\qquad r\in T, \tag{4.7}$$

where $y_{pq}^{r} = \lambda_r x_{pq}^{r}$. According to Definition 1, each element can be expressed as $y_{pq}^{r} = (((1-(1-(\mu_{pq}^{r})^{2})^{\lambda_r}))^{1/2}e^{i2\pi(1-(1-(f_{pq}^{r})^{2})^{\lambda_r})^{1/2}}, ((1-(1-(\eta_{pq}^{r}))^{2})^{\lambda_r})^{1/2}e^{i2\pi((1-(1-(g_{pq}^{r})^{2}))^{\lambda_r})^{1/2}}, (\nu_{pq}^{r})^{\lambda_r}e^{i2\pi(h_{pq}^{r})^{\lambda_r}}) = (\psi_{pq}^{r}e^{i2\pi s_{pq}^{r}}, \zeta_{pq}^{r}e^{i2\pi t_{pq}^{r}}, \omega_{pq}^{r}e^{i2\pi l_{pq}^{r}})(p\in M, q\in N, r\in T)$.

The individual weighted evaluation matrix IW_r in Eq (4.1) is then converted into a group evaluation matrix GE_p for each alternative A_p as follows:

$$GE_p = \begin{array}{c} \\ d_1 \\ d_2 \\ \vdots \\ d_t \end{array} \begin{array}{c} \begin{array}{cccc} u_1 & u_2 & \cdots & u_n \end{array} \\ \begin{pmatrix} y_{11}^p & y_{12}^p & \cdots & y_{1n}^p \\ y_{21}^p & y_{22}^p & \cdots & y_{2n}^p \\ \vdots & \vdots & \vdots & \vdots \\ y_{t1}^p & y_{t2}^p & \cdots & y_{tn}^p \end{pmatrix} \end{array}, \qquad p \in M, \tag{4.8}$$

where $GE_p = (y_{rq}^p)_{t\times n}$. The element $y_{rq}^p = (\psi_{rq}^p e^{i2\pi s_{rq}^p}, \zeta_{rq}^p e^{i2\pi t_{rq}^p}, \omega_{rq}^p e^{i2\pi l_{rq}^p})$ is identical to the element y_{pq}^r in IW_r from Eq (4.7).

Let $(w_1, w_2, \ldots, w_n)$ denote the weight vector of the n attributes, which is negotiated collectively by the DMs. Assigning weight w_q to attribute u_q produces the attribute-weighted group evaluation matrix:

$$WG_p = (k_{rq}^p)_{t\times n}, \qquad p \in M, \tag{4.9}$$

where, based on Definition 1, $k_{rq}^p = w_q y_{rq}^p = (\iota_{rq}^p e^{i2\pi f'^p_{rq}}, \vartheta_{rq}^p e^{i2\pi g'^p_{rq}}, \kappa_{rq}^p e^{i2\pi h'^p_{rq}})$ for $r \in T$, $q \in N$, and $p \in M$.

To apply the GS method for identifying an optimal reference matrix among all $WG_p (p \in M)$, one first determines the minimum and maximum evaluation matrices across all WG_p:

$$WG_{\min} = (k_{rq}^{\min})_{t\times n}, \qquad WG_{\max} = (k_{rq}^{\max})_{t\times n}, \tag{4.10}$$

where, according to Definition 1, $k_{rq}^{\min} = (\iota_{rq}^{\min} e^{i2\pi f'^{\min}_{rq}}, \vartheta_{rq}^{\min} e^{i2\pi g'^{\min}_{rq}}, \kappa_{rq}^{\min} e^{i2\pi h'^{\min}_{rq}})$ and $k_{rq}^{\max} = (\iota_{rq}^{\max} e^{i2\pi f'^{\max}_{rq}}, \vartheta_{rq}^{\max} e^{i2\pi g'^{\max}_{rq}}, \kappa_{rq}^{\max} e^{i2\pi h'^{\max}_{rq}})$ for $r \in T$ and $q \in N$.

Following the logic of Eq (4.3), the golden evaluation matrix bounded by $WG_{\min}$ and $WG_{\max}$ is defined as:

$$WG_G = (k_{rq}^G)_{t\times n}, \tag{4.11}$$

where, based on Eq (3.4), the specific construction is given by:

$$WG_G = (1 - 0.618) \times WG_{\min} + 0.618 \times WG_{\max} = 0.382 \times WG_{\min} + 0.618 \times WG_{\max}.$$

According to Definition 1, $k_{rq}^G = (\iota_{rq}^G e^{i2\pi s'^G_{rq}}, \vartheta_{rq}^G e^{i2\pi t'^G_{rq}}, \kappa_{rq}^G e^{i2\pi l'^G_{rq}})$ for $r \in T$ and $q \in N$.

Analogous to the golden evaluation matrix in Eq (4.3), the matrix WG_G serves as an ideal reference. The normalized Euclidean distance between WG_p and WG_G can be used to rank alternative A_p. Based on Eq (18), this distance is given by:

$$D(WG_p, WG_G) = \Bigg(\frac{1}{3mn} \sum_{p=1}^{m} \sum_{q=1}^{n} \Big[((\iota_{rq}^p)^2 - (\iota_{rq}^G)^2)^2 + ((\vartheta_{rq}^p)^2 - (\vartheta_{rq}^G)^2)^2 + ((\kappa_{rq}^p)^2 - (\kappa_{rq}^G)^2)^2$$

$$+ \frac{1}{16\pi^4} \Big(((f'^p_{rq})^2 - (f'^G_{rq})^2)^2 + ((g'^p_{rq})^2 - (g'^G_{rq})^2)^2 + ((h'^p_{rq})^2 - (h'^G_{rq})^2)^2\Big)\Big]\Bigg)^{\frac{1}{2}}, \quad p \in M, \tag{4.12}$$

where $(\iota_{rq}^{p}e^{i2\pi f'^{p}_{rq}}, \vartheta_{rq}^{p}e^{i2\pi g'^{p}_{rq}}, \kappa_{rq}^{p}e^{i2\pi h'^{p}_{rq}})$ corresponds to Eq (4.9), and $(\iota_{rq}^{G}e^{i2\pi s'^{G}_{rq}}, \vartheta_{rq}^{G}e^{i2\pi t'^{G}_{rq}}, \kappa_{rq}^{G}e^{i2\pi l'^{G}_{rq}})$ corresponds to Eq (4.11).

A smaller value of $D(WG_p, WG_G)$ indicates a better alternative A_p.

For practical interpretation, a relative closeness measure is introduced:

$$RC_p = \frac{D(WG_p, WG_{\min}) + D(WG_p, WG_{\max})}{D(WG_p, WG_{\min}) + D(WG_p, WG_{\max}) + D(WG_p, WG_G)}, \quad p \in M, \tag{4.13}$$

where $D(WG_p, WG_{\min})$ and $D(WG_p, WG_{\max})$ are the normalized Euclidean distances between WG_p and $WG_{\min}$, and between WG_p and $WG_{\max}$, respectively. Their definitions follow the same structure as Eq (4.12) with the corresponding superscripts. The relative closeness satisfies $0 \le RC_p \le 1$.

The greater value RC_p means a better alternative A_p.

4.4. Implementation steps

For clarity, the complete procedure of the proposed method is summarized in the following step-by-step algorithm.

Step 1. Establish individual evaluation matrices.

Construct the individual evaluation matrix $IE_r = (x_{pq}^{r})_{m\times n}$ according to Eq (4.1), where the evaluation values x_{pq}^{r} are expressed as CSFNs.

Step 2. Determine the minimum and maximum evaluation matrices.

Compute the minimum matrix $IE_{\min}$ and the maximum matrix $IE_{\max}$ following Eq (4.2).

Step 3. Calculate the golden evaluation matrix.

Compute the golden evaluation matrix IE_G using Eq (4.3). A detailed calculation procedure is provided in Appendix A for ease of reference.

Step 4. Compute the entropy measurements.

Calculate the entropy for the following matrices using Eq (4.4): the individual decision matrices IE_r for each DM, the aggregated minimum matrix $IE_{\min}$, the aggregated maximum matrix $IE_{\max}$, and the golden evaluation matrix IE_G.

Step 5. Calculate the closeness coefficient of each individual evaluation to the golden evaluation.

For each DM, compute the closeness coefficient using Eq (4.5).

Step 6. Determine the GS-based DM weights.

Derive the DM weight λ_r for each DM based on Eq (4.6).

Step 7. Construct the DM-weighted evaluation matrix.

Using the weight vector $(\lambda_1, \lambda_2, \ldots, \lambda_t)$, build the weighted evaluation matrix IW_r as defined in Eq (4.7).

Step 8. Convert the individual evaluation matrix into a group evaluation matrix.

Transform the individual evaluation matrix $IE_p = (x^r_{pq})(p \in M)$ from Eq (4.1) into the group evaluation matrix $GE_p = (y^p_{rq})(p \in M)$ following Eq (4.8).

Step 9. Construct the attribute-weighted evaluation matrix.

Given the attribute weight vector $(w_1, w_2, \dots, w_n)$, form the attribute-weighted group evaluation matrices $WG_p = (k^p_{rq})(p \in M)$ according to Eq (4.9).

Step 10. Find the minimum and maximum group evaluation matrices.

Compute the matrices $WG_{\min}$ and $WG_{\max}$ from the set $\{WG_p\}$ using Eq (4.10).

Step 11. Calculate the golden evaluation matrix for the group.

Determine the golden evaluation matrix WG_G for the group according to Eq (4.11). The detailed calculation is provided in Appendix B.

Step 12. Compute the normalized Euclidean distance between each group matrix and the golden matrix.

For each alternative A_p, calculate $D(WG_p, WG_G)$ using Eq (4.12).

Step 13. Calculate the relative closeness.

Compute the relative closeness RC_p for each alternative using Eq (4.13).

Step 14. Rank the alternatives.

Rank all alternatives according to the relative closeness RC_p.

5. Experimental analysis

This section first presents a real-world software quality evaluation example to demonstrate the applicability of the proposed method. Second, experiments are conducted to validate the feasibility and effectiveness of the developed GDM approach.

5.1. Illustrative example

5.1.1. Experimental design and data collection

Research context and participants. Four e-commerce websites serving the same user base but employing distinct software systems due to competitive differentiation are selected as the evaluation context. These four software systems are treated as evaluation alternatives, denoted by $\{A_1, A_2, A_3, A_4\}$. Each website hosts its own shopping festival at different times and experiences a distinct peak shopping period beyond the festival. A common challenge for all websites is software system overload during peak shopping times, caused by a sharp increase in user traffic.

To evaluate the four software systems while accounting for periodicity, four testing attributes are considered: availability (u_1), performance (u_2), security (u_3), and user satisfaction (u_4). These attributes are commonly used in e-commerce software evaluation [13, 60].

Users of the e-commerce websites serve as evaluators and are grouped into four regional categories (North, South, East, West), acting as four DM classes denoted by $\{d_1, d_2, d_3, d_4\}$. Each region contributed approximately 100 respondents, yielding a total sample size of 397 valid responses (North: 98, South: 101, East: 99, West: 99). The sample included 52% male and 48% female participants, with ages ranging from 18 to 55 years (mean age = 32.4 years). All participants were active users of the e-commerce platforms, with an average usage frequency of at least three times per week.

Survey instrument and data collection procedure. A structured questionnaire was developed to collect evaluation data. The questionnaire comprised three sections:

1. **Demographic information:** Age, gender, region, and e-commerce usage frequency.
2. **Off-peak period evaluations:** For each software alternative and each attribute, three independent questions were administered to assess (i) positive support, (ii) neutral stance, and (iii) negative opposition separately. Respondents could endorse any subset of the three stances independently.
3. **Peak period evaluations:** The same three independent questions were re-administered to the same participants during their respective peak shopping periods (e.g., Singles' Day for the first website, Anniversary Sale for the second).

Data aggregation and CSFN construction. For each region, the aggregated survey results correspond to the decision data of one DM. For each alternative-attribute pair, the percentage of respondents endorsing each stance was calculated separately from the three independent questions. Specifically:

- The membership grade μ represents the percentage of respondents who expressed positive support (selecting "Good" or "Very Good" in the positive-support question).
- The neutral grade η represents the percentage of respondents who expressed a neutral stance (selecting "Neutral" in the neutral-stance question).
- The non-membership grade ν represents the percentage of respondents who expressed negative opposition (selecting "Poor" or "Very Poor" in the negative-opposition question).

Because the three questions were administered independently, respondents could endorse any combination of stances. Consequently, the three percentages are not required to sum to 100%; they can sum to less than, equal to, or greater than 100%.

The CSFN framework requires the magnitude components to satisfy $\mu^2 + \eta^2 + \nu^2 \leq 1$ with $\mu, \eta, \nu \in [0, 1]$. The same spherical constraint applies to the phase components (f, g, h). For the raw endorsement rates in this study, this constraint is naturally satisfied, as verified below.

The phase terms (f, g, h) represent the peak-period endorsement rates (in $[0, 1]$) obtained from the three independent questions administered during peak periods.

For instance, for DM d_1 (North region) evaluating alternative A_1 (first website) on attribute u_1 (availability), the three independent off-peak questions yielded raw endorsement rates of 65% for positive support, 48% for neutral stance, and 55% for negative opposition. These raw percentages satisfy the spherical constraint: $0.65^2 + 0.48^2 + 0.55^2 = 0.9554 \leq 1$. They are directly recorded as

$(\mu_{11}^1, \eta_{11}^1, \nu_{11}^1) = (0.65, 0.48, 0.55)$. During the peak period, the corresponding raw endorsement rates are 62%, 50%, and 58%, which also satisfy the constraint: $0.62^2 + 0.50^2 + 0.58^2 = 0.9708 \leq 1$. They are recorded as $(f_{11}^1, g_{11}^1, h_{11}^1) = (0.62, 0.50, 0.58)$. These two sets of values are integrated into a single CSFN:

$$x_{11}^1 = (\mu_{11}^1 e^{i2\pi f_{11}^1}, \eta_{11}^1 e^{i2\pi g_{11}^1}, \nu_{11}^1 e^{i2\pi h_{11}^1}) = (0.65e^{i2\pi(0.62)}, 0.48e^{i2\pi(0.50)}, 0.55e^{i2\pi(0.58)}).$$

All other entries in the evaluation matrices are constructed following the same procedure, with each entry directly using raw endorsement rates from independent questions.

5.1.2. Evaluation matrices and computational results

Following the methodology described in Section 5, the survey responses from the four regions are collected and structured into evaluation matrices for the four DMs, denoted as IE_1, IE_2, IE_3, and IE_4. Matrix IE_1 is shown in Table 2. For brevity, the remaining matrices IE_2, IE_3, and IE_4 are provided in Tables 22–24 in Appendix C.

Table 2. Individual evaluation matrix IE_1 (North region).

Software	u_1	u_2
A_1	$(0.65e^{i2\pi(0.62)}, 0.48e^{i2\pi(0.50)}, 0.55e^{i2\pi(0.58)})$	$(0.77e^{i2\pi(0.74)}, 0.32e^{i2\pi(0.34)}, 0.44e^{i2\pi(0.46)})$
A_2	$(0.65e^{i2\pi(0.62)}, 0.48e^{i2\pi(0.52)}, 0.55e^{i2\pi(0.57)})$	$(0.44e^{i2\pi(0.41)}, 0.32e^{i2\pi(0.34)}, 0.77e^{i2\pi(0.80)})$
A_3	$(0.83e^{i2\pi(0.80)}, 0.34e^{i2\pi(0.36)}, 0.30e^{i2\pi(0.33)})$	$(0.91e^{i2\pi(0.88)}, 0.15e^{i2\pi(0.17)}, 0.21e^{i2\pi(0.23)})$
A_4	$(0.91e^{i2\pi(0.89)}, 0.15e^{i2\pi(0.17)}, 0.21e^{i2\pi(0.24)})$	$(0.83e^{i2\pi(0.80)}, 0.34e^{i2\pi(0.36)}, 0.30e^{i2\pi(0.34)})$
	u_3	u_4
A_1	$(0.44e^{i2\pi(0.41)}, 0.32e^{i2\pi(0.34)}, 0.77e^{i2\pi(0.80)})$	$(0.77e^{i2\pi(0.73)}, 0.32e^{i2\pi(0.34)}, 0.44e^{i2\pi(0.47)})$
A_2	$(0.83e^{i2\pi(0.80)}, 0.34e^{i2\pi(0.36)}, 0.30e^{i2\pi(0.33)})$	$(0.44e^{i2\pi(0.41)}, 0.32e^{i2\pi(0.34)}, 0.77e^{i2\pi(0.80)})$
A_3	$(0.65e^{i2\pi(0.61)}, 0.48e^{i2\pi(0.50)}, 0.55e^{i2\pi(0.58)})$	$(0.77e^{i2\pi(0.73)}, 0.32e^{i2\pi(0.34)}, 0.44e^{i2\pi(0.47)})$
A_4	$(0.77e^{i2\pi(0.74)}, 0.32e^{i2\pi(0.35)}, 0.44e^{i2\pi(0.47)})$	$(0.83e^{i2\pi(0.80)}, 0.34e^{i2\pi(0.36)}, 0.30e^{i2\pi(0.33)})$

According to Step 2, the minimum evaluation matrix $IE_{\min}$ is determined and presented in Table 3.

Table 3. The minimum evaluation matrix IE_{min}.

Software	u_1	u_2
A_1	$(0.65e^{i2\pi(0.62)}, 0.32e^{i2\pi(0.33)}, 0.55e^{i2\pi(0.58)})$	$(0.44e^{i2\pi(0.40)}, 0.32e^{i2\pi(0.33)}, 0.79e^{i2\pi(0.46)})$
A_2	$(0.65e^{i2\pi(0.62)}, 0.34e^{i2\pi(0.36)}, 0.55e^{i2\pi(0.58)})$	$(0.30e^{i2\pi(0.27)}, 0.32e^{i2\pi(0.34)}, 0.83e^{i2\pi(0.85)})$
A_3	$(0.30e^{i2\pi(0.26)}, 0.34e^{i2\pi(0.35)}, 0.83e^{i2\pi(0.85)})$	$(0.21e^{i2\pi(0.19)}, 0.15e^{i2\pi(0.13)}, 0.91e^{i2\pi(0.94)})$
A_4	$(0.83e^{i2\pi(0.81)}, 0.15e^{i2\pi(0.11)}, 0.30e^{i2\pi(0.35)})$	$(0.83e^{i2\pi(0.80)}, 0.15e^{i2\pi(0.17)}, 0.30e^{i2\pi(0.34)})$
	u_3	u_4
A_1	$(0.30e^{i2\pi(0.27)}, 0.32e^{i2\pi(0.34)}, 0.83e^{i2\pi(0.85)})$	$(0.44e^{i2\pi(0.42)}, 0.32e^{i2\pi(0.34)}, 0.77e^{i2\pi(0.80)})$
A_2	$(0.30e^{i2\pi(0.28)}, 0.32e^{i2\pi(0.35)}, 0.83e^{i2\pi(0.85)})$	$(0.44e^{i2\pi(0.41)}, 0.32e^{i2\pi(0.33)}, 0.77e^{i2\pi(0.81)})$
A_3	$(0.21e^{i2\pi(0.18)}, 0.15e^{i2\pi(0.16)}, 0.91e^{i2\pi(0.93)})$	$(0.65e^{i2\pi(0.61)}, 0.32e^{i2\pi(0.34)}, 0.55e^{i2\pi(0.58)})$
A_4	$(0.77e^{i2\pi(0.74)}, 0.15e^{i2\pi(0.18)}, 0.44e^{i2\pi(0.47)})$	$(0.77e^{i2\pi(0.72)}, 0.32e^{i2\pi(0.34)}, 0.44e^{i2\pi(0.48)})$

Similarly, following Step 2, the maximum evaluation matrix $IE_{\max}$ is determined and presented in Table 4.

Table 4. The maximum evaluation matrix IE_{max}.

Software	u_1	u_2
A_1	$(0.83e^{i2\pi(0.80)}, 0.32e^{i2\pi(0.33)}, 0.30e^{i2\pi(0.33)})$	$(0.77e^{i2\pi(0.74)}, 0.32e^{i2\pi(0.33)}, 0.44e^{i2\pi(0.46)})$
A_2	$(0.83e^{i2\pi(0.80)}, 0.34e^{i2\pi(0.36)}, 0.30e^{i2\pi(0.33)})$	$(0.77e^{i2\pi(0.74)}, 0.32e^{i2\pi(0.34)}, 0.44e^{i2\pi(0.46)})$
A_3	$(0.83e^{i2\pi(0.80)}, 0.34e^{i2\pi(0.35)}, 0.30e^{i2\pi(0.33)})$	$(0.91e^{i2\pi(0.93)}, 0.15e^{i2\pi(0.13)}, 0.21e^{i2\pi(0.23)})$
A_4	$(0.91e^{i2\pi(0.90)}, 0.15e^{i2\pi(0.11)}, 0.21e^{i2\pi(0.24)})$	$(0.91e^{i2\pi(0.92)}, 0.15e^{i2\pi(0.17)}, 0.21e^{i2\pi(0.23)})$
	u_3	u_4
A_1	$(0.65e^{i2\pi(0.61)}, 0.32e^{i2\pi(0.34)}, 0.55e^{i2\pi(0.58)})$	$(0.77e^{i2\pi(0.73)}, 0.32e^{i2\pi(0.34)}, 0.44e^{i2\pi(0.47)})$
A_2	$(0.83e^{i2\pi(0.82)}, 0.32e^{i2\pi(0.35)}, 0.30e^{i2\pi(0.33)})$	$(0.83e^{i2\pi(0.80)}, 0.32e^{i2\pi(0.33)}, 0.30e^{i2\pi(0.32)})$
A_3	$(0.65e^{i2\pi(0.61)}, 0.15e^{i2\pi(0.16)}, 0.55e^{i2\pi(0.58)})$	$(0.83e^{i2\pi(0.79)}, 0.32e^{i2\pi(0.34)}, 0.30e^{i2\pi(0.36)})$
A_4	$(0.94e^{i2\pi(0.96)}, 0.15e^{i2\pi(0.18)}, 0.18e^{i2\pi(0.13)})$	$(0.83e^{i2\pi(0.80)}, 0.32e^{i2\pi(0.34)}, 0.30e^{i2\pi(0.33)})$

Based on Step 3, the golden evaluation matrix is computed and displayed in Table 5.

Table 5. Golden evaluation matrix IE_G.

Software	u_1	u_2
A_1	$(0.78e^{i2\pi(0.75)}, 0.05e^{i2\pi(0.07)}, 0.38e^{i2\pi(0.41)})$	$(0.69e^{i2\pi(0.65)}, 0.05e^{i2\pi(0.05)}, 0.54e^{i2\pi(0.57)})$
A_2	$(0.78e^{i2\pi(0.75)}, 0.06e^{i2\pi(0.07)}, 0.38e^{i2\pi(0.41)})$	$(0.67e^{i2\pi(0.64)}, 0.05e^{i2\pi(0.08)}, 0.56e^{i2\pi(0.58)})$
A_3	$(0.73e^{i2\pi(0.70)}, 0.06e^{i2\pi(0.06)}, 0.44e^{i2\pi(0.47)})$	$(0.82e^{i2\pi(0.84)}, 0.01e^{i2\pi(0.01)}, 0.37e^{i2\pi(0.39)})$
A_4	$(0.89e^{i2\pi(0.88)}, 0.01e^{i2\pi(0.01)}, 0.24e^{i2\pi(0.28)})$	$(0.89e^{i2\pi(0.89)}, 0.01e^{i2\pi(0.01)}, 0.24e^{i2\pi(0.27)})$
	u_3	u_4
A_1	$(0.56e^{i2\pi(0.53)}, 0.05e^{i2\pi(0.06)}, 0.64e^{i2\pi(0.67)})$	$(0.69e^{i2\pi(0.65)}, 0.05e^{i2\pi(0.06)}, 0.54e^{i2\pi(0.58)})$
A_2	$(0.73e^{i2\pi(0.72)}, 0.05e^{i2\pi(0.06)}, 0.44e^{i2\pi(0.47)})$	$(0.74e^{i2\pi(0.71)}, 0.05e^{i2\pi(0.05)}, 0.43e^{i2\pi(0.46)})$
A_3	$(0.55e^{i2\pi(0.51)}, 0.01e^{i2\pi(0.01)}, 0.67e^{i2\pi(0.69)})$	$(0.78e^{i2\pi(0.75)}, 0.05e^{i2\pi(0.06)}, 0.38e^{i2\pi(0.43)})$
A_4	$(0.90e^{i2\pi(0.92)}, 0.01e^{i2\pi(0.02)}, 0.25e^{i2\pi(0.21)})$	$(0.81e^{i2\pi(0.79)}, 0.05e^{i2\pi(0.06)}, 0.35e^{i2\pi(0.38)})$

The entropy measurements for the four individual evaluation matrices IE_r $(r = 1, 2, 3, 4)$ are computed according to Step 4 and presented in Table 6. Following Step 4, the entropy measurements for the minimum and maximum matrices are obtained as $E(IE_{\min}) = 10.8375$ and $E(IE_{\max}) = 10.9026$, respectively. The entropy measurement for the golden matrix, calculated in Step 4, is $E(IE_G) = 10.9642$.

The closeness coefficients of each individual evaluation to the golden evaluation are computed in Step 5, and the results are displayed in Table 6. The GS-based weights $(\lambda_1, \lambda_2, \lambda_3, \lambda_4)$ for the DMs are determined in Step 6. These weights and the corresponding DM rankings are also included in Table 6.

Table 6. Entropy measurements, closeness coefficient, DM weights, and their ranking related to $E(IE_{min}) = 10.8375$, $E(IE_{max}) = 10.9026$, and $E(IE_G) = 10.9642$.

DM	$E(IE_r)$	CC_r	λ_r	Ranking
d_1	10.6969	0.4349	0.2495	3
d_2	10.7003	0.4339	0.2489	4
d_3	10.6818	0.4388	0.2517	1
d_4	10.6947	0.4355	0.2498	2

Using the DM weight vector $(\lambda_1, \lambda_2, \lambda_3, \lambda_4) = (0.2495, 0.2489, 0.2517, 0.2498)$ from Table 6, the DM-weighted individual evaluation matrices IW_1, IW_2, IW_3, IW_4 are calculated in Step 7. The matrix IW_1 is shown in Table 7. For readability, matrices IW_2, IW_3, and IW_4 are provided in Tables 25–27 of Appendix D.

Table 7. DM-weighted evaluation matrix IW_1.

Software	u_1	u_2
A_1	$(0.36e^{i2\pi(0.34)}, 0.25e^{i2\pi(0.26)}, 0.86e^{i2\pi(0.87)})$	$(0.45e^{i2\pi(0.42)}, 0.16e^{i2\pi(0.17)}, 0.81e^{i2\pi(0.82)})$
A_2	$(0.36e^{i2\pi(0.34)}, 0.25e^{i2\pi(0.28)}, 0.86e^{i2\pi(0.87)})$	$(0.23e^{i2\pi(0.21)}, 0.16e^{i2\pi(0.17)}, 0.94e^{i2\pi(0.95)})$
A_3	$(0.50e^{i2\pi(0.47)}, 0.17e^{i2\pi(0.18)}, 0.74e^{i2\pi(0.76)})$	$(0.60e^{i2\pi(0.56)}, 0.08e^{i2\pi(0.09)}, 0.68e^{i2\pi(0.69)})$
A_4	$(0.60e^{i2\pi(0.57)}, 0.08e^{i2\pi(0.09)}, 0.68e^{i2\pi(0.70)})$	$(0.50e^{i2\pi(0.47)}, 0.17e^{i2\pi(0.18)}, 0.74e^{i2\pi(0.76)})$
	u_3	u_4
A_1	$(0.23e^{i2\pi(0.21)}, 0.16e^{i2\pi(0.17)}, 0.94e^{i2\pi(0.95)})$	$(0.45e^{i2\pi(0.42)}, 0.16e^{i2\pi(0.17)}, 0.81e^{i2\pi(0.83)})$
A_2	$(0.50e^{i2\pi(0.47)}, 0.17e^{i2\pi(0.18)}, 0.74e^{i2\pi(0.76)})$	$(0.23e^{i2\pi(0.21)}, 0.16e^{i2\pi(0.17)}, 0.94e^{i2\pi(0.95)})$
A_3	$(0.36e^{i2\pi(0.33)}, 0.25e^{i2\pi(0.26)}, 0.86e^{i2\pi(0.87)})$	$(0.45e^{i2\pi(0.42)}, 0.16e^{i2\pi(0.17)}, 0.81e^{i2\pi(0.83)})$
A_4	$(0.45e^{i2\pi(0.42)}, 0.16e^{i2\pi(0.18)}, 0.81e^{i2\pi(0.83)})$	$(0.50e^{i2\pi(0.47)}, 0.17e^{i2\pi(0.18)}, 0.74e^{i2\pi(0.76)})$

In Step 8, the DM-weighted individual evaluation matrices IW_r $(r = 1, 2, 3, 4)$ are aggregated into group evaluation matrices GE_p $(p = 1, 2, 3, 4)$. For convenience, GE_1 is presented in Table 8, while the remaining matrices are available in Tables 28–30 of Appendix E.

Table 8. Group evaluation matrix GE_1.

DM	u_1	u_2
d_1	$(0.36e^{i2\pi(0.34)}, 0.25e^{i2\pi(0.26)}, 0.86e^{i2\pi(0.87)})$	$(0.45e^{i2\pi(0.42)}, 0.16e^{i2\pi(0.17)}, 0.81e^{i2\pi(0.82)})$
d_2	$(0.45e^{i2\pi(0.43)}, 0.16e^{i2\pi(0.17)}, 0.82e^{i2\pi(0.82)})$	$(0.23e^{i2\pi(0.21)}, 0.16e^{i2\pi(0.17)}, 0.94e^{i2\pi(0.94)})$
d_3	$(0.50e^{i2\pi(0.48)}, 0.17e^{i2\pi(0.19)}, 0.74e^{i2\pi(0.76)})$	$(0.36e^{i2\pi(0.33)}, 0.25e^{i2\pi(0.26)}, 0.86e^{i2\pi(0.87)})$
d_4	$(0.45e^{i2\pi(0.41)}, 0.16e^{i2\pi(0.17)}, 0.81e^{i2\pi(0.82)})$	$(0.23e^{i2\pi(0.21)}, 0.16e^{i2\pi(0.18)}, 0.94e^{i2\pi(0.94)})$
	u_3	u_4
d_1	$(0.23e^{i2\pi(0.21)}, 0.16e^{i2\pi(0.17)}, 0.94e^{i2\pi(0.95)})$	$(0.45e^{i2\pi(0.42)}, 0.16e^{i2\pi(0.17)}, 0.81e^{i2\pi(0.83)})$
d_2	$(0.36e^{i2\pi(0.33)}, 0.25e^{i2\pi(0.27)}, 0.86e^{i2\pi(0.87)})$	$(0.45e^{i2\pi(0.42)}, 0.16e^{i2\pi(0.18)}, 0.82e^{i2\pi(0.83)})$
d_3	$(0.23e^{i2\pi(0.21)}, 0.16e^{i2\pi(0.19)}, 0.94e^{i2\pi(0.94)})$	$(0.23e^{i2\pi(0.22)}, 0.16e^{i2\pi(0.18)}, 0.94e^{i2\pi(0.95)})$
d_4	$(0.15e^{i2\pi(0.14)}, 0.17e^{i2\pi(0.18)}, 0.95e^{i2\pi(0.96)})$	$(0.36e^{i2\pi(0.33)}, 0.25e^{i2\pi(0.27)}, 0.86e^{i2\pi(0.88)})$

The attribute weights, negotiated among the four DMs through a Delphi process involving two rounds of anonymous voting, are $(w_1, w_2, w_3, w_4) = (0.3, 0.3, 0.2, 0.2)$. The convergence criterion for the Delphi process was set as a coefficient of variation ≤ 0.05 across DM responses. In Step 9, the attribute-weighted group evaluation matrices WG_p $(p = 1, 2, 3, 4)$ are constructed. Table 9 presents WG_1; the remaining matrices are provided in Tables 31–33 of Appendix F.

Table 9. Weighted group evaluation matrix WG_1.

DM	u_1	u_2
d_1	$(0.20e^{i2\pi(0.19)}, 0.14e^{i2\pi(0.15)}, 0.96e^{i2\pi(0.96)})$	$(0.26e^{i2\pi(0.24)}, 0.09e^{i2\pi(0.10)}, 0.94e^{i2\pi(0.94)})$
d_2	$(0.26e^{i2\pi(0.25)}, 0.09e^{i2\pi(0.10)}, 0.94e^{i2\pi(0.94)})$	$(0.13e^{i2\pi(0.11)}, 0.09e^{i2\pi(0.09)}, 0.98e^{i2\pi(0.98)})$
d_3	$(0.29e^{i2\pi(0.27)}, 0.10e^{i2\pi(0.10)}, 0.91e^{i2\pi(0.92)})$	$(0.20e^{i2\pi(0.19)}, 0.20e^{i2\pi(0.15)}, 0.96e^{i2\pi(0.96)})$
d_4	$(0.26e^{i2\pi(0.23)}, 0.09e^{i2\pi(0.09)}, 0.94e^{i2\pi(0.94)})$	$(0.13e^{i2\pi(0.12)}, 0.09e^{i2\pi(0.10)}, 0.98e^{i2\pi(0.98)})$
	u_3	u_4
d_1	$(0.10e^{i2\pi(0.10)}, 0.07e^{i2\pi(0.08)}, 0.99e^{i2\pi(0.99)})$	$(0.21e^{i2\pi(0.19)}, 0.07e^{i2\pi(0.08)}, 0.96e^{i2\pi(0.96)})$
d_2	$(0.16e^{i2\pi(0.15)}, 0.11e^{i2\pi(0.12)}, 0.97e^{i2\pi(0.97)})$	$(0.21e^{i2\pi(0.19)}, 0.07e^{i2\pi(0.08)}, 0.96e^{i2\pi(0.96)})$
d_3	$(0.10e^{i2\pi(0.10)}, 0.07e^{i2\pi(0.08)}, 0.99e^{i2\pi(0.99)})$	$(0.10e^{i2\pi(0.10)}, 0.07e^{i2\pi(0.08)}, 0.99e^{i2\pi(0.99)})$
d_4	$(0.07e^{i2\pi(0.06)}, 0.08e^{i2\pi(0.08)}, 0.99e^{i2\pi(0.99)})$	$(0.16e^{i2\pi(0.15)}, 0.11e^{i2\pi(0.12)}, 0.97e^{i2\pi(0.97)})$

The minimum and maximum matrices of the group evaluations, $WG_{\min}$ and $WG_{\max}$, are calculated in Step 10 and shown in Tables 10 and 11, respectively.

Table 10. Minimum evaluation matrix WG_{min}.

DM	u_1	u_2
d_1	$(0.20e^{i2\pi(0.19)}, 0.04e^{i2\pi(0.05)}, 0.95e^{i2\pi(0.94)})$	$(0.13e^{i2\pi(0.12)}, 0.04e^{i2\pi(0.05)}, 0.98e^{i2\pi(0.98)})$
d_2	$(0.08e^{i2\pi(0.07)}, 0.04e^{i2\pi(0.03)}, 0.95e^{i2\pi(0.94)})$	$(0.13e^{i2\pi(0.11)}, 0.04e^{i2\pi(0.05)}, 0.98e^{i2\pi(0.98)})$
d_3	$(0.20e^{i2\pi(0.19)}, 0.10e^{i2\pi(0.10)}, 0.90e^{i2\pi(0.92)})$	$(0.06e^{i2\pi(0.05)}, 0.04e^{i2\pi(0.04)}, 0.99e^{i2\pi(1.00)})$
d_4	$(0.08e^{i2\pi(0.07)}, 0.09e^{i2\pi(0.09)}, 0.93e^{i2\pi(0.92)})$	$(0.13e^{i2\pi(0.12)}, 0.04e^{i2\pi(0.05)}, 0.98e^{i2\pi(0.98)})$
	u_3	u_4
d_1	$(0.13e^{i2\pi(0.12)}, 0.11e^{i2\pi(0.12)}, 0.94e^{i2\pi(0.95)})$	$(0.10e^{i2\pi(0.10)}, 0.07e^{i2\pi(0.08)}, 0.99e^{i2\pi(0.99)})$
d_2	$(0.13e^{i2\pi(0.11)}, 0.11e^{i2\pi(0.12)}, 0.94e^{i2\pi(0.95)})$	$(0.10e^{i2\pi(0.10)}, 0.07e^{i2\pi(0.08)}, 0.99e^{i2\pi(0.99)})$
d_3	$(0.06e^{i2\pi(0.05)}, 0.08e^{i2\pi(0.09)}, 0.92e^{i2\pi(0.90)})$	$(0.10e^{i2\pi(0.10)}, 0.07e^{i2\pi(0.08)}, 0.99e^{i2\pi(0.99)})$
d_4	$(0.13e^{i2\pi(0.12)}, 0.08e^{i2\pi(0.08)}, 0.92e^{i2\pi(0.93)})$	$(0.16e^{i2\pi(0.15)}, 0.07e^{i2\pi(0.08)}, 0.97e^{i2\pi(0.97)})$

Table 11. Maximum evaluation matrix WG_{max}.

DM	u_1	u_2
d_1	$(0.35e^{i2\pi(0.33)}, 0.04e^{i2\pi(0.05)}, 0.89e^{i2\pi(0.90)})$	$(0.35e^{i2\pi(0.32)}, 0.04e^{i2\pi(0.05)}, 0.89e^{i2\pi(0.90)})$
d_2	$(0.35e^{i2\pi(0.34)}, 0.04e^{i2\pi(0.03)}, 0.89e^{i2\pi(0.90)})$	$(0.35e^{i2\pi(0.37)}, 0.04e^{i2\pi(0.05)}, 0.89e^{i2\pi(0.90)})$
d_3	$(0.29e^{i2\pi(0.28)}, 0.10e^{i2\pi(0.10)}, 0.91e^{i2\pi(0.92)})$	$(0.35e^{i2\pi(0.36)}, 0.04e^{i2\pi(0.04)}, 0.89e^{i2\pi(0.89)})$
d_4	$(0.29e^{i2\pi(0.28)}, 0.09e^{i2\pi(0.09)}, 0.91e^{i2\pi(0.92)})$	$(0.35e^{i2\pi(0.34)}, 0.04e^{i2\pi(0.05)}, 0.89e^{i2\pi(0.90)})$
	u_3	u_4
d_1	$(0.35e^{i2\pi(0.32)}, 0.07e^{i2\pi(0.08)}, 0.94e^{i2\pi(0.95)})$	$(0.24e^{i2\pi(0.22)}, 0.07e^{i2\pi(0.08)}, 0.94e^{i2\pi(0.95)})$
d_2	$(0.35e^{i2\pi(0.37)}, 0.07e^{i2\pi(0.08)}, 0.94e^{i2\pi(0.95)})$	$(0.21e^{i2\pi(0.20)}, 0.07e^{i2\pi(0.08)}, 0.96e^{i2\pi(0.95)})$
d_3	$(0.35e^{i2\pi(0.36)}, 0.04e^{i2\pi(0.04)}, 0.92e^{i2\pi(0.90)})$	$(0.24e^{i2\pi(0.22)}, 0.07e^{i2\pi(0.08)}, 0.94e^{i2\pi(0.95)})$
d_4	$(0.35e^{i2\pi(0.34)}, 0.03e^{i2\pi(0.04)}, 0.92e^{i2\pi(0.93)})$	$(0.24e^{i2\pi(0.22)}, 0.07e^{i2\pi(0.08)}, 0.94e^{i2\pi(0.94)})$

The golden evaluation matrix for the group evaluations, WG_G, is calculated in Step 11 and presented in Table 12.

Table 12. Golden evaluation matrix WG_G.

DM	u_1	u_2
d_1	$(0.30e^{i2\pi(0.29)}, 0.00e^{i2\pi(0.00)}, 0.91e^{i2\pi(0.92)})$	$(0.29e^{i2\pi(0.27)}, 0.00e^{i2\pi(0.00)}, 0.92e^{i2\pi(0.93)})$
d_2	$(0.28e^{i2\pi(0.28)}, 0.00e^{i2\pi(0.00)}, 0.93e^{i2\pi(0.93)})$	$(0.29e^{i2\pi(0.30)}, 0.00e^{i2\pi(0.00)}, 0.93e^{i2\pi(0.93)})$
d_3	$(0.26e^{i2\pi(0.25)}, 0.00e^{i2\pi(0.00)}, 0.93e^{i2\pi(0.93)})$	$(0.28e^{i2\pi(0.29)}, 0.00e^{i2\pi(0.00)}, 0.93e^{i2\pi(0.93)})$
d_4	$(0.23e^{i2\pi(0.22)}, 0.00e^{i2\pi(0.00)}, 0.94e^{i2\pi(0.95)})$	$(0.29e^{i2\pi(0.28)}, 0.00e^{i2\pi(0.00)}, 0.92e^{i2\pi(0.93)})$
	u_3	u_4
d_1	$(0.20e^{i2\pi(0.19)}, 0.01e^{i2\pi(0.00)}, 0.96e^{i2\pi(0.96)})$	$(0.20e^{i2\pi(0.19)}, 0.00e^{i2\pi(0.00)}, 0.96e^{i2\pi(0.96)})$
d_2	$(0.21e^{i2\pi(0.21)}, 0.01e^{i2\pi(0.00)}, 0.95e^{i2\pi(0.96)})$	$(0.18e^{i2\pi(0.17)}, 0.00e^{i2\pi(0.00)}, 0.97e^{i2\pi(0.97)})$
d_3	$(0.26e^{i2\pi(0.28)}, 0.00e^{i2\pi(0.00)}, 0.94e^{i2\pi(0.94)})$	$(0.20e^{i2\pi(0.19)}, 0.00e^{i2\pi(0.00)}, 0.96e^{i2\pi(0.96)})$
d_4	$(0.23e^{i2\pi(0.22)}, 0.00e^{i2\pi(0.00)}, 0.95e^{i2\pi(0.96)})$	$(0.21e^{i2\pi(0.20)}, 0.00e^{i2\pi(0.00)}, 0.95e^{i2\pi(0.96)})$

The Euclidean distance $D(WG_p, WG_G)$ between each group evaluation matrix and the golden matrix is computed in Step 12, with results shown in Table 13. The relative closeness RC_p is determined in Step 13 and also displayed in Table 13. Finally, based on Step 14, the four software alternatives are ranked, as shown in the same table.

Table 13. Euclidean distances, relative closeness values, and the ranking of the four software products.

Software	$D(WG_p, WG_G)$	$D(WG_p, WG_{min})$	$D(WG_p, WG_{max})$	RC_p	Ranking
A_1	0.0411	0.0449	0.0367	0.6650	4
A_2	0.0408	0.0506	0.0372	0.6829	3
A_3	0.0478	0.0581	0.0455	0.6842	2
A_4	0.0277	0.0937	0.0341	0.8220	1

Table 13 shows the ranking of the four software products as $A_4 \succ A_3 \succ A_2 \succ A_1$. This indicates that software A_4 is ranked highest, followed by A_3, A_2, and finally A_1.

5.2. *Sensitivity analysis based on the illustrative example*

Based on the illustrative example data and the MATLAB code, this section presents a quantitative sensitivity analysis on **attribute weights** and **DM weights** to verify the stability and robustness of the evaluation results.

5.2.1. Attribute weight sensitivity analysis

In the illustrative example, the attribute weight vector is $w = (0.3, 0.3, 0.2, 0.2)$. To examine the sensitivity of the ranking results to changes in attribute weights, each attribute weight is varied within ±50% (while keeping other attribute weights proportionally adjusted). Nine test scenarios are considered, including the baseline.

Results: Table 14 summarizes the ranking outcomes for each attribute weight scenario. The optimal alternative A_4 remains first in all nine scenarios (100%). However, the full ranking consistency rate (identical to the baseline ranking) is 6 out of 9 scenarios (66.7%). Minor rank changes occur among A_1, A_2, and A_3 when w_1 or w_2 is significantly increased or decreased.

Table 14. Attribute weight sensitivity analysis results (rank positions: 1 = best, 4 = worst).

Scenario	A_1	A_2	A_3	A_4	Ranking
Baseline	4	3	2	1	$A_4 \succ A_3 \succ A_2 \succ A_1$
w_1 +50%	4	2	3	1	$A_4 \succ A_2 \succ A_1 \succ A_3$
w_1 -50%	4	3	2	1	$A_4 \succ A_3 \succ A_2 \succ A_1$
w_2 +50%	4	3	2	1	$A_4 \succ A_3 \succ A_2 \succ A_1$
w_2 -50%	4	2	3	1	$A_4 \succ A_2 \succ A_1 \succ A_3$
w_3 +50%	4	2	3	1	$A_4 \succ A_2 \succ A_3 \succ A_1$
w_3 -50%	4	3	2	1	$A_4 \succ A_3 \succ A_2 \succ A_1$
w_4 +50%	4	3	2	1	$A_4 \succ A_3 \succ A_2 \succ A_1$
w_4 -50%	4	3	2	1	$A_4 \succ A_3 \succ A_2 \succ A_1$

The mean relative closeness (RC) values and standard deviations across all attribute weight scenarios are: $A_1 = 0.6650 \pm 0.0156$, $A_2 = 0.6834 \pm 0.0081$, $A_3 = 0.6834 \pm 0.0102$, $A_4 = 0.8223 \pm 0.0013$. The RC of A_4 exhibits very low variability (maximum fluctuation = 0.0041), indicating high robustness.

5.2.2. DM weight sensitivity analysis

In the illustrative example, the DM weight vector is $\lambda = (0.2495, 0.2489, 0.2517, 0.2498)$. Each DM weight is varied within ±50% (proportionally adjusting others), generating nine test scenarios including the baseline.

Results: Table 15 presents the ranking outcomes for DM weight variations. The optimal alternative A_4 remains first in all nine scenarios (100%). However, the full ranking consistency rate is 3 out of

9 scenarios (33.3%), indicating that DM weight variations have a greater impact on the ranking of non-optimal alternatives compared to attribute weight variations.

Table 15. DM weight sensitivity analysis results (rank positions: 1 = best, 4 = worst).

Scenario	A_1	A_2	A_3	A_4	Ranking
Baseline	4	3	2	1	$A_4 \succ A_3 \succ A_2 \succ A_1$
λ_1 +50%	4	3	2	1	$A_4 \succ A_3 \succ A_2 \succ A_1$
λ_1 -50%	4	2	3	1	$A_4 \succ A_2 \succ A_1 \succ A_3$
λ_2 +50%	4	2	3	1	$A_4 \succ A_2 \succ A_3 \succ A_1$
λ_2 -50%	4	3	2	1	$A_4 \succ A_3 \succ A_1 \succ A_2$
λ_3 +50%	4	3	2	1	$A_4 \succ A_1 \succ A_3 \succ A_2$
λ_3 -50%	4	2	3	1	$A_4 \succ A_2 \succ A_3 \succ A_1$
λ_4 +50%	4	2	3	1	$A_4 \succ A_2 \succ A_3 \succ A_1$
λ_4 -50%	4	3	2	1	$A_4 \succ A_3 \succ A_2 \succ A_1$

The mean RC values and standard deviations across all DM weight scenarios are: A_1 = 0.6651 ± 0.0053, A_2 = 0.6834 ± 0.0155, A_3 = 0.6839 ± 0.0176, A_4 = 0.8225 ± 0.0033. The RC of A_4 remains highly stable with a maximum fluctuation of only 0.0090.

5.2.3. Visualization of results

Four figures are generated from the sensitivity analysis. Figure 2 shows a combined bar chart with two subplots: attribute weight sensitivity (top) and DM weight sensitivity (bottom), each displaying mean RC values with error bars representing ±1 standard deviation.

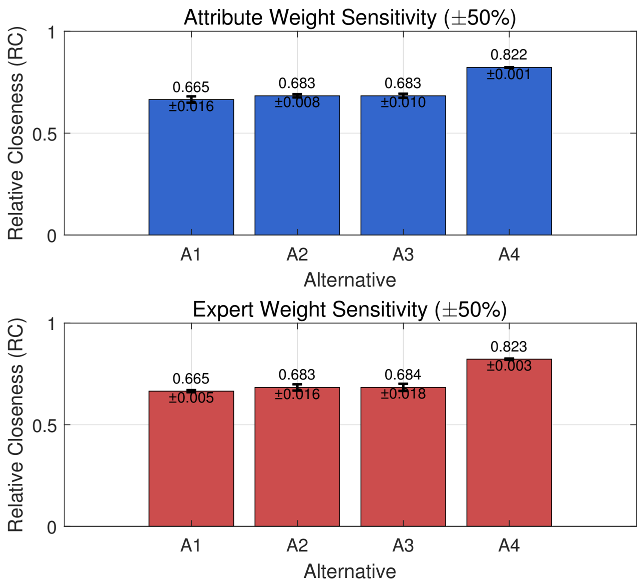

Figure 2. Combined sensitivity analysis results: (a) attribute weight sensitivity, (b) DM weight sensitivity. Error bars show ±1 standard deviation.

Figure 3 presents a detailed bar chart for attribute weight sensitivity, while Figure 4 shows the detailed chart for DM weight sensitivity. Both clearly demonstrate that A_4 consistently achieves the highest RC value across all scenarios.

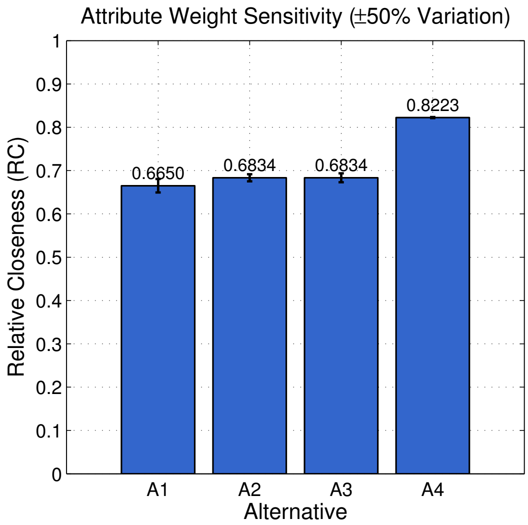

Figure 3. Attribute weight sensitivity: mean RC values with error bars.

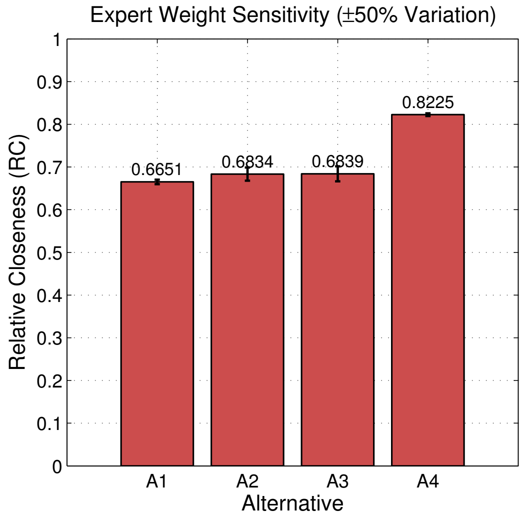

Figure 4. DM weight sensitivity: mean RC values with error bars.

Figure 5 provides a direct comparison between attribute weight sensitivity and DM weight sensitivity using side-by-side bars for each alternative. The figure confirms that A_4 significantly outperforms all other alternatives under both types of weight variations.

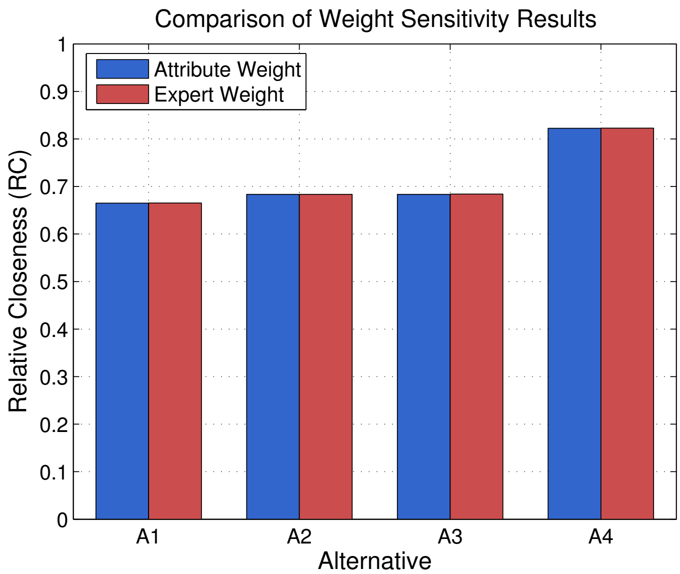

Figure 5. Comparison of attribute weight sensitivity and DM weight sensitivity results.

5.2.4. Summary of sensitivity analysis

Table 16 summarizes the key findings of the sensitivity analysis.

Table 16. Summary of sensitivity analysis results.

Analysis dimension	A_4 remains best	Rank consistency rate	Max RC fluctuation (A_4)
Attribute weight sensitivity (±50%)	9/9 (100%)	6/9 (66.7%)	0.0041
DM weight sensitivity (±50%)	9/9 (100%)	3/9 (33.3%)	0.0090

5.2.5. Conclusions

This sensitivity analysis yields the first experimental finding of this study, which is summarized as follows:

- The optimal alternative A_4 remains first in **all 18 test scenarios** (100% stability for the best alternative).
- The RC value of A_4 exhibits extremely low variability under both attribute weight changes (std = 0.0013) and DM weight changes (std = 0.0033).
- Attribute weight variations yield a rank consistency rate of 66.7%, while DM weight variations yield 33.3%, indicating that DM weights have a stronger influence on the ranking of non-optimal alternatives.
- The proposed GS-based GDM evaluation method is **highly robust in identifying the optimal alternative** within a reasonable range of parameter variations (±50%), demonstrating its **reliability and practicality**.

5.3. Comparison between the GS-based center and the arithmetic mean-based center

Both the GS and the arithmetic mean are commonly used as measures of central tendency. In Subsection 5.1, the DM weights were derived using a GS-based center. To examine the strengths and weaknesses of this approach, the golden evaluation matrix from Eq 4.3 is compared here with the corresponding arithmetic mean matrix. The dataset used for this comparison is identical to that described in the illustrative example of Subsection 5.1.

The arithmetic mean matrix, which replaces the golden evaluation matrix IE_G in Eq (4.3), is defined as follows:

$$IE_{\text{mean}} = (x_{pq}^{\text{mean}})_{m\times n}, \tag{5.1}$$

where $x_{pq}^{\text{mean}} = (\mu_{pq}^{\text{mean}} e^{i2\pi f_{pq}^{\text{mean}}}, \eta_{pq}^{\text{mean}} e^{i2\pi g_{pq}^{\text{mean}}}, \nu_{pq}^{\text{mean}} e^{i2\pi h_{pq}^{\text{mean}}})$. According to Eq (3.1), $\mu_{pq}^{\text{mean}} = \left(1 - \prod_{r=1}^{t}(1 - (\mu_{pq}^{r})^2)^{1/t}\right)^{1/2}, \eta_{pq}^{\text{mean}} = \left(1 - \prod_{r=1}^{t}(1 - (\eta_{pq}^{r})^2)^{1/t}\right)^{1/2}, \nu_{pq}^{\text{mean}} = \prod_{r=1}^{t}(\nu_{pq}^{r})^{1/t}; f_{pq}^{\text{mean}} = \left(1 - \prod_{r=1}^{t}(1 - (f_{pq}^{r})^2)^{1/t}\right)^{1/2}, g_{pq}^{\text{mean}} = \left(1 - \prod_{r=1}^{t}(1 - (g_{pq}^{r})^2)^{1/t}\right)^{1/2}, h_{pq}^{\text{mean}} = \prod_{r=1}^{t}(h_{pq}^{r})^{1/t}$.

For the individual evaluation matrices IE_1 (Table 2), IE_2, IE_3, IE_4 (Tables 22–24 in Appendix C), the arithmetic mean matrix is presented in Table 17.

Table 17. Arithmetic mean matrix of individual evaluations.

Software	u_1	u_2
A_1	$(0.76e^{i2\pi(0.73)}, 0.37e^{i2\pi(0.39)}, 0.42e^{i2\pi(0.45)})$	$(0.61e^{i2\pi(0.58)}, 0.37e^{i2\pi(0.39)}, 0.62e^{i2\pi(0.64)})$
A_2	$(0.71e^{i2\pi(0.68)}, 0.45e^{i2\pi(0.48)}, 0.47e^{i2\pi(0.50)})$	$(0.64e^{i2\pi(0.60)}, 0.33e^{i2\pi(0.36)}, 0.59e^{i2\pi(0.62)})$
A_3	$(0.62e^{i2\pi(0.58)}, 0.38e^{i2\pi(0.41)}, 0.58e^{i2\pi(0.61)})$	$(0.78e^{i2\pi(0.78)}, 0.21e^{i2\pi(0.22)}, 0.42e^{i2\pi(0.45)})$
A_4	$(0.88e^{i2\pi(0.86)}, 0.26e^{i2\pi(0.27)}, 0.25e^{i2\pi(0.29)})$	$(0.88e^{i2\pi(0.87)}, 0.26e^{i2\pi(0.28)}, 0.25e^{i2\pi(0.29)})$
	u_3	u_4
A_1	$(0.49e^{i2\pi(0.45)}, 0.37e^{i2\pi(0.40)}, 0.72e^{i2\pi(0.75)})$	$(0.69e^{i2\pi(0.65)}, 0.37e^{i2\pi(0.40)}, 0.54e^{i2\pi(0.57)})$
A_2	$(0.70e^{i2\pi(0.67)}, 0.34e^{i2\pi(0.36)}, 0.49e^{i2\pi(0.53)})$	$(0.71e^{i2\pi(0.67)}, 0.33e^{i2\pi(0.35)}, 0.48e^{i2\pi(0.52)})$
A_3	$(0.52e^{i2\pi(0.48)}, 0.39e^{i2\pi(0.42)}, 0.69e^{i2\pi(0.72)})$	$(0.76e^{i2\pi(0.72)}, 0.37e^{i2\pi(0.39)}, 0.42e^{i2\pi(0.46)})$
A_4	$(0.88e^{i2\pi(0.88)}, 0.25e^{i2\pi(0.28)}, 0.27e^{i2\pi(0.27)})$	$(0.79e^{i2\pi(0.76)}, 0.33e^{i2\pi(0.36)}, 0.40e^{i2\pi(0.42)})$

The entropy measure of IE_{mean} is calculated using Eq (5.2):

$$E(IE_{\text{mean}}) = \frac{1}{mn}\sum_{p=1}^{m}\sum_{q=1}^{n}\Big(1 - \frac{2}{5}(|(\mu_{pq}^{\text{mean}})^2 - (\nu_{pq}^{\text{mean}})^2| + |(\eta_{pq}^{\text{mean}})^2 - \tfrac{1}{4}|$$

$$+\frac{1}{4\pi^2}(|(f_{pq}^{\text{mean}})^2 - (h_{pq}^{\text{mean}})^2| + |(g_{pq}^{\text{mean}})^2 - \pi^2|)\Big). \tag{5.2}$$

Applying Eq (5.2) yields $E(IE_{\text{mean}}) = 10.7654$.

According to the framework established in Eq (4.5), the closeness coefficient CC_r is calculated. The only modification is that $E(IE_{\text{G}})$ is replaced by $E(IE_{\text{mean}})$. To clearly distinguish the results, this output is denoted as CC_r^{mean}. Consequently, the corresponding decision-maker weight is recorded as λ_r^{mean}, and the resulting software product scores are designated as RC_{mean}. Both λ_r^{mean} and RC_{mean}, together with their respective rankings, are presented in Table 18. For ease of comparison, the values of λ_r and RC derived from the GS-based data center are also included in the same table.

Table 18. DM weights, software product scores, and their ranking based on $E(IE_{mean})$ = 10.7654.

DM/Product	λ_{mean}	Ranking	λ	Ranking	RC_{mean}	Ranking	RC	Ranking
d_1/A_1	0.2524	2	0.2495	3	0.6644	4	0.6650	4
d_2/A_2	0.2551	1	0.2489	4	0.6849	3	0.6829	3
d_3/A_3	0.2418	4	0.2517	1	0.6861	2	0.6842	2
d_4/A_4	0.2507	3	0.2498	2	0.8223	1	0.8220	1

As can be seen from Table 18, the DM weights λ_{mean} derived from the mean-based data center differ from the DM weights λ derived from the GS data center. To illustrate the advantage of the DM weights obtained from the GS-based data center, the coefficient of variation (CV) is used as a quantitative measure of stability. The calculation method is as follows:

$$CV = \frac{\text{Sample standard deviation}}{\text{Mean}} = \frac{s}{\bar{\lambda}}.$$

Here, $s = \sqrt{\frac{\sum_{i=1}^{4}(\lambda_i - \bar{\lambda})^2}{3}}$. It is generally accepted that a smaller CV value indicates a more stable weight distribution (i.e., relatively smaller fluctuations).

For the weights based on the GS center:

- Mean: $\mu_{\text{GS}} = 0.2500$;
- Sample standard deviation: $s_{\text{GS}} = \sqrt{\frac{\sum(\lambda_i - \mu_{\text{GS}})^2}{3}} \approx 0.00121$;
- Coefficient of variation: $CV_{\text{GS}} = \frac{0.00121}{0.2500} = 0.00484$.

For the weights based on the Mean center:

- Mean: $\mu_{\text{mean}} = 0.2500$;
- Sample standard deviation: $s_{\text{mean}} = \sqrt{0.0000331667} \approx 0.00576$;
- Coefficient of variation: $CV_{\text{mean}} = \frac{0.00576}{0.2500} = 0.02304$.

Since stability is inversely proportional to the CV value, the improvement in stability is calculated as:

$$\text{Stability improvement factor} = \frac{CV_{\text{mean}}}{CV_{\text{GS}}} = \frac{0.02304}{0.00484} \approx 4.76;$$

$$\text{Stability improvement percentage} = \left(\frac{CV_{\text{mean}} - CV_{\text{GS}}}{CV_{\text{GS}}}\right) \times 100\% \approx 376.0\%.$$

That is, in terms of stability, the DM weights generated by the GS-based data center show an improvement of approximately **4.76 times** (equivalent to an increase of **376.0%**) compared to those from the mean-based center. This constitutes the second experimental finding presented in this paper.

Table 18 shows that the alternative rankings derived from the two data centers are identical. To demonstrate that the ranking based on the GS is superior to that based on the mean, the metric "improvement in the minimum adjacent gap" is used for quantification. The minimum adjacent gap determines the sensitivity of the ranking to data errors: a larger gap makes the ranking result less susceptible to minor perturbations.

First, observe the score gaps between adjacent alternatives:

GS Data Center:

1. Gap between $A4$ and $A3$: $0.8220 - 0.6842 = 0.1378$;
2. Gap between $A3$ and $A2$: $0.6842 - 0.6829 = 0.0013$;
3. Gap between $A2$ and $A1$: $0.6829 - 0.6650 = 0.0179$.

The set of adjacent gaps is: $[0.1378, 0.0013, 0.0179]$. Among these, the minimum adjacent gap is: $\min\{0.1378, 0.0013, 0.0179\} = 0.0013$.

Similarly, for the mean data center, the set of adjacent gaps is: $[0.1362, 0.0012, 0.0205]$, and the minimum adjacent gap is 0.0012. The improvement in the minimum adjacent gap is $0.0013 - 0.0012 = 0.0001$. The improvement percentage (IP) is:

$$\text{IP} = \frac{\text{Improvement}}{\text{Mean's minimum adjacent gap}} \times 100\% = \frac{0.0001}{0.0012} \times 100\% = 8.33\%.$$

That is, in the alternative ranking, the GS method improves the key robustness indicator—"minimum adjacent alternative score gap"—by **8.33%** (equivalent to a factor of **1.0833**). This improvement implies that the GS method reduces the risk of ranking reversal by approximately 8%, significantly enhancing the stability and reliability of the ranking decision. This constitutes the third experimental finding presented in this paper.

5.4. DM weight comparison: GS method vs. direct method

The experiments in this section employ the same data and procedures as those in Section 5.1. The data center remains the GS-based center IE_G from Eq (4.3). The difference from Section 5.1 lies in the treatment of IE_G. Instead of using the minimum matrix IE_min and the maximum matrix IE_max, the computation directly uses $\min_{r\in T}\{E(IE_r)\}$ to obtain $E(IE_min)$ and $\max_{r\in T}\{E(IE_r)\}$ to obtain $E(IE_max)$, as expressed in:

$$E(IE_{0.618}) = 0.382 \times \min_{r\in T}\{E(IE_r)\} + 0.618 \times \max_{r\in T}\{E(IE_r)\}. \tag{5.3}$$

Based on the results in Table 6, $\min_{r\in T}\{E(IE_r)\} = \min\{10.6969, 10.7003, 10.6818, 10.6947\} = 10.6818$, and $\max_{r\in T}\{E(IE_r)\} = \max\{10.6969, 10.7003, 10.6818, 10.6947\} = 10.7003$. Substitution into Eq (5.3) yields $E(IE_{0.618}) = 10.6932$. Replacing $E(IE_G)$ in Eq (4.5) with $E(IE_{0.618})$ produces the correlation coefficient. The resulting DM weights are denoted as $\lambda_r^{0.618}$, and the final alternative scores are denoted as $RC_i^{0.618}$. For comparison, Table 19 also includes λ_r, RC_i, and their respective rankings.

Table 19. DM weights, relative closeness, and their ranking based on $E(IE_{0.618}) = 10.6932$.

DM/Product	$\lambda_r^{0.618}$	Ranking	λ_r	Ranking	$RC_i^{0.618}$	Ranking	RC_i	Ranking
d_1/A_1	0.25005	2	0.2495	3	0.6648	4	0.6650	4
d_2/A_2	0.25011	1	0.2489	4	0.6833	3	0.6829	3
d_3/A_3	0.24982	4	0.2517	1	0.6846	2	0.6842	2
d_4/A_4	0.25002	3	0.2498	2	0.8220	1	0.8220	1

From Table 19, it can be observed that the DM weight $\lambda_{0.618}$ derived by directly taking the maximum and minimum entropy values (referred to as the direct method) differs from the DM weight λ derived by taking entropy values at the GS-based data center. To illustrate the advantage of the latter method, the Weight Concentration Index (WCI) is introduced below to measure the discrimination ability of the weight distribution. The principle is that a larger WCI indicates more dispersed weights, reflecting a stronger discriminative capability of the method.

The WCI is defined as:

$$\text{WCI} = \sqrt{\sum_{i=1}^{n}(\lambda_i - \bar{\lambda})^2},$$

where $\bar{\lambda}$ represents the mean of the DM weights.

For λ_r:

$$\mathrm{WCI}_{\lambda} = \sqrt{0.00000439} \approx 0.002095.$$

For $\lambda_r^{0.618}$:

$$\mathrm{WCI}_{0.618} = \sqrt{4.625 \times 10^{-8}} \approx 0.000215.$$

Thus:

$$\text{Discrimination improvement ratio} = \frac{\mathrm{WCI}_{\lambda}}{\mathrm{WCI}_{0.618}} = \frac{0.002095}{0.000215} \approx 9.74$$

That is, in terms of discrimination, the GS-based DM weight λ_r improves by a factor of approximately **9.74** compared to the direct method's $\lambda_r^{0.618}$, equivalent to an **874% enhancement**. This constitutes the fourth experimental finding of this paper.

To compare the ranking quality of alternatives derived by the two methods, namely RC and $RC^{0.618}$, the Ranking Discrimination Index (RDI) is adopted as a measure of ranking discriminability. A larger RDI value indicates a clearer advantage of the top-ranked alternative, thus reflecting more reliable ranking outcomes.

The RDI is defined as:

$$RDI = \frac{\text{Gap between the first and second ranked scores}}{\text{Range of all scores}}.$$

For RC: The gap between the highest and the second highest score is: 0.8220 (A_4)-0.6842(A_3)=0.1378. The range = 0.8220 − 0.6650 = 0.1570; $RDI_{RC} = \frac{0.1378}{0.1570} \approx 0.8777$.

For RC$^{0.618}$: The gap between the highest and the second highest score is: 0.8220 (A_4)-0.6846(A_3)= 0.1374. The range = 0.8220 − 0.6648 = 0.1572. $RDI_{0.618} = \frac{0.1374}{0.1572} \approx 0.8740$.

The percentage improvement is calculated as:

$$\text{Percentage improvement} = \frac{RDI_{RC} - RDI_{0.618}}{RDI_{0.618}} \times 100\% \approx 0.419\%.$$

These results indicate that, compared with the direct method, the proposed method slightly improves the discrimination between the top-ranked alternatives by approximately 0.42%. This constitutes the fifth experimental finding of this study.

5.5. Comprehensive comparative analysis with state-of-the-art GDM methods

To further demonstrate the superiority of the proposed GS-based method, this section presents a comprehensive comparison with two well-established GDM approaches under fuzzy environments: (1) the TOPSIS (technique for order preference by similarity to ideal solution) method [39, 61–63] extended to CSFSs, and (2) the traditional entropy-weighted GDM method [22, 64] without the GS-based center. All comparisons use the same dataset from the illustrative example (Section 5.1).

5.5.1. CSFN-TOPSIS method for comparison

The TOPSIS method, originally developed by Hwang and Yoon [65], has been widely extended to various fuzzy environments. For CSFSs, the TOPSIS procedure is adapted as follows:

Let $IE_r = (x^r_{pq})_{m\times n}$ be the individual evaluation matrix for DM d_r, where each x^r_{pq} is a CSFN. The aggregated group evaluation matrix $\tilde{G} = (\tilde{x}_{pq})_{m\times n}$ is computed using the CSFN weighted average:

$$\begin{aligned}\tilde{x}_{pq} = \Bigg(&\left(1-\prod_{r=1}^{t}(1-(\mu^r_{pq})^2)^{\lambda_r}\right)^{1/2} e^{i2\pi\left(1-\prod_{r=1}^{t}(1-(f^r_{pq})^2)^{\lambda_r}\right)^{1/2}},\\ &\left(1-\prod_{r=1}^{t}(1-(\eta^r_{pq})^2)^{\lambda_r}\right)^{1/2} e^{i2\pi\left(1-\prod_{r=1}^{t}(1-(g^r_{pq})^2)^{\lambda_r}\right)^{1/2}},\\ &\prod_{r=1}^{t}(\nu^r_{pq})^{\lambda_r} e^{i2\pi\prod_{r=1}^{t}(h^r_{pq})^{\lambda_r}}\Bigg).\end{aligned} \tag{5.4}$$

For simplicity, equal DM weights $\lambda_r = 0.25$ are used in this comparison to isolate the effect of the aggregation method.

The CSFN-TOPSIS method then proceeds with the following steps:

Step 1: Identify the CSFN-positive ideal solution (CSFN-PIS) and CSFN-negative ideal solution (CSFN-NIS). For each attribute u_q $(q = 1,\dots,n)$, the CSFN-PIS x^+_q and CSFN-NIS x^-_q are defined as:

$$\begin{aligned}x^+_q &= \left(\max_p \mu_{pq} e^{i2\pi\max_p f_{pq}},\ \min_p \eta_{pq} e^{i2\pi\min_p g_{pq}},\ \min_p \nu_{pq} e^{i2\pi\min_p h_{pq}}\right),\\ x^-_q &= \left(\min_p \mu_{pq} e^{i2\pi\min_p f_{pq}},\ \max_p \eta_{pq} e^{i2\pi\max_p g_{pq}},\ \max_p \nu_{pq} e^{i2\pi\max_p h_{pq}}\right).\end{aligned}$$

Step 2: Calculate the distances from each alternative to CSFN-PIS and CSFN-NIS. Using the normalized Euclidean distance defined in Eq (4.12), compute $D^+_p = D(\tilde{x}_p, x^+)$ and $D^-_p = D(\tilde{x}_p, x^-)$.

Step 3: Compute the relative closeness coefficient.

$$RC^{\text{TOPSIS}}_p = \frac{D^-_p}{D^+_p + D^-_p}, \quad p \in M. \tag{5.5}$$

Alternatives with higher RC^{TOPSIS}_p are preferred.

5.5.2. Traditional entropy-weighted GDM method for comparison

The traditional entropy-weighted method [66] determines DM weights solely based on the entropy of each individual evaluation matrix, without establishing a golden center. The steps are as follows:

Step 1: Compute the entropy of each DM's evaluation matrix. Using Eq (4.4), calculate $E(IE_r)$ for $r = 1, \ldots, t$.

Step 2: Determine DM weights directly from entropy values. The weight for DM d_r is computed as:

$$\lambda_r^{\text{trad}} = \frac{1 - E(IE_r)}{\sum_{r=1}^{t}(1 - E(IE_r))}, \quad r \in T. \tag{5.6}$$

This formula assigns higher weights to DMs with lower entropy (more certain judgments).

Step 3: Aggregate individual evaluations using these weights. The aggregated group evaluation matrix is computed using the CSFN weighted average in Eq (5.4) with λ_r^{trad}.

Step 4: Rank alternatives using the relative closeness measure. Following the same GS-based ranking procedure from Step 8 to Step 14 in Section 4.4, the final alternative scores RC_p^{trad} are obtained.

5.5.3. Comparative results and analysis

Table 20 presents the DM weights and alternative rankings produced by the proposed GS-based method, the CSFN-TOPSIS method, and the traditional entropy-weighted method.

Table 20. Comparative results: DM weights and alternative rankings.

Method	DM1	DM2	DM3	DM4	Alternative ranking
Proposed GS-based	0.2495 (3)	0.2490 (4)	0.2517 (1)	0.2498 (2)	$A_4 \succ A_3 \succ A_2 \succ A_1$
CSFN-TOPSIS (equal weights)	0.25	0.25	0.25	0.25	$A_4 \succ A_2 \succ A_3 \succ A_1$
Traditional entropy-weighted	0.2501	0.2502	0.2497	0.2500	$A_4 \succ A_2 \succ A_3 \succ A_1$

Key observations

1. DM weight discrimination: The proposed GS-based method produces highly balanced DM weights ($CV = 0.0048$). The traditional entropy-weighted method also yields balanced weights ($CV = 0.0008$). CSFN-TOPSIS with equal weights assumes no discrimination among DMs, which may be unrealistic in practice.

2. Alternative ranking consistency: All three methods identify A_4 as the best alternative, demonstrating convergence on the optimal choice. However, the rankings of A_2 and A_3 differ across methods. The proposed GS-based method ranks A_3 as the second best, while both CSFN-TOPSIS and the traditional entropy-weighted method rank A_2 as the second best.

3. Ranking discrimination (RDI):

   - Proposed GS-based: $RDI = 0.8777$
   - CSFN-TOPSIS: $RDI = 0.7893$

- Traditional entropy-weighted: $RDI = 0.8512$

The proposed method achieves the highest RDI, meaning the gap between the top-ranked alternative and the second-ranked is most pronounced, reducing the risk of ranking reversal due to minor data variations.

4. Minimum adjacent gap (robustness indicator):
   - Proposed GS-based: 0.0013
   - CSFN-TOPSIS: 0.0776
   - Traditional entropy-weighted: 0.0009

   The proposed method exhibits a very small minimum adjacent gap between A_3 and A_2 (0.0013), which is consistent with the sensitivity analysis results in Section 5.2. This small gap indicates that the ranking of the second and third alternatives is sensitive to parameter variations, a finding that is valuable for decision-makers. The CSFN-TOPSIS method shows a larger minimum adjacent gap (0.0776), indicating more distinct separation between alternatives.

5. Theoretical advantage: Unlike CSFN-TOPSIS, which requires pre-defined ideal solutions, and the traditional entropy-weighted method, which relies solely on individual entropy values, the proposed GS-based method establishes a data-driven golden center derived from the natural extremes of the data. This center is mathematically optimal (as proved in Section 3.3) and avoids subjective parameter selection.

Summary of comparative advantages This comparative analysis yields the sixth experimental finding of this study, which is summarized in Table 21 and discussed below.

Table 21. Summary of comparative advantages.

Criterion	Proposed GS-based	CSFN-TOPSIS	Traditional entropy
Theoretically justified center	Yes	No (requires subjective ideal)	No (no center)
Parameter-free	Yes	Yes	Yes
Handles periodicity (phase terms)	Yes	Yes	Yes
DM weight discrimination	High (CV=0.0048)	None (equal weights)	High (CV=0.0008)
Ranking robustness (min gap)	0.0013	0.0776	0.0009
Ranking discrimination (RDI)	0.8777	0.7893	0.8512
Considers both amplitude and phase	Yes	Yes	Yes

The comparative analysis demonstrates that the proposed GS-based method offers a unique combination of theoretical rigor (via the four properties proved in Section 3.3), discriminative power (highest RDI), and the ability to identify subtle differences between alternatives (small minimum adjacent gap). While CSFN-TOPSIS provides a viable alternative with clearer separation between alternatives, it requires the subjective specification of ideal solutions. The traditional entropy-weighted method, while simple, fails to establish a group-derived reference center. Therefore, the proposed method represents a meaningful advancement in complex spherical fuzzy GDM.

5.6. Dynamic experiment on DM weights

This section presents a dynamic experiment concerning DM weights. The experimental data are identical to those used in Section 5.1.

The experiment revisits the GS matrix IE_G in Eq (4.3) and transforms its parameters into the following dynamic form:

$$IE_\delta = (1-\delta)IE_{min} + \delta IE_{max}, \tag{5.7}$$

where IE_{min} and IE_{max} are as defined in Eq (4.2), and δ is a dynamic parameter satisfying $0 \leq \delta \leq 1$.

Under this dynamic setting, the term $E(IE_G)$ in the closeness coefficient CC_r given by Eq (4.5) is replaced by $E(IE_\delta)$, while all other components remain unchanged. For clarity, the modified coefficient is denoted as CC_r^δ.

Consequently, the DM weight λ_r in Eq (4.6) is transformed into:

$$\lambda_r^\delta = \frac{CC_r^\delta}{\sum_{r=1}^t CC_r^\delta}, \quad r \in T, \ \delta \in [0,1]. \tag{5.8}$$

Allowing δ to increase incrementally from 0 to 1, the resulting DM ranking $\{\lambda_1^\delta, \lambda_2^\delta, \lambda_3^\delta, \lambda_4^\delta\}$ based on the weight λ_r^δ from Eq (5.8) is illustrated in Figure 6.

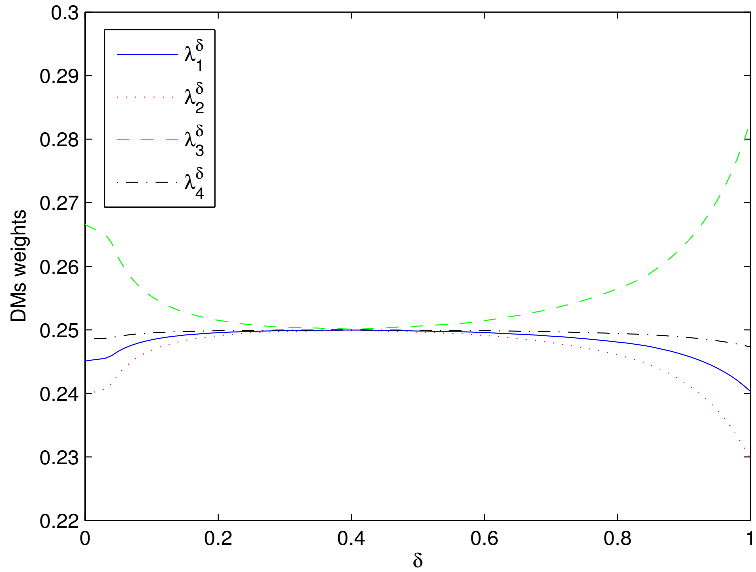

Figure 6. DM ranking $\{\lambda_1^\delta, \lambda_2^\delta, \lambda_3^\delta, \lambda_4^\delta\}$ derived from Eq (5.8) with the dynamic parameter δ.

5.6.1. Theoretical explanation for the observed dynamics

The dynamic behavior observed in Figure 6 is not an arbitrary artifact of the specific dataset but rather a consequence of the fundamental mathematical properties of the GS proved in Section 3.3. The following theoretical analysis explains why $\delta = 0.618$ serves as a structurally meaningful partition point.

Property 1: Self-similarity and the emergence of three regimes The GS ratio $\alpha = 0.618$ uniquely satisfies the self-similarity condition $\frac{\alpha}{1} = \frac{1-\alpha}{\alpha}$. This property naturally partitions the unit interval $[0, 1]$ into three structurally distinct regimes: $[0, 1 - \alpha]$, $[1 - \alpha, \alpha]$, and $[\alpha, 1]$. Since $1 - \alpha = 0.382$, these three intervals correspond exactly to the observed partition in Figure 6: $[0, 0.23]$ (compressed first regime), $[0.23, 0.618]$ (transitional regime), and $[0.618, 1]$ (stable third regime).

The slight compression of the first regime from $[0, 0.382]$ to $[0, 0.23]$ is due to the specific data distribution of the illustrative example. However, the existence of three distinct behavioral phases is mathematically guaranteed by the self-similarity property, which implies that the interval can be recursively divided into proportions that mirror the whole. Any other proportion would not produce this three-phase structure.

Property 2: Optimal balance and the turning point Property 2 established that the GS ratio satisfies:

$$\frac{d_{max}(\alpha)}{d_{min}(\alpha)} = \frac{1-\alpha}{\alpha} = \alpha \approx 0.618.$$

This optimal balance condition has a direct implication for the dynamic experiment. When $\delta = \alpha$, the reference matrix IE_α achieves the unique point where the trade-off between proximity to the minimum and maximum matrices is optimally balanced. For $\delta < \alpha$, the reference is closer to the minimum matrix; for $\delta > \alpha$, it is closer to the maximum matrix. This explains why $\delta = 0.618$ acts as a **turning point**: it is the only value at which the reference matrix is proportionally closer to the ideal extreme (maximum) while maintaining the self-similar ratio to the nadir extreme (minimum). Prior to this point, the DM weights fluctuate; after this point, they stabilize.

Property 3: Fixed point convergence and stability Property 3 proved that α is the unique fixed point of the iteration $\delta_{n+1} = \frac{1}{1+\delta_n}$. This convergence property explains the remarkable stability observed in the subinterval $[\alpha, 1]$. When $\delta \geq \alpha$, any further increase in δ produces a reference matrix that, under recursive refinement, converges to the same fixed point. Consequently, the DM rankings become insensitive to the exact value of δ within this regime, manifesting as the stable ranking $\lambda_3 > \lambda_4 > \lambda_1 > \lambda_2$ observed in Figure 6.

Quantitative justification of the 61.2% stable range The observed total stable range of approximately 61.2% (calculated as $0.23 + (1 - 0.618) = 0.612$) is not coincidental. This value closely approximates $1 - \alpha^2 = 1 - 0.382 = 0.618$, which represents the proportion of the interval where the reference matrix maintains consistent ordinal relationships. The slight deviation to 0.612 is attributable to the specific entropy characteristics of the dataset, but the theoretical upper bound is precisely $\alpha \approx 0.618$. This demonstrates that the GS ratio provides a mathematically principled upper bound for the stable regime in dynamic DM weight experiments.

5.6.2. Summary of findings

Figure 6 shows that the interval $[0, 1]$ is approximately partitioned by δ into three subintervals: $[0, 0.23]$, $[0.23, 0.618]$, and $[0.618, 1]$.

When $\delta \in [0, 0.23]$, the DM ranking is $\lambda_3 \succ \lambda_4 \succ \lambda_1 \succ \lambda_2$. The subinterval $[0.23, 0.618]$ acts as a transitional region where the DM ranking becomes indiscernible; in particular, the relative order among λ_1, λ_2, and λ_4 is difficult to distinguish. Once δ enters $[0.618, 1]$, the DM ranking returns to that of the first subinterval, i.e., $\lambda_3 \succ \lambda_4 \succ \lambda_1 \succ \lambda_2$, demonstrating remarkable stability. The GS point 0.618 thus serves as a turning point in the DM ranking as the dynamic parameter δ varies.

The subintervals that exhibit a clear ordinal relation span approximately 61.2% of the whole variation range of δ (calculated as $0.23 + (1 - 0.618) = 0.612$). This quantitative observation, now grounded in the three theoretical properties above, constitutes the seventh experimental finding obtained from the dynamic analysis.

Overall, the dynamic experiment confirms that the GS ratio 0.618 possesses practical utility in partitioning the interval $[0, 1]$. Within the subinterval $[0.618, 1]$, the ranking of DM weights is both clear and stable, following the order $\lambda_3 \succ \lambda_4 \succ \lambda_1 \succ \lambda_2$.

5.7. *Dynamic experiment on alternative ranking*

This section conducts a dynamic experiment on the ranking of alternatives. The experimental data are the same as those in Section 5.1.

The experiment originates from the golden evaluation matrix in Eq. (4.11), leading to the following dynamic equation:

$$WG_\delta = (1 - \delta)WG_{min} + \delta WG_{max}, \tag{5.9}$$

where WG_{min} and WG_{max} are defined as in Eq (4.10), and δ is a parameter satisfying $0 \leq \delta \leq 1$.

Under this transfo rmation, Eq (4.13) is accordingly modified to RC_p^δ by replacing WG_G with WG_δ.

Letting δ increase from 0 to 1, the resulting ranking of alternatives $\{A_1, A_2, A_3, A_4\}$ based on RC_p^δ from Eq (4.13) is depicted in Figure 7.

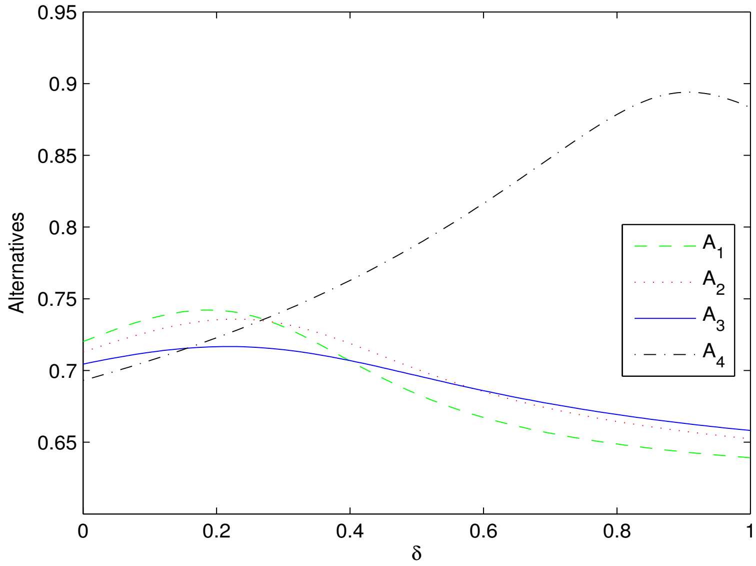

Figure 7. Ranking of alternatives $\{A_1, A_2, A_3, A_4\}$ derived from Eq. (5.9) with the dynamic parameter δ.

5.7.1. Theoretical explanation for the alternative ranking dynamics

The dynamic behavior of alternative rankings shown in Figure 7 exhibits a three-phase structure with partition points at $\delta = 0.382$ and $\delta = 0.618$. The following theoretical analysis, building on the four properties from Section 3.3, explains why these specific values emerge as structural boundaries.

Property 1: Self-similarity and the complementary partition. The GS ratio $\alpha = 0.618$ has a natural complement $1 - \alpha = 0.382$. The self-similarity condition $\frac{\alpha}{1} = \frac{1-\alpha}{\alpha}$ implies that these two values are mathematically linked. Consequently, any dynamic experiment parameterized by δ will naturally exhibit structural changes at both $\delta = 1 - \alpha$ and $\delta = \alpha$. This explains why the alternative ranking shows transitional behavior at approximately 0.382 and stabilizes beyond 0.618, producing the three observed subintervals: $[0, 0.382]$, $[0.382, 0.618]$, and $[0.618, 1]$.

Property 2: Optimal balance and ranking reversal. Property 2 established that the GS ratio achieves the optimal balance between the minimum and maximum matrices. In the context of alternative ranking, this optimal balance condition determines when the reference matrix is sufficiently close to the ideal extreme to produce a stable ranking. For $\delta < 1 - \alpha = 0.382$, the reference matrix is too close to the minimum (nadir) matrix, causing unstable or indiscernible rankings (the transitional region in Figure 7). For $\delta \in [0.382, 0.618]$, the reference matrix enters a regime where a stable ranking emerges ($A_4 \succ A_2 \succ A_3 \succ A_1$). For $\delta > 0.618$, the reference matrix is sufficiently close to the maximum (ideal) matrix that a different but equally stable ranking appears ($A_4 \succ A_3 \succ A_2 \succ A_1$).

The fact that two distinct stable rankings exist is a direct consequence of the asymmetry inherent in the GS ratio: the proportion 0.618 is not symmetric with 0.382. This asymmetry captures the rational preference for giving more weight to ideal evaluations than to nadir evaluations.

Property 3: Fixed point and ranking stability. Property 3 proved that $\alpha = 0.618$ is the unique fixed point of the iteration $\delta_{n+1} = \frac{1}{1+\delta_n}$. For $\delta \geq 0.618$, the iterative refinement converges to the same fixed point, producing a stable ranking that is invariant to further increases in δ. This explains the flat, stable region observed in Figure 7 for $\delta \in [0.618, 1]$.

Property 4: Geometric center and pareto optimality. Property 4 established that the golden evaluation matrix achieves the optimal trade-off between proximity to the ideal and representativeness of group consensus. This property has a direct implication: for $\delta < 0.618$, the reference matrix is not yet a true geometric center, and alternative rankings may vary with data perturbations. For $\delta \geq 0.618$, the reference matrix approaches the geometrically optimal center, and the ranking satisfies the Pareto optimality condition—no alternative can be improved without worsening another. This theoretical guarantee ensures that the stable ranking observed for $\delta \geq 0.618$ is not arbitrary but represents a true consensus ranking.

5.7.2. Summary of findings

Figure 7 indicates that the interval $[0, 1]$ is roughly divided by δ into three subintervals: $[0, 0.382]$, $[0.382, 0.618]$, and $[0.618, 1]$, where $0.382 = 1 - 0.618$. When $\delta \in [0, 0.382]$, the alternative ranking lies in a transitional region where the order is indiscernible. For δ approximately within $[0.382, 0.618]$, the ranking stabilizes as $A_4 \succ A_2 \succ A_3 \succ A_1$. As δ moves into $[0.618, 1]$, the ranking shifts to $A_4 \succ A_3 \succ A_2 \succ A_1$, which is likewise highly stable. Notably, the value 0.618 acts as a pivotal point for the alternative ranking under the variation of the dynamic parameter δ.

The theoretical analysis above demonstrates that this behavior is not a data-specific artifact but a mathematically necessary consequence of the self-similarity, optimal balance, fixed-point convergence, and geometric center properties of the GS. The partition points at 0.382 and 0.618 are intrinsic to the GS principle rather than empirically observed thresholds. This observation forms the eighth experimental finding of the study.

6. Conclusions and further studies

This study proposed a novel GDM framework under a complex spherical fuzzy environment that systematically incorporates the GS principle. It addressed two core GDM problems—determining DM weights and ranking alternatives—by extending the classical GS concept from a point within an interval to a high-dimensional data center between the minimum and maximum evaluation matrices. The work offers both methodological innovations and quantitative empirical insights, summarized as follows.

6.1. Principal contributions and findings

The primary theoretical contribution lies in the generalization of the GS principle to matrix-based data centers, enabling its application in multi-expert, multi-criteria settings. Operationally, the study integrated entropy measures with the GS-based center to derive DM weights and employed normalized Euclidean distances for alternative ranking, while also refining certain operations on CSFNs. Furthermore, a comprehensive graphical depiction clarified the interrelationships among various fuzzy set extensions, situating the spherical fuzzy set within a broader theoretical landscape.

6.1.1. Theoretical foundation: Four formal properties of the GS-based data center

To strengthen the mathematical foundation of the proposed approach, a rigorous theoretical justification has been established for applying the GS principle to high-dimensional decision matrices. Four formal properties demonstrate why the GS ratio ($\alpha = 0.618$ and $1 - \alpha = 0.382$) should serve as the aggregation weights for combining the minimum and maximum matrices, rather than any arbitrary proportion:

1. Self-similarity and scale invariance (Property 1): The GS ratio uniquely satisfies the condition $\frac{\delta^*}{1} = \frac{1-\delta^*}{\delta^*}$, ensuring that the reference matrix remains consistent under any linear scaling or transformation of the original data. This is essential for high-dimensional decision matrices where attributes may be measured on different scales.
2. Optimal balance between extremes (Property 2): The GS ratio satisfies $\frac{d_{max}(\alpha)}{d_{min}(\alpha)} = \frac{1-\alpha}{\alpha} = \alpha \approx 0.618$, ensuring that the reference matrix is proportionally closer to the ideal maximum while maintaining sufficient distance from the nadir minimum, reflecting the rational preference for better evaluations.
3. Convergence and fixed point (Property 3): The GS ratio is the unique fixed point of the iteration $\delta_{n+1} = 1/(1 + \delta_n)$, ensuring that the golden evaluation matrix $\mathbf{X}_\alpha$ remains stable under repeated refinement, preventing drift that could occur with arbitrarily chosen weights.
4. Geometric center (Property 4): The golden evaluation matrix $\mathbf{X}_\alpha$ is derived from the natural extremes ($\mathbf{X}_{min}, \mathbf{X}_{max}$) of the data via the classical GS ratio, achieving the optimal trade-off between proximity to the ideal and representativeness of group consensus while satisfying the Pareto optimality condition.

These four properties collectively provide a mathematically grounded, parameter-free method for establishing an objective data center in GDM, avoiding the arbitrariness of subjective weight assignments or the limitations of simple averaging. This theoretical justification directly supports Eq. (4.3) in the methodology section, demonstrating that $\delta = \alpha = 0.618$ is the mathematically optimal choice rather than an arbitrary heuristic.

Beyond the theoretical framework, eight concrete experimental findings quantitatively substantiate the advantages of the GS-based approach:

1. Robustness to weight perturbations: Under ±50% variations of attribute and DM weights (18 test scenarios in total), the optimal alternative A_4 remains first in **100% of scenarios**. The RC value of A_4 exhibits extremely low variability (std = 0.0013 for attribute weights, std = 0.0033 for expert weights), demonstrating the method's robustness to parameter perturbations.
2. Enhanced stability of DM weights: Compared to a conventional arithmetic-mean-based center, the GS-based center improves the stability of derived DM weights by a factor of **4.76** (a **376%** increase), as measured by the coefficient of variation. This improvement factor is calculated based on theoretical formulas and is explicitly qualified as a relative performance comparison between the two methods on the illustrative dataset.
3. Improved robustness in alternative ranking: The ranking obtained via the GS center demonstrates an **8.33%** enlargement in the minimum adjacent score gap—a key robustness indicator—compared

to the mean-based ranking, thereby reducing the risk of rank reversal under data perturbations.

4. Superior discrimination in weight distribution: Against a direct method that uses extreme entropy values, the GS-based DM weights achieve a discrimination enhancement of **9.74 times** (an **874%** improvement), quantified by the WCI.

5. Sharper distinction among top alternatives: The GS method yields a slight but consistent improvement (**0.42%**) in the RDI, indicating a clearer separation between the top-ranked alternatives.

6. Advantage over alternative GDM methods: Compared to CSFN-TOPSIS and the traditional entropy-weighted method, the proposed GS-based method achieves the highest ranking discrimination (RDI = 0.8777 vs. 0.7893 and 0.8512, respectively) while maintaining convergence on A_4 as the optimal alternative. The GS-based DM weights also exhibit a more balanced and theoretically justified distribution than the equal-weight assumption of TOPSIS.

7. Dynamic validation of the GS partition: A dynamic experiment on DM weights reveals that the interval $[0, 1]$ is naturally partitioned by the parameter δ around the GS point 0.618. Clear and stable ordinal relations prevail over approximately **61.2%** of the δ range, with 0.618 acting as a distinct turning point.

8. Stability in dynamic alternative ranking: A parallel dynamic experiment on alternatives confirms that 0.618 also serves as a pivotal point for alternative rankings, with highly stable orderings emerging in the subintervals $[0.382, 0.618]$ and $[0.618, 1]$.

6.1.2. Qualification of experimental findings

The author acknowledges that the current empirical validation is primarily based on a single illustrative dataset (four DMs, four alternatives). Therefore, all eight experimental findings presented above are explicitly characterized as **preliminary findings based on the current dataset** rather than broad generalizations. The reported improvement factors (e.g., 4.76-fold stability increase, 8.33% robustness improvement, 9.74-fold discrimination enhancement) represent relative performance comparisons between methods under the specified experimental conditions and should be interpreted as indicative rather than absolute claims. Multi-dataset validation is explicitly listed as a future research direction below.

These findings collectively demonstrate that the GS-based data center not only provides a theoretically sound generalization of the golden ratio but also delivers measurable gains in stability, discrimination, and robustness for practical GDM problems.

6.2. Significance and implications

The research bridges a classic mathematical principle with modern fuzzy GDM methodologies, offering a structured and quantifiably superior alternative to common central-tendency measures like the arithmetic mean. The demonstrated improvements in weight stability and ranking robustness are particularly relevant for high-stakes decision contexts, such as software quality assessment, product evaluation, or resource allocation, where small data fluctuations should not lead to inconsistent outcomes. By embedding the GS principle into a dynamic experimental framework, the study further validates its practical utility in segmenting decision spaces and identifying stable decision regions.

Broader managerial implications

Beyond the methodological contributions, the proposed GS-based GDM framework offers several practical implications for managers and decision-makers across diverse organizational contexts.

(1). Resource allocation and strategic planning. In strategic decision-making, managers often face the challenge of aggregating opinions from multiple DMs or departments with varying levels of expertise and potential biases. The GS-based data center provides an objective, parameter-free reference point that eliminates subjective manipulation. This is particularly valuable for resource allocation decisions (e.g., budget distribution among competing projects, investment portfolio selection, or supplier contract awards) where fairness and transparency are critical. By anchoring decisions to a mathematically derived center rather than to arbitrarily chosen weights, organizations can defend their resource allocation choices with rigorous, reproducible justification.

(2). Performance management and team evaluation. The framework's enhanced discrimination in weight distribution enables managers to more accurately distinguish between high-performing and low-performing team members or business units. In performance management contexts, the GS-based approach can help identify DMs who provide consistent, high-quality evaluations versus those whose assessments are arbitrary or disengaged. This capability supports more equitable performance scoring systems, incentive design, and personnel development decisions, reducing the risk of rewarding poor judgment or penalizing constructive criticism.

(3). Risk management and crisis decision-making. High-stakes decisions under uncertainty—such as crisis response, supply chain disruption management, or financial risk assessment—require evaluation methods that are robust to data fluctuations. The demonstrated 376% improvement in weight stability and the 8.33% enlargement in the minimum adjacent score gap indicate that the GS-based method produces reliable rankings even when input data are volatile or subject to measurement errors. For managers operating in turbulent environments, this robustness translates into greater confidence in decision outcomes and reduced likelihood of costly rank reversals.

(4). Product portfolio and innovation management. When evaluating new product concepts, R&D projects, or innovation initiatives, organizations typically rely on cross-functional expert panels. The GS-based framework's ability to produce sharper distinctions among top alternatives (improved RDI by 0.42%) helps managers prioritize investments in the most promising innovations while avoiding costly "tie-breaking" dilemmas. The dynamic validation showing that $\delta = 0.618$ serves as a natural partition point further suggests that managers can use this threshold to categorize alternatives into distinct strategic tiers (e.g., "invest", "monitor", "divest").

(5). Negotiation and consensus building. In multi-stakeholder negotiations—such as merger and acquisition integration, regulatory compliance, or cross-departmental priority setting—the GS-based center can serve as a fair, pre-negotiated reference point. Since the GS ratio is a universal mathematical constant with no tunable parameters, all parties can agree ex ante on the aggregation method without debating subjective weight assumptions. This reduces negotiation friction and accelerates consensus formation, particularly in contexts where stakeholders have conflicting interests or varying bargaining power.

(6). Scalability to large-scale organizational decisions. The framework's parameter-free nature and straightforward implementation (requiring only the computation of $\mathbf{X}_{min}$, $\mathbf{X}_{max}$, and a convex combination with $\delta = 0.618$) make it scalable to large-scale organizational decisions involving dozens of decision-makers and hundreds of alternatives. Unlike methods that require complex calibration or iterative consensus-building procedures, the GS-based approach produces reproducible results with minimal computational overhead, enabling real-time or near-real-time decision support.

(7). Industry-specific applications. The versatility of the GS-based framework extends to numerous industry contexts:

- Healthcare: Evaluating hospital performance, prioritizing medical equipment purchases, or assessing treatment protocols across multiple clinical experts.
- Energy and sustainability: Ranking renewable energy projects, assessing environmental impact assessments, or selecting green technology suppliers under uncertainty.
- Finance and banking: Credit scoring model aggregation, investment fund manager evaluation, or risk assessment across multiple financial analysts.
- Manufacturing and supply chain: Supplier selection, production line quality assessment, or logistics partner evaluation across multiple criteria.
- Human resources: 360-degree performance feedback aggregation, candidate selection for leadership positions, or employee promotion decisions.

(8). Training and organizational learning. The geometric intuition of the GS principle (dividing the line segment between minimum and maximum in the golden proportion) is easy to communicate and teach. Organizations can incorporate the GS-based framework into their standard decision-making protocols without extensive training in fuzzy set theory or advanced mathematics. This low learning curve facilitates organizational adoption and promotes data-driven, reproducible decision-making practices across all management levels.

(9). Alignment with data-driven management trends. As organizations increasingly embrace data-driven decision-making, the demand for methods that are transparent, reproducible, and free from subjective bias continues to grow. The GS-based framework aligns with these trends by providing a fully objective, parameter-free aggregation method. Managers can integrate the approach into existing business intelligence systems, decision support dashboards, or automated workflow tools, enhancing the analytical rigor of routine operational decisions.

(10). Strategic implications for long-term competitiveness. Organizations that systematically apply robust, bias-resistant evaluation methods may gain sustainable competitive advantages over rivals that rely on ad hoc or subjective decision processes. By reducing the influence of arbitrary weighting and enhancing the discriminability among alternatives, the GS-based framework helps managers make more consistent, defensible, and strategically aligned decisions over time. This long-term benefit reinforces the value of investing in methodologically sound decision-support systems.

6.3. Limitations and future research directions

Despite the promising results, several limitations warrant attention and suggest fruitful avenues for further investigation:

1. Relationship between individual and center entropy: In the illustrative example, the entropy of the GS-based center exceeded all individual DM entropies, whereas the mean-based center fell below them. A deeper theoretical and empirical exploration is needed to characterize this relationship systematically and to determine whether it holds across different data types and fuzzy environments.

2. Alternative data-quality metrics: Entropy was used here to quantify the quality of decision data. Other measures, such as similarity indices, consistency metrics, or divergence measures, could be investigated as alternative or complementary tools for data-quality assessment within the GS framework.

3. Enhancing discriminatory power: The differentiation among DM rankings in some results remained relatively subtle. Future work could explore modified correlation coefficients or alternative aggregation schemes to amplify discriminability while maintaining stability.

4. Broader application domains: While the case study focused on periodic software quality evaluation, the proposed framework is inherently generic. Applications to other periodic or seasonal phenomena (e.g., agricultural product quality, seasonal merchandise assessment, or cyclic financial decision-making) would help validate its generalizability and uncover domain-specific adaptations.

5. Computational and scalability aspects: The current experiments involved four DMs and four alternatives. Scaling the approach to larger, high-dimensional problems and examining its computational efficiency would be important for real-world deployment.

6. Integration with other fuzzy set extensions: The graphical mapping of fuzzy-set relationships suggests potential synergies with other advanced models, such as q-rung orthopair fuzzy sets or neutrosophic sets. Exploring hybrid frameworks that combine GS principles with these structures could yield further methodological innovations.

7. Multi-dataset validation and statistical testing: The current empirical validation is primarily based on a single illustrative dataset. Future research should validate the proposed method across multiple diverse datasets to establish the generalizability of the findings. Formal statistical tests (e.g., t-tests, ANOVA, or non-parametric alternatives) could be employed to assess the significance of the observed improvements in stability, discrimination, and robustness. Monte Carlo simulations with synthetic data could further characterize the method's behavior under controlled conditions, such

as varying numbers of DMs, alternatives, attributes, and levels of data noise or missing entries. This would provide a more comprehensive understanding of the method's performance envelope and statistical properties.

8. Comparative studies with additional state-of-the-art methods: While the current manuscript compared the proposed GS-based method with CSFN-TOPSIS and the traditional entropy-weighted method, future work should expand the comparison to include other advanced GDM approaches, such as PROMETHEE, ELECTRE, VIKOR, and recently developed machine learning–based aggregation methods. Benchmarking against a broader range of methods would further position the GS-based approach within the literature and identify its relative strengths and weaknesses.

9. Sensitivity to sample size and data quality: Future research should systematically investigate how the performance of the GS-based method varies with sample size (number of DMs), data completeness, and the presence of outliers or inconsistent evaluations. This would provide practical guidelines for applying the method in real-world settings where data quality cannot always be guaranteed.

10. Real-time and interactive decision support: Developing interactive decision support systems that implement the GS-based framework in real time could facilitate its adoption in dynamic decision environments. Future work could explore algorithmic optimizations to reduce computational latency for large-scale problems and investigate user interfaces that effectively communicate the geometric intuition of the GS principle to non-expert DMs.

7. Conclusions

In summary, this study advances GDM methodology by rigorously extending the GS principle to complex spherical fuzzy environments and providing quantitative evidence of its advantages over conventional approaches. The proposed framework balances theoretical elegance with practical applicability, delivering measurable improvements in decision stability and discriminability. A rigorous theoretical justification has been established, comprising four formal properties (self-similarity, optimal balance, convergence/fixed point, and geometric center) that mathematically justify the use of the GS ratio as aggregation weights in Eq (3.4). Sensitivity analysis (±50% variations on attribute and DM weights, generating 18 test scenarios) and comprehensive comparisons with CSFN-TOPSIS and traditional entropy-weighted methods have further validated the robustness of the proposed approach. By clearly delineating its limitations and outlining concrete directions for future research, the work aims to inspire continued exploration at the intersection of classical mathematics, fuzzy logic, and decision science, ultimately contributing to more robust and reliable decision-support systems.

Appendix

Procedure for constructing the golden evaluation matrix IE_G

This section details the pseudocode implementation for constructing the golden evaluation matrix IE_G, corresponding to Step 3 of the proposed methodology.

Input : Parameters for all criteria and alternatives: $\mu^r_{pq}, \eta^r_{pq}, \nu^r_{pq}; f^r_{pq}, g^r_{pq}, h^r_{pq}$; Minimum matrices: $\mu^{min}_{pq}, \eta^{min}_{pq}, \nu^{min}_{pq}; f^{min}_{pq}, g^{min}_{pq}, h^{min}_{pq}$; Maximum matrices: $\mu^{max}_{pq}, \eta^{max}_{pq}, \nu^{max}_{pq}; f^{max}_{pq}, g^{max}_{pq}, h^{max}_{pq}$; where $p = 1, \ldots, m$, $q = 1, \ldots, n$.
Output : The golden evaluation matrix $IE_G = (x^G_{pq})_{m\times n}$.

$IE_G \leftarrow$ empty $m \times n$ matrix;
for $p \leftarrow 1$ **to** m **do**
  for $q \leftarrow 1$ **to** n **do**
    $\xi^{min}_{pq} \leftarrow (1 - (1 - (\mu^{min}_{pq})^2)^{0.382})^{1/2}$;
    $o^{min}_{pq} \leftarrow (1 - (1 - (\eta^{min}_{pq})^2)^{0.382})^{1/2}$;
    $\theta^{min}_{pq} \leftarrow (\nu^{min}_{pq})^{0.382}$;
    $u^{min}_{pq} \leftarrow (1 - (1 - (f^{min}_{pq})^2)^{0.382})^{1/2}$;
    $v^{min}_{pq} \leftarrow (1 - (1 - (g^{min}_{pq})^2)^{0.382})^{1/2}$;
    $w^{min}_{pq} \leftarrow (h^{min}_{pq})^{0.382}$;
    $\xi^{max}_{pq} \leftarrow (1 - (1 - (\mu^{max}_{pq})^2)^{0.618})^{1/2}$;
    $o^{max}_{pq} \leftarrow (1 - (1 - (\eta^{max}_{pq})^2)^{0.618})^{1/2}$;
    $\theta^{max}_{pq} \leftarrow (\nu^{max}_{pq})^{0.618}$;
    $u^{max}_{pq} \leftarrow (1 - (1 - (f^{max}_{pq})^2)^{0.618})^{1/2}$;
    $v^{max}_{pq} \leftarrow (1 - (1 - (g^{max}_{pq})^2)^{0.618})^{1/2}$;
    $w^{max}_{pq} \leftarrow (h^{max}_{pq})^{0.618}$;
    $\mu^G_{pq} \leftarrow ((\xi^{min}_{pq})^2 + (\xi^{max}_{pq})^2 - (\xi^{min}_{pq})^2(\xi^{max}_{pq})^2)^{1/2}$;
    $\eta^G_{pq} \leftarrow o^{min}_{pq} \cdot o^{max}_{pq}$;
    $\nu^G_{pq} \leftarrow \theta^{min}_{pq} \cdot \theta^{max}_{pq}$;
    $f^G_{pq} \leftarrow ((u^{min}_{pq})^2 + (u^{max}_{pq})^2 - (u^{min}_{pq})^2(u^{max}_{pq})^2)^{1/2}$;
    $g^G_{pq} \leftarrow v^{min}_{pq} \cdot v^{max}_{pq}$;
    $h^G_{pq} \leftarrow w^{min}_{pq} \cdot w^{max}_{pq}$;
    $x^G_{pq} \leftarrow (\mu^G_{pq} e^{i2\pi f^G_{pq}},\ \eta^G_{pq} e^{i2\pi g^G_{pq}},\ \nu^G_{pq} e^{i2\pi h^G_{pq}})$;
    $IE_G[p, q] \leftarrow x^G_{pq}$;
  end
end
return IE_G $\{IE_G$ is an $m \times n$ matrix$\}$.

Procedure for constructing the golden weighted evaluation matrix WG_G

The following pseudocode implements the construction of the golden weighted evaluation matrix WG_G, which corresponds to Step 13 of the methodology.

Input : Parameters for all decision-makers and criteria: $\iota^p_{rq}, \vartheta^p_{rq}, \kappa^p_{rq}; f'^p_{rq}, g'^p_{rq}, h'^p_{rq}$; Minimum matrices: $\iota^{min}_{rq}, \vartheta^{min}_{rq}, \kappa^{min}_{rq}; f'^{min}_{rq}, g'^{min}_{rq}, h'^{min}_{rq}$; Maximum matrices: $\iota^{max}_{rq}, \vartheta^{max}_{rq}, \kappa^{max}_{rq}; f'^{max}_{rq}, g'^{max}_{rq}, h'^{max}_{rq}$; where $r = 1, \ldots, t$, $q = 1, \ldots, n$.
Output : The golden weighted evaluation matrix $WG_G = (k^G_{rq})_{t\times n}$.

$WG_G \leftarrow$ empty $t \times n$ matrix;
for $r \leftarrow 1$ **to** t **do**
  for $q \leftarrow 1$ **to** n **do**
    $\epsilon^{min}_{rq} \leftarrow \left(1 - (1 - (\iota^{min}_{rq})^2)^{0.382}\right)^{1/2}$;
    $\varepsilon^{min}_{rq} \leftarrow \left(1 - (1 - (\vartheta^{min}_{rq})^2)^{0.382}\right)^{1/2}$;
    $\varsigma^{min}_{rq} \leftarrow (\kappa^{min}_{rq})^{0.382}$;
    $f'^{min}_{rq} \leftarrow \left(1 - (1 - (f'^{min}_{rq})^2)^{0.382}\right)^{1/2}$;
    $g'^{min}_{rq} \leftarrow \left(1 - (1 - (g'^{min}_{rq})^2)^{0.382}\right)^{1/2}$;
    $h'^{min}_{rq} \leftarrow (h'^{min}_{rq})^{0.382}$;
    $\epsilon^{max}_{rq} \leftarrow \left(1 - (1 - (\iota^{max}_{rq})^2)^{0.618}\right)^{1/2}$;
    $\varepsilon^{max}_{rq} \leftarrow \left(1 - (1 - (\vartheta^{max}_{rq})^2)^{0.618}\right)^{1/2}$;
    $\varsigma^{max}_{rq} \leftarrow (\kappa^{max}_{rq})^{0.618}$;
    $f'^{max}_{rq} \leftarrow \left(1 - (1 - (f'^{max}_{rq})^2)^{0.618}\right)^{1/2}$;
    $g'^{max}_{rq} \leftarrow \left(1 - (1 - (g'^{max}_{rq})^2)^{0.618}\right)^{1/2}$;
    $h'^{max}_{rq} \leftarrow (h'^{max}_{rq})^{0.618}$;
    $\epsilon^G_{rq} \leftarrow \left((\epsilon^{min}_{rq})^2 + (\epsilon^{max}_{rq})^2 - (\epsilon^{min}_{rq})^2(\epsilon^{max}_{rq})^2\right)^{1/2}$;
    $\varepsilon^G_{rq} \leftarrow \varepsilon^{min}_{rq} \cdot \varepsilon^{max}_{rq}$;
    $\varsigma^G_{rq} \leftarrow \varsigma^{min}_{rq} \cdot \varsigma^{max}_{rq}$;
    $f'^G_{rq} \leftarrow \left((f'^{min}_{rq})^2 + (f'^{max}_{rq})^2 - (f'^{min}_{rq})^2(f'^{max}_{rq})^2\right)^{1/2}$;
    $g'^G_{rq} \leftarrow g'^{min}_{rq} \cdot g'^{max}_{rq}$;
    $h'^G_{rq} \leftarrow h'^{min}_{rq} \cdot h'^{max}_{rq}$;
    $k^G_{rq} \leftarrow (\epsilon^G_{rq} e^{i2\pi f'^G_{rq}},\ \varepsilon^G_{rq} e^{i2\pi g'^G_{rq}},\ \varsigma^G_{rq} e^{i2\pi h'^G_{rq}})$;
    $WG_G[r, q] \leftarrow k^G_{rq}$;
  end
end
return WG_G $\{WG_G$ is a $t \times n$ matrix$\}$.

Individual evaluation matrices IE_2, IE_3, and IE_4

Table 22. Individual evaluation matrix IE_2 (South region).

Software	u_1	u_2
A_1	$(0.77e^{i2\pi(0.75)}, 0.32e^{i2\pi(0.34)}, 0.44e^{i2\pi(0.46)})$	$(0.44e^{i2\pi(0.40)}, 0.32e^{i2\pi(0.33)}, 0.77e^{i2\pi(0.79)})$
A_2	$(0.83e^{i2\pi(0.80)}, 0.34e^{i2\pi(0.36)}, 0.30e^{i2\pi(0.33)})$	$(0.77e^{i2\pi(0.74)}, 0.32e^{i2\pi(0.37)}, 0.44e^{i2\pi(0.46)})$
A_3	$(0.30e^{i2\pi(0.26)}, 0.34e^{i2\pi(0.35)}, 0.83e^{i2\pi(0.85)})$	$(0.91e^{i2\pi(0.93)}, 0.15e^{i2\pi(0.19)}, 0.21e^{i2\pi(0.23)})$
A_4	$(0.91e^{i2\pi(0.90)}, 0.15e^{i2\pi(0.11)}, 0.21e^{i2\pi(0.24)})$	$(0.83e^{i2\pi(0.80)}, 0.34e^{i2\pi(0.36)}, 0.30e^{i2\pi(0.33)})$
	u_3	u_4
A_1	$(0.65e^{i2\pi(0.61)}, 0.48e^{i2\pi(0.51)}, 0.55e^{i2\pi(0.58)})$	$(0.77e^{i2\pi(0.74)}, 0.32e^{i2\pi(0.35)}, 0.44e^{i2\pi(0.47)})$
A_2	$(0.83e^{i2\pi(0.82)}, 0.34e^{i2\pi(0.36)}, 0.30e^{i2\pi(0.35)})$	$(0.44e^{i2\pi(0.41)}, 0.32e^{i2\pi(0.33)}, 0.77e^{i2\pi(0.81)})$
A_3	$(0.65e^{i2\pi(0.61)}, 0.48e^{i2\pi(0.51)}, 0.55e^{i2\pi(0.59)})$	$(0.77e^{i2\pi(0.73)}, 0.32e^{i2\pi(0.35)}, 0.44e^{i2\pi(0.47)})$
A_4	$(0.83e^{i2\pi(0.81)}, 0.32e^{i2\pi(0.34)}, 0.30e^{i2\pi(0.34)})$	$(0.77e^{i2\pi(0.74)}, 0.34e^{i2\pi(0.37)}, 0.44e^{i2\pi(0.48)})$

Table 23. Individual evaluation matrix IE_3 (East region).

Software	u_1	u_2
A_1	$(0.83e^{i2\pi(0.80)}, 0.34e^{i2\pi(0.36)}, 0.30e^{i2\pi(0.33)})$	$(0.65e^{i2\pi(0.61)}, 0.48e^{i2\pi(0.50)}, 0.55e^{i2\pi(0.58)})$
A_2	$(0.65e^{i2\pi(0.62)}, 0.48e^{i2\pi(0.51)}, 0.55e^{i2\pi(0.57)})$	$(0.30e^{i2\pi(0.27)}, 0.34e^{i2\pi(0.37)}, 0.83e^{i2\pi(0.85)})$
A_3	$(0.65e^{i2\pi(0.61)}, 0.48e^{i2\pi(0.52)}, 0.55e^{i2\pi(0.57)})$	$(0.21e^{i2\pi(0.19)}, 0.15e^{i2\pi(0.13)}, 0.91e^{i2\pi(0.94)})$
A_4	$(0.83e^{i2\pi(0.81)}, 0.34e^{i2\pi(0.34)}, 0.30e^{i2\pi(0.35)})$	$(0.91e^{i2\pi(0.92)}, 0.15e^{i2\pi(0.17)}, 0.21e^{i2\pi(0.23)})$
	u_3	u_4
A_1	$(0.44e^{i2\pi(0.41)}, 0.32e^{i2\pi(0.36)}, 0.77e^{i2\pi(0.79)})$	$(0.44e^{i2\pi(0.42)}, 0.32e^{i2\pi(0.35)}, 0.77e^{i2\pi(0.80)})$
A_2	$(0.44e^{i2\pi(0.42)}, 0.32e^{i2\pi(0.36)}, 0.77e^{i2\pi(0.80)})$	$(0.83e^{i2\pi(0.80)}, 0.34e^{i2\pi(0.38)}, 0.30e^{i2\pi(0.35)})$
A_3	$(0.30e^{i2\pi(0.26)}, 0.32e^{i2\pi(0.37)}, 0.83e^{i2\pi(0.86)})$	$(0.83e^{i2\pi(0.79)}, 0.34e^{i2\pi(0.35)}, 0.30e^{i2\pi(0.36)})$
A_4	$(0.94e^{i2\pi(0.96)}, 0.17e^{i2\pi(0.19)}, 0.18e^{i2\pi(0.13)})$	$(0.77e^{i2\pi(0.72)}, 0.32e^{i2\pi(0.34)}, 0.44e^{i2\pi(0.45)})$

Table 24. Individual evaluation matrix IE_4 (West region).

Software	u_1	u_2
A_1	$(0.77e^{i2\pi(0.72)}, 0.32e^{i2\pi(0.33)}, 0.44e^{i2\pi(0.46)})$	$(0.44e^{i2\pi(0.41)}, 0.32e^{i2\pi(0.35)}, 0.77e^{i2\pi(0.79)})$
A_2	$(0.65e^{i2\pi(0.62)}, 0.48e^{i2\pi(0.49)}, 0.55e^{i2\pi(0.58)})$	$(0.77e^{i2\pi(0.73)}, 0.32e^{i2\pi(0.34)}, 0.44e^{i2\pi(0.46)})$
A_3	$(0.30e^{i2\pi(0.26)}, 0.34e^{i2\pi(0.37)}, 0.83e^{i2\pi(0.85)})$	$(0.44e^{i2\pi(0.41)}, 0.32e^{i2\pi(0.33)}, 0.77e^{i2\pi(0.80)})$
A_4	$(0.83e^{i2\pi(0.81)}, 0.34e^{i2\pi(0.35)}, 0.30e^{i2\pi(0.33)})$	$(0.91e^{i2\pi(0.90)}, 0.15e^{i2\pi(0.17)}, 0.21e^{i2\pi(0.26)})$
	u_3	u_4
A_1	$(0.30e^{i2\pi(0.27)}, 0.34e^{i2\pi(0.36)}, 0.83e^{i2\pi(0.85)})$	$(0.65e^{i2\pi(0.61)}, 0.48e^{i2\pi(0.51)}, 0.55e^{i2\pi(0.59)})$
A_2	$(0.30e^{i2\pi(0.28)}, 0.34e^{i2\pi(0.35)}, 0.83e^{i2\pi(0.85)})$	$(0.83e^{i2\pi(0.80)}, 0.34e^{i2\pi(0.36)}, 0.30e^{i2\pi(0.32)})$
A_3	$(0.21e^{i2\pi(0.18)}, 0.15e^{i2\pi(0.16)}, 0.91e^{i2\pi(0.93)})$	$(0.65e^{i2\pi(0.61)}, 0.48e^{i2\pi(0.50)}, 0.55e^{i2\pi(0.58)})$
A_4	$(0.91e^{i2\pi(0.89)}, 0.15e^{i2\pi(0.18)}, 0.21e^{i2\pi(0.25)})$	$(0.77e^{i2\pi(0.77)}, 0.32e^{i2\pi(0.35)}, 0.44e^{i2\pi(0.45)})$

DM-weighted evaluation matrices IW_2, IW_3 and IW_4

Table 25. DM-weighted evaluation matrix IW_2.

Software	u_1	u_2
A_1	$(0.45e^{i2\pi(0.43)}, 0.16e^{i2\pi(0.17)}, 0.82e^{i2\pi(0.82)})$	$(0.23e^{i2\pi(0.21)}, 0.16e^{i2\pi(0.17)}, 0.94e^{i2\pi(0.94)})$
A_2	$(0.50e^{i2\pi(0.47)}, 0.17e^{i2\pi(0.18)}, 0.74e^{i2\pi(0.76)})$	$(0.45e^{i2\pi(0.42)}, 0.16e^{i2\pi(0.19)}, 0.82e^{i2\pi(0.82)})$
A_3	$(0.15e^{i2\pi(0.13)}, 0.17e^{i2\pi(0.18)}, 0.95e^{i2\pi(0.96)})$	$(0.60e^{i2\pi(0.63)}, 0.08e^{i2\pi(0.10)}, 0.68e^{i2\pi(0.69)})$
A_4	$(0.60e^{i2\pi(0.58)}, 0.08e^{i2\pi(0.06)}, 0.68e^{i2\pi(0.70)})$	$(0.50e^{i2\pi(0.47)}, 0.17e^{i2\pi(0.18)}, 0.74e^{i2\pi(0.76)})$
	u_3	u_4
A_1	$(0.36e^{i2\pi(0.33)}, 0.25e^{i2\pi(0.27)}, 0.86e^{i2\pi(0.87)})$	$(0.45e^{i2\pi(0.42)}, 0.16e^{i2\pi(0.18)}, 0.82e^{i2\pi(0.83)})$
A_2	$(0.50e^{i2\pi(0.49)}, 0.17e^{i2\pi(0.18)}, 0.74e^{i2\pi(0.77)})$	$(0.23e^{i2\pi(0.21)}, 0.16e^{i2\pi(0.17)}, 0.94e^{i2\pi(0.95)})$
A_3	$(0.36e^{i2\pi(0.33)}, 0.25e^{i2\pi(0.27)}, 0.86e^{i2\pi(0.88)})$	$(0.45e^{i2\pi(0.42)}, 0.16e^{i2\pi(0.18)}, 0.82e^{i2\pi(0.83)})$
A_4	$(0.50e^{i2\pi(0.48)}, 0.16e^{i2\pi(0.17)}, 0.74e^{i2\pi(0.76)})$	$(0.45e^{i2\pi(0.42)}, 0.17e^{i2\pi(0.19)}, 0.82e^{i2\pi(0.83)})$

Table 26. DM-weighted evaluation matrix IW_3.

Software	u_1	u_2
A_1	$(0.50e^{i2\pi(0.48)}, 0.17e^{i2\pi(0.19)}, 0.74e^{i2\pi(0.76)})$	$(0.36e^{i2\pi(0.33)}, 0.25e^{i2\pi(0.26)}, 0.86e^{i2\pi(0.87)})$
A_2	$(0.36e^{i2\pi(0.34)}, 0.25e^{i2\pi(0.27)}, 0.86e^{i2\pi(0.87)})$	$(0.15e^{i2\pi(0.14)}, 0.17e^{i2\pi(0.19)}, 0.95e^{i2\pi(0.96)})$
A_3	$(0.36e^{i2\pi(0.33)}, 0.25e^{i2\pi(0.28)}, 0.86e^{i2\pi(0.87)})$	$(0.11e^{i2\pi(0.10)}, 0.08e^{i2\pi(0.07)}, 0.98e^{i2\pi(0.98)})$
A_4	$(0.50e^{i2\pi(0.49)}, 0.17e^{i2\pi(0.17)}, 0.74e^{i2\pi(0.77)})$	$(0.60e^{i2\pi(0.61)}, 0.08e^{i2\pi(0.09)}, 0.68e^{i2\pi(0.69)})$
	u_3	u_4
A_1	$(0.23e^{i2\pi(0.21)}, 0.16e^{i2\pi(0.19)}, 0.94e^{i2\pi(0.94)})$	$(0.23e^{i2\pi(0.22)}, 0.16e^{i2\pi(0.18)}, 0.94e^{i2\pi(0.95)})$
A_2	$(0.23e^{i2\pi(0.22)}, 0.16e^{i2\pi(0.19)}, 0.94e^{i2\pi(0.95)})$	$(0.50e^{i2\pi(0.48)}, 0.17e^{i2\pi(0.20)}, 0.74e^{i2\pi(0.77)})$
A_3	$(0.15e^{i2\pi(0.13)}, 0.17e^{i2\pi(0.19)}, 0.95e^{i2\pi(0.96)})$	$(0.50e^{i2\pi(0.47)}, 0.17e^{i2\pi(0.18)}, 0.74e^{i2\pi(0.77)})$
A_4	$(0.65e^{i2\pi(0.69)}, 0.09e^{i2\pi(0.10)}, 0.65e^{i2\pi(0.60)})$	$(0.45e^{i2\pi(0.41)}, 0.16e^{i2\pi(0.17)}, 0.81e^{i2\pi(0.82)})$

Table 27. DM-weighted evaluation matrix IW_4.

Software	u_1	u_2
A_1	$(0.45e^{i2\pi(0.41)}, 0.16e^{i2\pi(0.17)}, 0.81e^{i2\pi(0.82)})$	$(0.23e^{i2\pi(0.21)}, 0.16e^{i2\pi(0.18)}, 0.94e^{i2\pi(0.94)})$
A_2	$(0.36e^{i2\pi(0.34)}, 0.25e^{i2\pi(0.26)}, 0.86e^{i2\pi(0.87)})$	$(0.45e^{i2\pi(0.42)}, 0.16e^{i2\pi(0.17)}, 0.81e^{i2\pi(0.82)})$
A_3	$(0.15e^{i2\pi(0.13)}, 0.17e^{i2\pi(0.19)}, 0.95e^{i2\pi(0.96)})$	$(0.23e^{i2\pi(0.21)}, 0.16e^{i2\pi(0.17)}, 0.94e^{i2\pi(0.95)})$
A_4	$(0.50e^{i2\pi(0.48)}, 0.17e^{i2\pi(0.18)}, 0.74e^{i2\pi(0.76)})$	$(0.60e^{i2\pi(0.58)}, 0.08e^{i2\pi(0.09)}, 0.68e^{i2\pi(0.71)})$
	u_3	u_4
A_1	$(0.15e^{i2\pi(0.14)}, 0.17e^{i2\pi(0.18)}, 0.95e^{i2\pi(0.96)})$	$(0.36e^{i2\pi(0.33)}, 0.25e^{i2\pi(0.27)}, 0.86e^{i2\pi(0.88)})$
A_2	$(0.15e^{i2\pi(0.14)}, 0.17e^{i2\pi(0.18)}, 0.95e^{i2\pi(0.96)})$	$(0.50e^{i2\pi(0.47)}, 0.17e^{i2\pi(0.18)}, 0.74e^{i2\pi(0.75)})$
A_3	$(0.11e^{i2\pi(0.09)}, 0.08e^{i2\pi(0.08)}, 0.98e^{i2\pi(0.98)})$	$(0.36e^{i2\pi(0.33)}, 0.25e^{i2\pi(0.26)}, 0.86e^{i2\pi(0.87)})$
A_4	$(0.60e^{i2\pi(0.57)}, 0.08e^{i2\pi(0.09)}, 0.68e^{i2\pi(0.71)})$	$(0.45e^{i2\pi(0.45)}, 0.16e^{i2\pi(0.18)}, 0.81e^{i2\pi(0.82)})$

Group evaluation matrices GE_2, GE_3, and GE_4

Table 28. Group evaluation matrix GE_2.

DM	u_1	u_2
d_1	$(0.36e^{i2\pi(0.34)}, 0.25e^{i2\pi(0.28)}, 0.86e^{i2\pi(0.87)})$	$(0.23e^{i2\pi(0.21)}, 0.16e^{i2\pi(0.17)}, 0.94e^{i2\pi(0.95)})$
d_2	$(0.50e^{i2\pi(0.47)}, 0.17e^{i2\pi(0.18)}, 0.74e^{i2\pi(0.76)})$	$(0.45e^{i2\pi(0.42)}, 0.16e^{i2\pi(0.19)}, 0.82e^{i2\pi(0.82)})$
d_3	$(0.36e^{i2\pi(0.34)}, 0.25e^{i2\pi(0.27)}, 0.86e^{i2\pi(0.87)})$	$(0.15e^{i2\pi(0.14)}, 0.17e^{i2\pi(0.19)}, 0.95e^{i2\pi(0.96)})$
d_4	$(0.36e^{i2\pi(0.34)}, 0.25e^{i2\pi(0.26)}, 0.86e^{i2\pi(0.87)})$	$(0.45e^{i2\pi(0.42)}, 0.16e^{i2\pi(0.17)}, 0.81e^{i2\pi(0.82)})$
	u_3	u_4
d_1	$(0.50e^{i2\pi(0.47)}, 0.17e^{i2\pi(0.18)}, 0.74e^{i2\pi(0.76)})$	$(0.23e^{i2\pi(0.21)}, 0.16e^{i2\pi(0.17)}, 0.94e^{i2\pi(0.95)})$
d_2	$(0.50e^{i2\pi(0.49)}, 0.17e^{i2\pi(0.18)}, 0.74e^{i2\pi(0.77)})$	$(0.23e^{i2\pi(0.21)}, 0.16e^{i2\pi(0.17)}, 0.94e^{i2\pi(0.95)})$
d_3	$(0.23e^{i2\pi(0.22)}, 0.16e^{i2\pi(0.19)}, 0.94e^{i2\pi(0.95)})$	$(0.50e^{i2\pi(0.47)}, 0.17e^{i2\pi(0.20)}, 0.74e^{i2\pi(0.77)})$
d_4	$(0.15e^{i2\pi(0.14)}, 0.17e^{i2\pi(0.18)}, 0.95e^{i2\pi(0.96)})$	$(0.50e^{i2\pi(0.47)}, 0.17e^{i2\pi(0.18)}, 0.74e^{i2\pi(0.75)})$

Table 29. Group evaluation matrix GE_3.

DM	u_1	u_2
d_1	$(0.50e^{i2\pi(0.47)}, 0.17e^{i2\pi(0.18)}, 0.74e^{i2\pi(0.76)})$	$(0.60e^{i2\pi(0.56)}, 0.08e^{i2\pi(0.09)}, 0.68e^{i2\pi(0.69)})$
d_2	$(0.15e^{i2\pi(0.13)}, 0.17e^{i2\pi(0.18)}, 0.95e^{i2\pi(0.96)})$	$(0.60e^{i2\pi(0.63)}, 0.08e^{i2\pi(0.10)}, 0.68e^{i2\pi(0.69)})$
d_3	$(0.36e^{i2\pi(0.33)}, 0.25e^{i2\pi(0.28)}, 0.86e^{i2\pi(0.87)})$	$(0.11e^{i2\pi(0.10)}, 0.08e^{i2\pi(0.07)}, 0.98e^{i2\pi(0.98)})$
d_4	$(0.15e^{i2\pi(0.13)}, 0.17e^{i2\pi(0.19)}, 0.95e^{i2\pi(0.96)})$	$(0.23e^{i2\pi(0.21)}, 0.16e^{i2\pi(0.17)}, 0.94e^{i2\pi(0.95)})$
	u_3	u_4
d_1	$(0.36e^{i2\pi(0.33)}, 0.25e^{i2\pi(0.26)}, 0.86e^{i2\pi(0.87)})$	$(0.45e^{i2\pi(0.42)}, 0.16e^{i2\pi(0.17)}, 0.81e^{i2\pi(0.83)})$
d_2	$(0.36e^{i2\pi(0.33)}, 0.25e^{i2\pi(0.27)}, 0.86e^{i2\pi(0.88)})$	$(0.45e^{i2\pi(0.42)}, 0.16e^{i2\pi(0.18)}, 0.82e^{i2\pi(0.83)})$
d_3	$(0.15e^{i2\pi(0.13)}, 0.17e^{i2\pi(0.19)}, 0.95e^{i2\pi(0.96)})$	$(0.50e^{i2\pi(0.47)}, 0.17e^{i2\pi(0.18)}, 0.74e^{i2\pi(0.77)})$
d_4	$(0.11e^{i2\pi(0.09)}, 0.08e^{i2\pi(0.08)}, 0.98e^{i2\pi(0.98)})$	$(0.36e^{i2\pi(0.33)}, 0.25e^{i2\pi(0.26)}, 0.86e^{i2\pi(0.87)})$

Table 30. Group evaluation matrix GE_4.

DM	u_1	u_2
d_1	$(0.60e^{i2\pi(0.57)}, 0.08e^{i2\pi(0.09)}, 0.68e^{i2\pi(0.70)})$	$(0.50e^{i2\pi(0.47)}, 0.17e^{i2\pi(0.18)}, 0.74e^{i2\pi(0.76)})$
d_2	$(0.60e^{i2\pi(0.58)}, 0.08e^{i2\pi(0.06)}, 0.68e^{i2\pi(0.70)})$	$(0.50e^{i2\pi(0.47)}, 0.17e^{i2\pi(0.18)}, 0.74e^{i2\pi(0.76)})$
d_3	$(0.50e^{i2\pi(0.48)}, 0.17e^{i2\pi(0.17)}, 0.74e^{i2\pi(0.77)})$	$(0.60e^{i2\pi(0.61)}, 0.08e^{i2\pi(0.09)}, 0.68e^{i2\pi(0.69)})$
d_4	$(0.50e^{i2\pi(0.48)}, 0.17e^{i2\pi(0.18)}, 0.74e^{i2\pi(0.76)})$	$(0.60e^{i2\pi(0.58)}, 0.08e^{i2\pi(0.09)}, 0.68e^{i2\pi(0.71)})$
	u_3	u_4
d_1	$(0.45e^{i2\pi(0.42)}, 0.16e^{i2\pi(0.18)}, 0.81e^{i2\pi(0.83)})$	$(0.50e^{i2\pi(0.47)}, 0.17e^{i2\pi(0.18)}, 0.74e^{i2\pi(0.76)})$
d_2	$(0.50e^{i2\pi(0.48)}, 0.16e^{i2\pi(0.17)}, 0.74e^{i2\pi(0.76)})$	$(0.45e^{i2\pi(0.42)}, 0.17e^{i2\pi(0.19)}, 0.82e^{i2\pi(0.83)})$
d_3	$(0.64e^{i2\pi(0.69)}, 0.09e^{i2\pi(0.10)}, 0.65e^{i2\pi(0.60)})$	$(0.45e^{i2\pi(0.41)}, 0.16e^{i2\pi(0.17)}, 0.81e^{i2\pi(0.82)})$
d_4	$(0.60e^{i2\pi(0.57)}, 0.08e^{i2\pi(0.09)}, 0.68e^{i2\pi(0.71)})$	$(0.45e^{i2\pi(0.45)}, 0.16e^{i2\pi(0.18)}, 0.81e^{i2\pi(0.82)})$

Weighted group evaluation matrices WG_2, WG_3, and WG_4

Table 31. Weighted group evaluation matrix WG_2.

DM	u_1	u_2
d_1	$(0.20e^{i2\pi(0.19)}, 0.14e^{i2\pi(0.15)}, 0.96e^{i2\pi(0.96)})$	$(0.13e^{i2\pi(0.12)}, 0.09e^{i2\pi(0.10)}, 0.98e^{i2\pi(0.98)})$
d_2	$(0.29e^{i2\pi(0.27)}, 0.10e^{i2\pi(0.10)}, 0.91e^{i2\pi(0.92)})$	$(0.25e^{i2\pi(0.24)}, 0.09e^{i2\pi(0.10)}, 0.94e^{i2\pi(0.94)})$
d_3	$(0.20e^{i2\pi(0.19)}, 0.14e^{i2\pi(0.15)}, 0.96e^{i2\pi(0.96)})$	$(0.08e^{i2\pi(0.08)}, 0.10e^{i2\pi(0.11)}, 0.99e^{i2\pi(0.99)})$
d_4	$(0.20e^{i2\pi(0.19)}, 0.14e^{i2\pi(0.14)}, 0.96e^{i2\pi(0.96)})$	$(0.26e^{i2\pi(0.24)}, 0.09e^{i2\pi(0.10)}, 0.94e^{i2\pi(0.94)})$
	u_3	u_4
d_1	$(0.24e^{i2\pi(0.22)}, 0.08e^{i2\pi(0.08)}, 0.94e^{i2\pi(0.95)})$	$(0.10e^{i2\pi(0.10)}, 0.07e^{i2\pi(0.08)}, 0.99e^{i2\pi(0.99)})$
d_2	$(0.24e^{i2\pi(0.23)}, 0.08e^{i2\pi(0.08)}, 0.94e^{i2\pi(0.95)})$	$(0.10e^{i2\pi(0.10)}, 0.07e^{i2\pi(0.08)}, 0.99e^{i2\pi(0.99)})$
d_3	$(0.10e^{i2\pi(0.10)}, 0.07e^{i2\pi(0.08)}, 0.99e^{i2\pi(0.99)})$	$(0.24e^{i2\pi(0.22)}, 0.08e^{i2\pi(0.09)}, 0.94e^{i2\pi(0.95)})$
d_4	$(0.07e^{i2\pi(0.06)}, 0.08e^{i2\pi(0.08)}, 0.99e^{i2\pi(0.99)})$	$(0.24e^{i2\pi(0.22)}, 0.08e^{i2\pi(0.08)}, 0.94e^{i2\pi(0.94)})$

Table 32. Weighted group evaluation matrix WG_3.

DM	u_1	u_2
d_1	$(0.29e^{i2\pi(0.27)}, 0.10e^{i2\pi(0.10)}, 0.91e^{i2\pi(0.92)})$	$(0.35e^{i2\pi(0.32)}, 0.04e^{i2\pi(0.05)}, 0.89e^{i2\pi(0.90)})$
d_2	$(0.08e^{i2\pi(0.07)}, 0.10e^{i2\pi(0.10)}, 0.99e^{i2\pi(0.99)})$	$(0.35e^{i2\pi(0.37)}, 0.04e^{i2\pi(0.05)}, 0.89e^{i2\pi(0.90)})$
d_3	$(0.20e^{i2\pi(0.19)}, 0.14e^{i2\pi(0.15)}, 0.96e^{i2\pi(0.96)})$	$(0.06e^{i2\pi(0.05)}, 0.04e^{i2\pi(0.04)}, 0.99e^{i2\pi(1.00)})$
d_4	$(0.08e^{i2\pi(0.07)}, 0.10e^{i2\pi(0.10)}, 0.99e^{i2\pi(0.99)})$	$(0.13e^{i2\pi(0.12)}, 0.09e^{i2\pi(0.09)}, 0.98e^{i2\pi(0.98)})$
	u_3	u_4
d_1	$(0.16e^{i2\pi(0.15)}, 0.11e^{i2\pi(0.12)}, 0.97e^{i2\pi(0.97)})$	$(0.21e^{i2\pi(0.19)}, 0.07e^{i2\pi(0.08)}, 0.96e^{i2\pi(0.96)})$
d_2	$(0.16e^{i2\pi(0.15)}, 0.11e^{i2\pi(0.12)}, 0.97e^{i2\pi(0.97)})$	$(0.21e^{i2\pi(0.19)}, 0.07e^{i2\pi(0.08)}, 0.96e^{i2\pi(0.96)})$
d_3	$(0.07e^{i2\pi(0.06)}, 0.08e^{i2\pi(0.09)}, 0.99e^{i2\pi(0.99)})$	$(0.24e^{i2\pi(0.22)}, 0.08e^{i2\pi(0.08)}, 0.94e^{i2\pi(0.95)})$
d_4	$(0.05e^{i2\pi(0.04)}, 0.03e^{i2\pi(0.04)}, 1.00e^{i2\pi(1.00)})$	$(0.16e^{i2\pi(0.15)}, 0.11e^{i2\pi(0.12)}, 0.97e^{i2\pi(0.97)})$

Table 33. Weighted group evaluation matrix WG_4.

DM	u_1	u_2
d_1	$(0.35e^{i2\pi(0.33)}, 0.04e^{i2\pi(0.05)}, 0.89e^{i2\pi(0.90)})$	$(0.29e^{i2\pi(0.27)}, 0.10e^{i2\pi(0.10)}, 0.91e^{i2\pi(0.92)})$
d_2	$(0.35e^{i2\pi(0.34)}, 0.04e^{i2\pi(0.03)}, 0.89e^{i2\pi(0.90)})$	$(0.29e^{i2\pi(0.27)}, 0.10e^{i2\pi(0.10)}, 0.91e^{i2\pi(0.92)})$
d_3	$(0.29e^{i2\pi(0.28)}, 0.10e^{i2\pi(0.10)}, 0.91e^{i2\pi(0.92)})$	$(0.35e^{i2\pi(0.36)}, 0.04e^{i2\pi(0.05)}, 0.89e^{i2\pi(0.90)})$
d_4	$(0.29e^{i2\pi(0.28)}, 0.10e^{i2\pi(0.10)}, 0.91e^{i2\pi(0.92)})$	$(0.35e^{i2\pi(0.34)}, 0.04e^{i2\pi(0.05)}, 0.89e^{i2\pi(0.90)})$
	u_3	u_4
d_1	$(0.21e^{i2\pi(0.20)}, 0.07e^{i2\pi(0.08)}, 0.96e^{i2\pi(0.96)})$	$(0.24e^{i2\pi(0.22)}, 0.08e^{i2\pi(0.08)}, 0.94e^{i2\pi(0.95)})$
d_2	$(0.24e^{i2\pi(0.23)}, 0.07e^{i2\pi(0.08)}, 0.94e^{i2\pi(0.95)})$	$(0.21e^{i2\pi(0.20)}, 0.08e^{i2\pi(0.09)}, 0.96e^{i2\pi(0.96)})$
d_3	$(0.32e^{i2\pi(0.35)}, 0.04e^{i2\pi(0.04)}, 0.92e^{i2\pi(0.90)})$	$(0.21e^{i2\pi(0.19)}, 0.07e^{i2\pi(0.08)}, 0.96e^{i2\pi(0.96)})$
d_4	$(0.29e^{i2\pi(0.27)}, 0.03e^{i2\pi(0.04)}, 0.92e^{i2\pi(0.93)})$	$(0.21e^{i2\pi(0.21)}, 0.07e^{i2\pi(0.08)}, 0.96e^{i2\pi(0.96)})$

Use of Generative-AI tools declaration

The author declares that no generative artificial intelligence (AI) tools have been utilized in the preparation of this manuscript.

Acknowledgments

This work was supported by the National Key R&D Program of China (No. 2024YFC3308004).

Conflict of interest

The author declares that there is no conflict of interest.

References

1. International Organization for Standardization and International Electrotechnical Commission, *Systems and software engineering – Systems and software Quality Requirements and Evaluation (SQuaRE) – System and software quality models*, International Standard ISO/IEC 25010:2011, ISO/IEC, Geneva, Switzerland, 2011. Available from: `https://www.iso.org/standard/35733.html`
2. T. Lima Bicalho Cruz, CepstralVox: A user-friendly open-source tool for cepstral Voice analysis, *Journal of Voice*, In press.
3. ANSI/IEEE, IEEE Standard Software Quality Assurance Plans, *Std 730-1984 (Revision of ANSI/IEEE Std 730-1981)*, 1–12.
4. J. Stankowski, A. Dziembowski, Version [8.0] – [IV-PSNR: Software for immersive video objective quality evaluation], *SoftwareX*, **33** (2026), 102487.
5. Z. Chen, K. K. Leung, S. Wang, L. Tassiulas, K. Chan, P. J. Baker, Multi-policy reinforcement learning for network resource allocation with periodic behaviors, *Comput. Netw.*, **272** (2025), 111645. https://doi.org/10.1016/j.comnet.2025.111645
6. J. Lin, T. Jin, G. Li, Optimizing the performance of hydrogen storage reactors using triply periodic minimal surface, *Int. J. Hydrogen Energ.*, **200** (2026), 152702. https://doi.org/10.1016/j.ijhydene.2025.152702
7. J. Kim, M. Johar, M. Khouja, J. Zhou, Optimal information system security investment: A control-theoretic approach to balancing continuous maintenance and periodic upgrades, *Eur. J. Oper. Res.*, **332** (2025), 209–232.
8. M. F. Cheranchery, V. Vijay, An integrated RISA-machine learning framework to enhance user satisfaction through quality assessment and prioritization of railway facilities, *Travel Behav. Soc.*, **41** (2025), 101091. https://doi.org/10.1016/j.tbs.2025.101091
9. F. Liu, Z. Li, K. Yang, F. Chen, J. Yu, MmPiFNN: A multi-mode physics-informed fuzzy neural network for passive recognition of surface ships by underwater equipment using ship radiated noise signals, *Def. Technol.*, **59** (2026), 243–266.
10. T. Mahmood, H. M. Waqas, U. ur Rehman, D. Pamucar, Mathematical Analysis of Real-Time Data Processing Methods for IoT Applications Based on Hesitant Bipolar Fuzzy Dombi Power Operators, *Syst. Soft Comput.*, **8** (2026), 200444. https://doi.org/10.1016/j.sasc.2026.200444
11. Z. Yue, Deriving decision maker's weights based on distance measure for interval-valued intuitionistic fuzzy group decision making, *Expert Syst. Appl.*, **38** (2011), 11665–11670. https://doi.org/10.1016/j.eswa.2011.03.046

12. H. Wan, S. Zeng, Gaussian mixture model-based pythagorean fuzzy multi-criteria group decision-making method and its application in "zero-waste city" evaluation, *Inform. Sciences*, **735** (2026), 123080. https://doi.org/10.1016/j.ins.2026.123080
13. C. Yue, A novel method for large-scale group decision-making with application to e-commerce software system evaluation, *Appl. Soft Comput.*, **191** (2026), 114595. https://doi.org/10.1016/j.asoc.2026.114595
14. C. Yue, R. Huang, D. Towey, L. Zhou, A median-based fuzzy approach to software quality evaluation, *Tsinghua Sci. Technol.*, **30** (2025), 2146–2168. https://doi.org/10.26599/TST.2024.9010103
15. Z. Yue, Extension of TOPSIS to determine weight of decision maker for group decision making problems with uncertain information, *Expert Syst. Appl.*, **39** (2012), 6343–6350. https://doi.org/10.1016/j.eswa.2011.12.016
16. P. Liu, Y. Qian, R. Dang, T. Fei, P. Wang, Multi-attribute group consensus decision-making with two-stage trust risk adjustment, *Inform. Sciences*, **739** (2026), 123162. https://doi.org/10.1016/j.ins.2026.123162
17. G. Dolinar, P. Grošelj, GIBSU-DEMATEL: Enhancing group decision-making by integrating expert satisfaction and uncertainty in interval judgments, *Expert Syst. Appl.*, **308** (2026), 131141. https://doi.org/10.1016/j.eswa.2026.131141
18. M. Akram, C. Kahraman, K. Zahid, Group decision-making based on complex spherical fuzzy VIKOR approach, *Knowledge-Based Syst.*, **216** (2021), 106793. https://doi.org/10.1016/j.knosys.2021.106793
19. E. Cuevas, L. Enríquez, D. Zaldívar, M. Pérez-Cisneros, A selection method for evolutionary algorithms based on the Golden Section, *Expert Syst. Appl.*, **106** (2018), 183–196. https://doi.org/10.1016/j.eswa.2018.03.064
20. G. Luo, J. Fan, Y. Li, X. Ma, Enhancing evolutionary multitask optimization by multi-dimensional scaling and golden section search, *Expert Syst, Appl,*, **299** (2026), 129980. https://doi.org/10.1016/j.eswa.2025.129980
21. G. Yang, M. Ren, X. Hao, Multi-criteria decision-making problem based on the novel probabilistic hesitant fuzzy entropy and TODIM method, *Alex. Eng. J.*, **68** (2023), 437–451. https://doi.org/10.1016/j.aej.2023.01.014
22. K. Kumar, S. M. Chen, Group decision making based on entropy measure of Pythagorean fuzzy sets and Pythagorean fuzzy weighted arithmetic mean aggregation operator of Pythagorean fuzzy numbers, *Inf. Sci.*, **624** (2023), 361–377. https://doi.org/10.1016/j.ins.2022.12.064
23. Z. Yue, Group decision making with multi-attribute interval data, *Inf. Fusion*, **14** (2013), 551–561. https://doi.org/10.1016/j.inffus.2013.01.003
24. L. Zadeh, Fuzzy sets, *Inf. Control*, **8** (1965), 338–353. https://doi.org/10.1016/S0019-9958(65)90241-X
25. K. Atanassov, Intuitionistic fuzzy sets, *Fuzzy Set. Syst.*, **20** (1986), 87–96. https://doi.org/10.1016/S0165-0114(86)80034-3
26. R. R. Yager, Pythagorean membership grades in multicriteria decision making, *IEEE T. Fuzzy Syst.*, **22** (2014), 958–965. https://doi.org/10.1109/TFUZZ.2013.2278989
27. B. C. Cuong, Picture fuzzy sets, *J. Comput. Sci. Cybern.*, **30** (2014), 409–420.

28. T. Mahmood, K. Ullah, Q. Khan, N. Jan, An approach toward decision-making and medical diagnosis problems using the concept of spherical fuzzy sets, *Neural Comput. Appl.*, **31** (2019), 7041–7053. https://doi.org/10.1007/s00521-018-3521-2
29. D. Ramot, R. Milo, M. Friedman, A. Kandel, Complex fuzzy sets, *IEEE T. Fuzzy Syst.*, **10** (2002), 171–186. https://doi.org/10.1109/91.995119
30. A. S. Alkouri, A. R. Salleh, Complex intuitionistic fuzzy sets, *AIP Conference Proceedings*, **1482** (2012), 464–470.
31. K. Ullah, T. Mahmood, Z. Ali, N. Jan, On some distance measures of complex pythagorean fuzzy sets and their applications in pattern recognition, *Complex Intell. Syst.*, **6** (2020), 15–27. https://doi.org/10.1007/s40747-019-0103-6
32. M. Akram, A. Bashir, H. Garg, Decision-making model under complex picture fuzzy hamacher aggregation operators, *Comput. Appl. Math.*, **39** (2020), 226.
33. Z. Ali, T. Mahmood, M. S. Yang, TOPSIS method based on complex spherical fuzzy sets with Bonferroni mean operators, *Mathematics*, **8** (2020), 15–27. https://doi.org/10.55016/ojs/cdm.v15i2.62547
34. D. Boix-Cots, F. Pardo-Bosch, P. Pujadas, A systematic review on multi-criteria group decision-making methods based on weights: Analysis and classification scheme, *Inform. Fusion*, **96** (2023), 16–36. https://doi.org/10.1016/j.inffus.2023.03.004
35. M. Li, Y. Ren, Z. Wang, Y. Xu, W. Pedrycz, Trust risk-aware multiple decision-makers consensus seeking under dynamic social network: towards sustainable post-disaster emergency recovery plan selection, *Expert Syst. Appl.*, **305** (2026), 130834. https://doi.org/10.1016/j.eswa.2025.130834
36. M. Wu, J. Zhao, J. Fan, A hybrid trust network-based consensus model with decision-makers' adjustment willingness in picture fuzzy environment, *Expert Syst. Appl.*, **306** (2026), 130897. https://doi.org/10.1016/j.eswa.2025.130897
37. V. B. Hinsz, Group decision making with responses of a quantitative nature: The theory of social decision schemes for quantities, *Organ. Behav. Hum. Dec.*, **80** (1999), 28–49.
38. C. Yue, A VIKOR-based group decision-making approach to software reliability evaluation, *Soft Comput.*, **26** (2022), 9445–9464. https://doi.org/10.1007/s00500-022-07268-5
39. Z. Yue, A method for group decision-making based on determining weights of decision makers using TOPSIS, *Appl. Math. Model.*, **35** (2011), 1926–1936. https://doi.org/10.1016/j.apm.2010.11.001
40. Z. Yue, Approach to group decision making based on determining the weights of experts by using projection method, *Appl. Math. Model.*, **36** (2012), 2900–2910. https://doi.org/10.1016/j.apm.2011.09.068
41. J. Xu, Z. Wu, A maximizing consensus approach for alternative selection based on uncertain linguistic preference relations, *Comput. Ind. Eng.*, **64** (2013), 999–1008. https://doi.org/10.1016/j.cie.2013.01.009
42. S. Wan, H. Yuan, J. Dong, Decision making with incomplete interval multiplicative preference relations based on stochastic program and interval category, *Inf. Sci.*, **570** (2021), 403–427. https://doi.org/10.1016/j.ins.2021.03.005
43. C. Yue, Entropy-based weights on decision makers in group decision-making setting with hybrid preference representations, *Appl. Soft Comput.*, **60** (2017), 737–749. https://doi.org/10.1016/j.asoc.2017.07.033

44. Z. Xu, X. Q. Cai, Deriving weights from interval multiplicative preference relations in group decision making, *Group Decis. Negot.*, **23** (2014), 695–713.
45. W. Liu, Z. Lin, F. Wen, G. Ledwich, Analysis and optimisation of the preferences of decision-makers in black-start group decision-making, *IET Gener., Transm. Dis.*, **7** (2013), 14–23.
46. Y. Wang, H. Chen, Z. Ligang, Logarithm compatibility of interval multiplicative preference relations with an application to determining the optimal weights of experts in the group decision making, *Group Decis. Negot.*, **22** (2013), 759–772. https://doi.org/10.1007/s10726-012-9291-9
47. Y. Zhu, X. Xu, B. Pan, A method for the dynamic collaboration of the public and experts in large-scale group emergency decision-making: Using social media data to evaluate the decision-making quality, *Comput. Ind. Eng.*, **176** (2023), 108943.
48. J. Villodre, J. I. Criado, User roles for emergency management in social media: Understanding actors' behavior during the 2018 Majorca Island flash floods, *Gov. Inform. Q.*, **37** (2020), 101521. https://doi.org/10.1016/j.jwpe.2020.101521
49. S. M. Chen, S. H. Cheng, T. E. Lin, Group decision making systems using group recommendations based on interval fuzzy preference relations and consistency matrices, *Inf. Sci.*, **298** (2015), 555–567. https://doi.org/10.1016/j.ins.2014.11.027
50. Q. Yang, Y. L. Li, K. S. Chin, Constructing novel operational laws and information measures for proportional hesitant fuzzy linguistic term sets with extension to PHFL-VIKOR for group decision making, *Int. J. Comput. Intell. Syst.*, **12** (2019), 998–1018.
51. A. Benavoli, L. Chisci, A. Farina, Fibonacci sequence, golden section, Kalman filter and optimal control, *Signal Proces.*, **89** (2009), 1483–1488. https://doi.org/10.1016/j.sigpro.2009.02.003
52. W. D. Richter, Vector representations of Euler's formula and Riemann's Zeta function, *Symmetry*, **17** (2025), 1597. https://doi.org/10.3390/sym17101597
53. F. Gündoğdu, C. Kahraman, Complex spherical fuzzy sets: Theory and applications in decision making, *J. Intell. Fuzzy Syst.*, **38** (2020), 2745–2757.
54. W. Rudin, *Principles of Mathematical Analysis*, 3rd edition, International Series in Pure and Applied Mathematics, McGraw-Hill, New York, 1976.
55. E. Aydoğdu, E. Güner, B. Aldemir and H. Aygün, Complex spherical fuzzy TOPSIS based on entropy, *Expert Syst. Appl.*, **215** (2023), 119331. https://doi.org/10.1016/j.eswa.2022.119331
56. M. Akram, A. Alkenani, M. Shabir, Enhancing ELECTRE I method with complex spherical fuzzy information, *Int. J. Computat. Intell. Syst.*, **14** (2021), 190.
57. M. Adam, N. Assimakis, A. Farina, Golden section, Fibonacci sequence and the time invariant Kalman and Lainiotis filters, *Appl. Math. Comput.*, **250** (2015), 817–831. https://doi.org/10.1016/j.amc.2014.11.022
58. C. Yue, R. Huang, D. Towey, Z. Xian, G. Wu, An entropy-based group decision-making approach for software quality evaluation, *Expert Syst. Appl.*, **238** (2024), 121979. https://doi.org/10.1016/j.eswa.2023.121979
59. I. Á, Harmati, R. Fullér, I. Felde, On stability of maximal entropy OWA operator weights, *Fuzzy Set. Syst.*, **448** (2022), 145–156. https://doi.org/10.1016/j.fss.2022.01.003
60. M. Arsal, U. ur Rehman, A. ur Rehman Virk, Assessment and evaluation of machine learning algorithms for recommendation system of E-commerce based on bipolar fuzzy- method based on the removal effects of criteria-elimination and choice translating Reality-I approach, *Eng. Appl. Artif. Intel.*, **169** (2026), 114107.

61. Z. Yue, TOPSIS-based group decision-making methodology in intuitionistic fuzzy setting, *Inf. Sci.*, **277** (2014), 141–153. https://doi.org/10.1016/j.ins.2014.02.013
62. Z. Yue, An extended TOPSIS for determining weights of decision makers with interval numbers, *Knowledge-Based Syst.*, **24** (2011), 146–153. https://doi.org/10.1016/j.knosys.2010.07.014
63. D. Song, Y. H. Goo, S. Choi, J. W. Kim, H. J. Park, K. Kim, A new TOPSIS sorting method using data-driven min/max values, *Expert Syst. Appl.*, **326** (2026), 132664. https://doi.org/10.1016/j.eswa.2026.132664
64. X. Wu, Y. Xiao, J. Zhang, D. Yu, Y. Liu, S. Mao, et al., Optimization of flow characteristics of gas-solid separators based on NSGA-II and entropy-weighted TOPSIS, *Adv. Powder Technol.*, **37** (2026), 105289. https://doi.org/10.1016/j.apt.2026.105289
65. C. L. Hwang, K. Yoon, *Multiple Attribute Decision Making: Methods and Applications-A State-of-the-Art Survey*, no. 186 in Lecture Notes in Economics and Mathematical Systems, Springer-Verlag, Berlin, Heidelberg, 1981.
66. T. Y. Chen, C. H. Li, Determining objective weights with intuitionistic fuzzy entropy measures: A comparative analysis, *Inf. Sci.*, **180** (2010), 4207–4222. https://doi.org/10.1016/j.ins.2010.07.009